

A New Electrokinetic Technology for Revitalization of Oily Sludge

Shiva Habibi

A Thesis
in
The Department
of
Building, Civil, and Environmental Engineering

Presented in Partial Fulfillment of the Requirements
for the Degree of Doctor of Philosophy (Ph.D.)
Concordia University
Montreal, Quebec, Canada

March 2004

© Shiva Habibi, 2004



National Library
of Canada

Bibliothèque nationale
du Canada

Acquisitions and
Bibliographic Services

Acquisitons et
services bibliographiques

395 Wellington Street
Ottawa ON K1A 0N4
Canada

395, rue Wellington
Ottawa ON K1A 0N4
Canada

Your file Votre référence

ISBN: 0-612-90386-9

Our file Notre référence

ISBN: 0-612-90386-9

The author has granted a non-exclusive licence allowing the National Library of Canada to reproduce, loan, distribute or sell copies of this thesis in microform, paper or electronic formats.

L'auteur a accordé une licence non exclusive permettant à la Bibliothèque nationale du Canada de reproduire, prêter, distribuer ou vendre des copies de cette thèse sous la forme de microfiche/film, de reproduction sur papier ou sur format électronique.

The author retains ownership of the copyright in this thesis. Neither the thesis nor substantial extracts from it may be printed or otherwise reproduced without the author's permission.

L'auteur conserve la propriété du droit d'auteur qui protège cette thèse. Ni la thèse ni des extraits substantiels de celle-ci ne doivent être imprimés ou autrement reproduits sans son autorisation.

In compliance with the Canadian Privacy Act some supporting forms may have been removed from this dissertation.

Conformément à la loi canadienne sur la protection de la vie privée, quelques formulaires secondaires ont été enlevés de ce manuscrit.

While these forms may be included in the document page count, their removal does not represent any loss of content from the dissertation.

Bien que ces formulaires aient inclus dans la pagination, il n'y aura aucun contenu manquant.

Canada

**CONCORDIA UNIVERSITY
SCHOOL OF GRADUATE STUDIES**

This is to certify that the thesis prepared

By: **Shiva Habibi**
Entitled: **A New Electrokinetic Technology for Revitalization of Oily Sludge**

and submitted in partial fulfillment of the requirements for the degree of

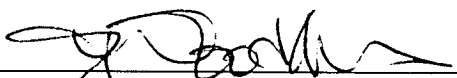
DOCTOR OF PHILOSOPHY (Civil Engineering)

complies with the regulations of the University and meets the accepted standards with respect to originality and quality.

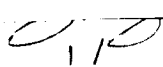
Signed by the final examining committee:

Dr. M. Debbabi  _____ Chair

Dr. I. D. Buchanan _____ External Examiner



Dr. P. Wood Adams _____ External to Program

Dr. F. Haghighat  _____ Examiner

Dr. J. Hadjinicolaou  _____ Examiner

Dr. M. Electedrowicz _____ Thesis Supervisor

Approved by _____
Dr. K. Ha-Huy, Graduate Program Director

MAY 06 2004

✓ _____
Dr. N. Esmail, Dean
Faculty of Engineering & Computer Science

Abstract

A New Electrokinetic Technology for Revitalization of Oily Sludge

Shiva Habibi, Ph.D.

Concordia University, 2004

Petroleum industries are burdened with the problem of handling large quantities of sludge having properties that depend on the nature of the crude oil, the processing capacity, the down-stream capacities, and the design of effluent treatment plants. Oily sludge is a complex mixture of hydrocarbons, water, metals, and suspended fine solids. This composition makes management of the sludge a complicated and costly undertaking. The objective of this research is to develop a technique that would significantly improve the separation of phases so as to allow for their further reuse. This investigation focused on the application of electrokinetic phenomenon for the remediation of oily sludge. To assess the effect of surfactant on the electrokinetic mobilization of organic contaminants in oily sludge, an amphoteric surfactant was used. Tests were performed in a series of electrokinetic cells with different electrical potentials. During 32 days of the experimental, electrical parameters and pH were measured daily, while samples collected at strategic intervals were analyzed by UV/VIS and FTIR methods. This research lies at the forefront of electrokinetic technology and embraces a combination of several processes including electrocoagulation, electrocoalescence, desorption, electrophoresis, and electroosmosis. The results obtained permit an assessment of the thermodynamics of the proposed process and introduce new theories on the behavior of the colloidal

component of oily sludge under different electrical potentials. The results demonstrated an excellent separation of phases; these consisted of water, hydrocarbon, and solid phases. The recovered solid phase exhibited high hydrocarbon content, so it could be reused. The separated liquid hydrocarbon could be reused in other processes. Some volatile hydrocarbons were released during the process. Advantageously, these gaseous hydrocarbons may be captured and burned as fuel. The results showed that the separated water had a low concentration of hydrocarbon, suitable for sending to the wastewater treatment plant. The method allows for the recycling of the hydrocarbon residue of a waste stream into a usable refinery product by achieving a 63% reduction in water content, and, thereby, reduces or eliminates the potential liability for environmental contamination arising from the disposal of waste stream products.

Acknowledgments

I would like to express my deepest sense of gratitude to my supervisor Dr. Maria Elektorowicz for her patient guidance, encouragement and excellent advice through this study.

My sincere thanks to Dr. Chifrina for her comments and suggestions in this work.

A special thanks to my great parents, who thought the goof things that really matter in life. I deeply appreciate your unconditional love, support and sacrifices and thanks for being a source of pride for me.

To my amazing brother, Hamed, my kind sisters, Sepideh and Shideh for their deep love and encouragement.

My appreciation to my friends in Iran and Canada.

To my beloved husband, Ali, whose endless support has allowed me to chase a dream. Thanks for your love, patience, understanding, and believing in me.

And at last I dedicate this work to my great friend and mentor in every step of my life, Dr. Gholam Reza Khajehpoor.

Contents

	<u>Pages</u>
List of Figures	xiii
List of Tables	xviii
Chapter 1: Introduction	1
1-1) Objective	4
Chapter 2: Literature review	5
2-1) Emulsions and emulsion stability	5
2-2) Effect of crude oil compositions on stabilization of water-in-oil emulsions	11
2-2-1) Asphaltene	12
2-2-2) Resins	16
2-2-3) Waxes	16
2-3) Oily sludge	17
2-4) Effects on environment	22
2-5) Wastes in refinery	24
2-6) Methods for treating of oily sludges	26
2-6-1) Incineration	29
2-6-2) Coking	30

2-6-3) Biological treatment	31
2-6-4) Land farming	32
2-6-5) Propane solvent extraction	33
2-6-6) Carver-Greenfield process	34
2-6-7) Ohsol process	35
2-6-8) Retech / Tetral	35
2-6-9) Sarex process	36
2-6-10) SoilTech process	36
2-6-11) Waste-Tech process	37
2-6-12) Scaltech process	37
2-6-13) TaBoRR process	38
2-6-14) Centech process	38
2-6-15) Hydrothermal processing	39
2-6-16) Conclusion	41
2-7) Electrokinetic method	42
2-7-1) Electrokinetic effect	45
2-7-2) Electroosmosis	48
2-7-3) Electrophoresis	49
2-8) Coagulation	50

2-8-1) Fractal approach	53
2-9) Surfactant	54
2-9-1) Anionic surfactants	55
2-9-2) Nonionic surfactants	55
2-9-3) Cationic surfactants	55
2-9-4) Amphoteric surfactants	56
2-9-5) Solubility	56
2-9-6) Adsorption	58
2-9-7) Micelle formation	58
2-9-8) Critical micelle concentration	60
2-9-9) Electrokinetic transport	61
Chapter 3: Experimental methodology	62
3-1) Experimental installation and cell configuration	64
3-2) Apparatus, reagents and equipment	67
3-2-1) Initial oily sludge	68
3-3) Characteristics of oily sludge before and after the experiment	68
3-3-1) Parameters measured	68
3-3-2) Water content	69
3-3-3) Light hydrocarbon content	70

3-3-4) Solids content	70
3-3-5) Non-volatile hydrocarbon content	71
3-4) Surfactant preparation	71
3-5) Cell preparation procedures	71
3-6) Duration of experiment	72
3-7) pH measurement procedure	72
3-8) Electrical Parameters	73
3-9) Sampling procedures during the experiment	73
3-10) UV/VIS analysis	74
3-11) FTIR analysis	75
3-12) Fractal analysis	77
Chapter 4: Results	78
4-1) Different fractions in oily sludge	80
4-2) Volume reductions in the cells	83
4-3) Electrical parameters	84
4-3-1) Electrical changes in cells with surfactant only	84
4-3-1-1) Cell with higher voltage - AE (1.5)	84
4-3-1-2) Cell with lower voltage - AE (0.5)	85
4-3-2) Resistance changes in cells containing sludge	86

4-3-2-1) Cell with higher voltage - SAE (1.5)	86
4-3-2-2) Cell with lower voltage - SAE (0.5)	87
4-3-2-3) Cell without addition of surfactant, higher voltage - SE (1.5)	89
4-3-2-4) Cell without addition of surfactant, lower voltage -SE (0.5)	90
4-4) pH measurements	92
4-4-1) pH changes in cells with surfactant only	92
4-4-1-1) Cell with higher voltage - AE (1.5)	92
4-4-1-2) Cell with lower voltage - AE (0.5)	96
4-4-2) pH changes in cells containing sludge	99
4-4-2-1) Cell with higher voltage - SAE (1.5)	99
4-4-2-2) Cell with lower voltage - SAE (0.5)	102
4-4-2-3) Cell without addition of surfactant, higher voltage - SE (1.5)	107
4-4-2-4) Cell without addition of surfactant, lower voltage - SE (0.5)	111
4-5) Relative aromatic hydrocarbon content	115
4-6) Relative aliphatic hydrocarbon content	124
4-7) Fractal analysis	133
4-8) Power and energy consumption	133

Chapter 5: Theory of electro-separation and model development	137
5-1) New developed model	139
5-1-1) Momentum balance between forces in x- axis (F_x)	140
5-1-2) Momentum balance between forces in y- axis (F_y)	142
5-1-3) Momentum balance (F_{xy})	143
5-2) Rate of electro-demulsification of aromatic hydrocarbons	145
5-3) Demulsification rate	148
5-4) Effect of resistance distribution on the dynamics of the process	149
5-5) Amphoteric surfactant behavior under the electrical field	152
5-6) Effect of electrical potential on the polarity of the hydrocarbon	153
5-7) Effect of pH distribution on the dynamics of the process	157
5-8) Effect of temperature on the dynamics of the process	159
5-9) Fractal analysis	159
5-10) New theory of colloids behavior in electrokinetic cell	160
Chapter 6: Impact of the new technology on environment and sustainable development	163
6-1) Average volume reduction rate	163
6-2) Emission mitigation	163
6-3) Value-added products	164
6-3-1) Separated solid fraction	165

6-3-2) Separated liquid fraction	166
6-3-3) Separated volatile fraction	167
6-4) Energy consumption analysis	167
Chapter 7: Case Study- Validation of the new theories	169
Chapter 8: Conclusion	176
Chapter 9: Future work	179
References	180
Appendix A	191
A-1) Characteristics of oily sludge before and after the experiment	192
A-2) Sustainable development	194
A-3) Pollution prevention and waste minimization	196
A-4) Environmental regulations	198
Appendix B - Glossary	205

List of Figures

	<u>Pages</u>
Figure 2-1 Different types of emulsions	6
Figure 2-2 Processes taking place in an emulsion leading to emulsion breakdown and separation	7
Figure 2-3 The equilibrium position of a solid particle at an oil-water interface	10
Figure 2-4 Hypothetical molecular structures of the asphaltenes	13
Figure 2-5 Possible configurations of asphaltene molecules on the emulsion interface	15
Figure 2-6 Oil droplet size distribution and classification	25
Figure 2-7 Flow diagram of solvent extraction	33
Figure 2-8 Process flow diagram of hydrothermal treatment	39
Figure 2-9 Electrokinetic phenomena	45
Figure 2-10 Double layer charge distribution	46
Figure 2-11 The generation of a sedimentations potential	46
Figure 2-12 Temporary dipole of atoms	52
Figure 2-13 Typical solubility ranges of surfactant types	57
Figure 2-14 “Tail-biting “ in the isoelectric area	58
Figure 2-15 Relative sizes of hydrophilic and hydrophobic groups	59
Figure 2-16 Schematic diagram of sphere-to-rod transition	59
Figure 2-17 Viscosity vs. concentration, indicating micellar structures	60
Figure 2-18 Schematic diagram of CMC vs. pH for an amphoteric surfactant	61
Figure 3-1 Experimental methodology	65
Figure3-2 Configuration of electrokinetic cell	66
Figure 3-3 Distillation apparatus	69

Figure 4-1	Different movements and creation of phases during the experiment	79
Figure 4-2	Initial sludge	81
Figure 4-3	Electrokinetics separated solid phase - cell SE (0.5)	81
Figure 4-4	Electrokinetics separated solid phase from cell SE (1.5)	82
Figure 4-5	Separated solid phase with amphoteric surfactant from cell SE (0.5)	82
Figure 4-6	Electrokinetics separated solid phase with amphoteric surfactant from cell SE (1.5)	83
Figure 4-7	Resistance distribution in cell AE (1.5)	85
Figure 4-8	Resistance distribution in cell AE (0.5)	86
Figure 4-9	Resistance distribution in cell SAE (1.5)	87
Figure 4-10	Resistance distribution in cell SAE (0.5)	88
Figure 4-11	Resistance distribution in cell SE (1.5)	90
Figure 4-12	Resistance distribution in cell SE (0.5)	92
Figure 4-13	pH changes in the top level of cell AE (1.5)	93
Figure 4-14	pH changes in the bottom level of cell AE (1.5)	94
Figure 4-15	pH changes in the cathode and the anode areas of cell AE (1.5)	94
Figure 4-16	pH changes in the cathode, the middle and the anode areas of cell AE (1.5)	95
Figure 4-17	pH changes in the middle cathode and the middle anode areas of cell AE (1.5)	95
Figure 4-18	pH changes in the top level of cell AE (0.5)	96
Figure 4-19	pH changes in the bottom level of cell AE (0.5)	97
Figure 4-20	pH changes in the cathode and the anode areas of cell AE (0.5)	97
Figure 4-21	pH changes in the cathode, the middle, and the anode areas of cell AE (0.5)	98

Figure 4-22 pH changes in the middle cathode and the middle anode areas of cell AE (0.5)	98
Figure 4-23 pH changes in the top level of cell SAE (1.5)	100
Figure 4-24 pH changes in the bottom level of cell SAE (1.5)	100
Figure 4-25 pH changes in the cathode and the anode areas of cell SAE (1.5)	101
Figure 4-26 pH changes in the cathode, the middle and the anode areas of cell SAE (1.5)	101
Figure 4-27 pH changes in the middle cathode and the middle anode areas of cell SAE (1.5)	102
Figure 4-28 pH changes in the top level of cell SAE (0.5)	104
Figure 4-29 pH changes in the bottom level of cell SAE (0.5)	105
Figure 4-30 pH changes in the cathode and the anode areas of cell SAE (0.5)	105
Figure 4-31 pH changes in the cathode, the middle and the anode areas of cell SAE (0.5)	106
Figure 4-32 pH changes in the middle cathode and the middle anode areas of cell SAE (0.5)	106
Figure 4-33 pH changes in the top level of cell SE (1.5)	108
Figure 4-34 pH changes in the bottom level of cell SE (1.5)	109
Figure 4-35 pH changes in the cathode and the anode areas of cell SE (1.5)	109
Figure 4-36 pH changes in the cathode, the middle, and the anode areas of cell SE (1.5)	110
Figure 4-37 pH changes in the middle cathode and the middle anode areas of Cell SE (1.5)	110
Figure 4-38 pH changes in the top level of cell SE (0.5)	112
Figure 4-39 pH changes in the bottom level of cell SE (0.5)	113
Figure 4-40 pH changes in the cathode and the anode areas of cell SE (0.5)	113

Figure 4-41	pH changes in the cathode, the middle, and the anode areas of cell SE (0.5)	114
Figure 4-42	pH changes in the middle cathode and the middle anode areas of cell SE (0.5)	114
Figure 4-43	UV/VIS spectrometer results for cell SAE (1.5) in different days of sampling	118
Figure 4-44	UV/VIS spectrometer results for cell SAE (0.5) in different days of sampling	119
Figure 4-45	UV/VIS spectrometer results for cell SE (1.5) in different days of sampling	120
Figure 4-46	UV/VIS spectrometer results for cell SE (0.5) in different days of sampling	121
Figure 4-47	UV/VIS spectrometer results for cell S in different days of sampling	122
Figure 4-48	UV/VIS spectrometer results for cell SA in different days of sampling	123
Figure 4-49	FTIR test results for cell SAE (1.5) in different days of sampling	127
Figure 4-50	FTIR test results for cell SAE (0.5) in different days of sampling	128
Figure 4-51	FTIR test results for cell SE (1.5) in different days of sampling	129
Figure 4-52	FTIR test results for cell SE (0.5) in different days of sampling	130
Figure 4-53	FTIR test results for cell S in different days of sampling	131
Figure 4-54	FTIR test results for cell SE in different days of sampling	132
Figure 4-55	Power consumption distribution	134
Figure 4-56	Energy consumption in different cells	134
Figure 5-1	Behavior of colloidal particles	138
Figure 5-2	Fast and slow coagulation	139
Figure 5-3	(a) Forces acting on a colloid particle,	140

(b) The total driving force (F_{xy}) and its direction

Figure 5-4	Relative aromatic hydrocarbon content at different distances from the cathode	147
Figure 5-5	Polarity of hydrocarbon in the cells without surfactant	155
Figure 5-6	Polarity of hydrocarbon in the cells with surfactant	156
Figure 5-7	Behavior of colloidal particles in electrokinetic cell	162
Figure 6-1	Initial oily sludge	165
Figure 6-2	Remained solid phase after the elektrokinetic test	166
Figure 6-3	Remained liquid phase after the elektrokinetic test	167
Figure 7-1	Resistance changes in the cell SE' (1.5)	170
Figure 7-2	Resistance changes in the cell SE' (0.5)	171
Figure 7-3	Resistance changes in the cell SCE' (1.5)	173
Figure 7-4	Resistance changes in the cell SCE' (0.5)	173
Figure 7-5	Electrokinetic separated solid phase of the cell SE' (0.5)	175

List of Tables

	<u>Pages</u>
Table 2-1 Characteristics of purified refinery sludge (hydrocarbon fraction)	19
Table 2-2 Analysis of Typical API and DAF Float Sludges from Petroleum Refining	21
Table 2-3 Characteristics of wastewater treatment sludge in Bedok Plant	22
Table 2-4 Processes used for separation and waste minimization	28
Table 2-5 Summary of electrokinetic effect	45
Table 3-1 Summary of cells	63
Table 3-2 Schedule of sampling	74
Table 4-1 Samples description	80
Table 4-2 Volume reduction rate	84
Table 4-3 Results of fractal analysis	133
Table 4-4 Cost of power consumption in each cell	135
Table 5-1 Demulcification rate in electrokinetic cells	148
Table 7-1 Summary of cells in the case study experiment	169
Table A-1 Water content in the samples	192
Table A-2 Volatile hydrocarbon content in the samples	192
Table A-3 Solid content in the samples	193
Table A-4 Non - Volatile hydrocarbon content in the samples	193
Table A-5 Petroleum Sludge Hazardous Waste List	199
Table A-6 Hazardous Substances and Reportable Quantities	202
Table A-7 K-Listed Refinery U.S. Waste Generation	203

Symbols

M	Mass of particles
L	Linear measure of size
D_f	Mass fractal dimension
E	Electrical field strength
Q	Charge of the colloid particle
F_e	Electrophoretic force
ε	Dielectric constant of the liquid phase
a	Radius of the colloid particle
$1/k$	Thickness of the double layer
F_v	Resisting force in x-axis
f	Friction factor
v	Velocity of the colloidal particle
F_{xy}	Total driving force
ζ	Zeta potential
η	Viscosity of liquid
F_g	Gravity force
F_l	Lifting force
F_f	Frictional drag force
ρ_p	Density of the colloid particle
V_p	Volume of the colloid particle
g	Gravitational acceleration
ρ_l	Density of the liquid phase
C_d	Drag coefficient
A_p	Projected area of the particle perpendicular to the velocity
R_n	Reynolds number
m_t	Total mass of colloidal particle
m_w	Mass of water phase
m_{lh}	Mass of liquid hydrocarbon phase
m_s	Mass of solid phase

K	Rate of electro-demulsification
x	Distance from the cathode
V	electrical potential
C_s	Concentration of surfactant
H_0	Initial height of the emulsion
H	Height of the remained emulsion after the experiment
t	time
k	Overall demulsification rate constant
b	Function of electrical potential and the distance from the cathode
c	Function of electrical potential and the distance from the cathode
R	Resistance
P	polarity of hydrocarbon
C_{Ar}	Relative content of aromatic hydrocarbons
C_{Al}	Relative content of aliphatic hydrocarbons
v_{eo}	Electro-osmotic velocity of the liquid (m/s)
u_E	Electrophoretic mobility
u_{eo}	Electro-osmotic mobility,
V	Electrical potential (V)
I	Electrical current (A)
a_λ	Absorptivity coefficient of wavelength λ
λ	Wavelength
b	Optical thickness of sample
A_λ	Absorbency

Chapter 1

Introduction

Petroleum refining is one of the industries that produce large amount of hazardous waste. Petroleum industries are burdened with the problem of handling large quantities of sludge, whose properties, depend on the nature of the crude oil, processing capacity, down-stream capacities, and the design of effluent treatment plants. Accumulation of sludge in refineries is usually due to pump failures, desalter failure, oil draining from tanks and operation units, periodic cleaning of storage tank and pipeline ruptures, and other factors (Kuriakose and Manjooran, 2001).

This sludge has been categorized by regulatory agencies as hazardous wastes. Typically, these petroleum sludge wastes are water-in-oil emulsions that are stabilized by fine solids. The US Resource Conservation and Recovery Act (RCRA) has listed these wastes as F037 – F038 and K048 – K052 sludges (Appendix A-4). It is estimated that each refinery produces 30,000 tons of these sludges per year (US EPA, 1991). As a result of a 1990 ban on land disposal, costs for treatment and disposal of petroleum wastes have significantly increased. The government, the industry, and the public all feel the need for cost-effective alternatives to traditional physical and chemical methods.

The development of different technologies for recycling and treating of petroleum wastes is driven by strong restrictive disposal regulations (e.g. Ontario Environmental Protection Act, R.R.O. 1990, Regulation 347 (General- Waste Management) and Resource Conservation and Recovery Act (RCRA)). These legislations regulate the future use of land disposal for hazardous wastes; they also mandate the reduction of volume, toxicity, and mobility of the wastes. Besides these regulations, the options for

disposal of oily sludges are limited. Landfill incurs a long-term liability, and incineration results in pollution with no energy benefit. This situation has compelled us to investigate and develop permanent and cost-effective solutions that are acceptable to the public.

Recycling is the most environmentally friendly option to handle these wastes. Recycling makes it possible to reuse valuable oil for reprocessing, reformulating, or recovering energy through burning. The recycling of oil and sludge can minimize the disposal of pollutants outside the industrial zone and reduce overall contamination (Galil and Rebhun, 1992). At present, no easy and cost-effective technology for treating oily sludge exists that would recover the valuable fuel contained in the sludge.

Several process technology options for treating the petroleum sludge have emerged during the past several years in response to enhancement of environmental regulations governing these wastes. Current technologies for treatment of refinery wastes are very expensive, and are mostly inadequate for current and future regulations (Conaway, 1999). Some of these technologies are centrifugation, thermal desorption, solvent extraction, and hydrothermal processing. None of these technologies are quite successful. Some of them have operational problems and may produce low-quality solids; others that produce high-quality solids are very expensive. Most of them do not satisfy either a new sustainable development approach (Appendix A-2) or the elimination of the greenhouse effect leading to the climate changes. Therefore, investigation of a technology of high quality at a low price is needed; a universally applicable technology is needed for the treatment of petroleum wastes. The technology should be capable of recovering petroleum in a form that can be sent to a refinery for further processing to produce higher quality petroleum products (Ripley et al., 1998).

Electrokinetics is a developing technology that is used for in-situ remediation of heavy metals and organic contaminants from saturated or unsaturated soils, sludges, and sediments. Successful removals of polar organic compounds (Elektorowicz et al., 1996(a); and Pamukcu et al., 1995) and PAH (Elektorowicz and Hatim, 1999) have been reported. Several investigations have considered different emulsion components (Jahanbakhshi, 1996; Elektorowicz et al., 1995), different devices (Rizakos, 1994; Elektorowicz and Hatim, 1997), and various conditioning liquids (Jesien, 1995 and 1996; Yellamraju, 1995 and 1996; Norssair, 1995; Elektorowicz and Hatim, 1999). Investigations have demonstrated that electrokinetic phenomena, generated upon the application of an electrical field, play an active part in phase separation in diesel-fuel-contaminated soil (Norssair, 1996a and 1996b; Elektorowicz et al., 1995). Generally, the principal advantages of this method are as follows:

- The flow direction can be controlled
- The method is capable of removing a wide range of compounds
- The method has a low electric power consumption

In this investigation, electrokinetic phenomena have been used for remediation of oily sludge. To assess the effect of surfactant on solubilization, desorption and mobilization of organic compounds by electrokinetics in oily sludge, amphoteric surfactant was also applied.

1-1) Objective

The main objective of this research is to develop a new sustainable technology for oily sludge management using electrokinetic phenomena that can readily separate petroleum and return a high percentage of the refinable petroleum fraction to the refinery.

Specific objectives are formulated as follows:

- Separating phases for their further reuse
- Recovering petroleum from the waste stream and returning it to the refinery for processing into the usable products
- Achieving volume reduction
- Defining thermodynamic processes governing the separation of phases
- Indicating opportunities for further reuse of separated phases (value-added products, energy recovery, GHG mitigation, etc)
- Meeting all of the above objectives efficiently and economically.

Chapter 2

Literature review

Oily sludge, produced mostly in petroleum refineries and petrochemical industries, is one of the major industrial wastes that require treatment. This hazardous waste has caused extensive damage to the environment. I studied this problem for more than five years as I worked for a petrochemical company in Iran. This problem does not relate just to countries that are involved in the extraction and production of oil; it concerns all people worldwide because the green-house gas effect (GHG), global warming, and ozone depletion affect all living species.

Typically, these sludge wastes are water-in-oil emulsions that are stabilized by fine solids. In order to protect the environment, their oil content has to be minimized by breaking up these solids-stabilized oil droplets. In addition to environmental concerns, the high price of oil drives the economic need to recover from these oily sludges as much useable oil as possible. This chapter will present a brief literature review of these emulsions, including their stability and characteristics as well as current technologies. The chapter also includes information about the phenomena that can be applied to a new methodology.

2-1) Emulsions and emulsion stability

Emulsions can be found in many important areas of everyday life, such as in the food, cosmetic, and pharmaceutical industries. Emulsions are not always desired; in the petroleum industry they can result in high cost and large damages to the environment. An emulsion consists of a liquid dispersed in another immiscible liquid as droplets of

colloidal sizes ($\sim 0.1 - 10 \mu\text{m}$) or larger. If the oil is the dispersed phase, it is called oil-in-water emulsion, and if the water is the dispersed phase it is a water-in-oil emulsion. Sometimes, multiple emulsion oil-water-oil suspensions may also be found (Sjoblom et al., 2003) (Figure 2-1).

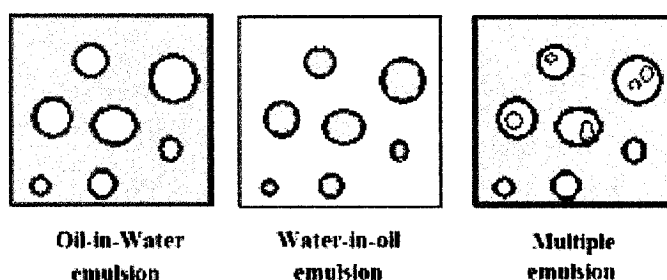


Figure 2-1 Different types of emulsions

The behavior of emulsions is often very complex. Emulsion morphology significantly influences the physico-chemical properties of emulsion products. Many factors influence emulsion morphologies including temperature, electrolyte, phase volume ratio, agitation, viscosity, wettability, hydrophile-lipophile balance (HLB), and interfacial tension (Lee et al., 2002). An emulsion may be either very tight and stable or loose, depending on a number of factors such as the properties of the oil and water, the percentage of water and oil in the emulsion, and the type and amount of emulsifying agents present. The common emulsifying agents in crude oil emulsions are asphaltenes, resins, organic acids, and finely divided minerals; each of them usually occurring as a film on the surface of the dispersed droplets (Ali and Aiqan, 2000).

Emulsions are not thermodynamically stable and tend to minimize their surface area by separating into the different phases. For this separation to occur, the droplets must merge with each other, or with the homophase continuum that gradually forms. Figure 2-

2 shows different processes that facilitate the separation: sedimentation and creaming, flocculation, and coalescence. In creaming and sedimentation, density differences between the two liquid phases create a droplet concentration gradient, resulting in a close packing of the droplets. Aggregation of droplets can occur when the droplets stay very close to one another for a much longer time than if no attractive forces existed between them (Sjoblom et al., 2003).

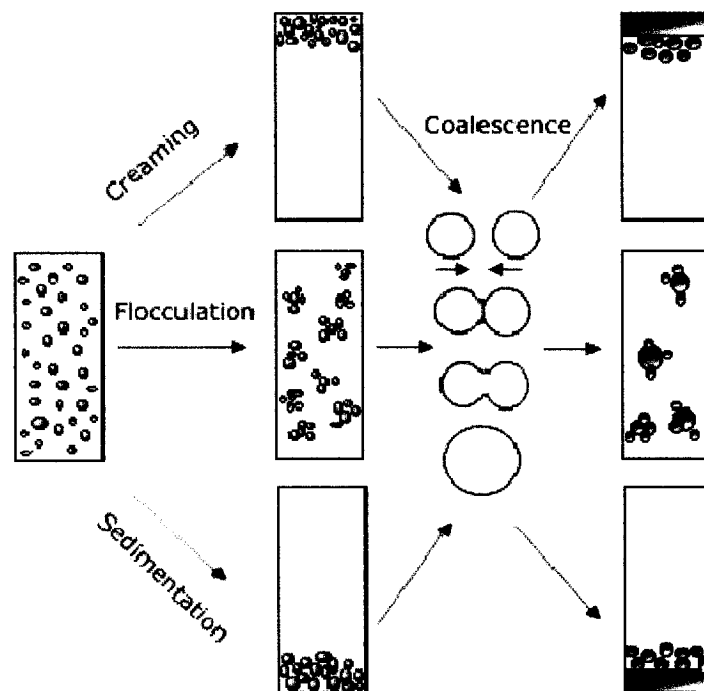


Figure 2-2 Processes taking place in an emulsion leading to emulsion breakdown and separation (Sjoblom et al., 2003).

The coalescent behavior can be described in three steps: droplets approaching each other, the process of film thinning and drainage, and film rupture leading to droplet-droplet coalescence. In the first step, the drops approach each other and are separated by a film of the continuous phase. The second step involves the thinning of this film to reduce

the interfacial area. When the film reaches a certain critical thickness, any significant disturbance or instability will cause film rupture, and coalescence will occur (Eow et al., 2001).

The external electrical forces can facilitate coalescence between small drops in order to attain suitable drop sizes for phase separation. It is believed that the interaction between the drops and the externally applied electrostatic field results in charging and agglomeration of the drops, and eventually coalescence. An external electric field can cause the coalescence of drops at an interface (Bhardwaj and Hartland, 1994). An electrical field can promote contact between drops to help in drop-drop coalescence.

Zhang et al. in 1995 believed that even a small external electric field induces changes of opposite sign on the closest surfaces of two aqueous drops when two drops are close to each other. The presence of one drop affects the potential field around the other drop, resulting in the drops flowing around each other. If two drops are sufficiently close, van der Waals attraction may also become important, helping to pull nearby drops into contact and holding them together during coalescence because of the tendency of interfacial tension to minimize the surface area.

The actual coalescence process depends on two factors: the dielectric break-down of the continuous phase film between adjacent drops, and the attractive force between drops due to their potential differences. The film may also rupture by means other than electrostatic break-down. Other factors, such as the average droplet size and the time that the liquid mixture exposed to the electric field, also affect coalescence efficiency.

The size of droplets in emulsions may vary considerably as a result of (i) variation of interfacial properties (surfactant effects); (ii) variation in the water hold-up; and (iii) variation in the level of shear to which the emulsion is subjected (Eow et al., 2001).

Certain factors may prevent the droplets from coming into contact with each other, such as electrical double layer repulsion and steric stabilization by polymers and surfactants. Polymers, surfactants, and adsorbed particles can create a strong interfacial film that acts as a barrier against aggregation and coalescence (Sjoblom et al., 2003).

Finely divided solids in contact with oil and water can also form solid-stabilized emulsions. These fine particles adsorb at the droplet surface and, by lowering the demulsification rate constant, act as a barrier that prevents droplet coalescence (Yan and Masliyah, 1997). When the contact angle of the particles is near to 90° , the particles will be collected at the interface, so the emulsion will reach its highest stability (Sjoblom et al., 2003).

It is generally accepted that hydrophilic solids with a contact angle slightly less than 90° stabilize oil-in-water emulsions, while hydrophobic solids with a contact angle slightly larger than 90° stabilize water-in-oil emulsions (Yan and Masliyah, 1996). Figure 2-3 shows the equilibrium position of a solid particle at an oil-water interface. If the particle has a contact angle less than 90° (hydrophobic), a large volume fraction of the particle will be in the water phase (Figure 2-3 a); but if it has contact angle higher than 90° (hydrophilic) a smaller volume fraction will be in the water phase and a large volume fraction will remain in the oil (Figure 2-3 b) (Yan and Masliyah, 1993).

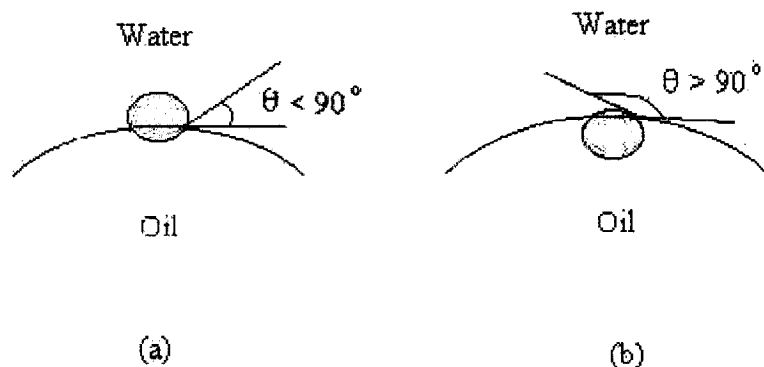


Figure 2-3 The equilibrium position of a solid particle at an oil-water interface

Asphaltenes are responsible for the hydrophobicity of the minerals. By using high pH aqueous phase or asphaltene-soluble solvents, the clay surface properties can be modified so that the clay will be desorbed from the oil-water interface, leading to a higher demulsification rate (Yan and Masliyah, 1996). The stability of water-in-oil emulsions stabilized by mineral particles depends on the formation of complex structures at the oil-water interface; the stability can be decreased by decreasing the asphaltene adsorption (Menon and Wasan, 1988).

Other factors that may increase the stability of an emulsion are low interfacial tension, high viscosity of the bulk phase, and relatively small volumes of dispersed phase (Sjoblom et al., 2003). Hano et al. in 1988 investigated the effect of oil phase viscosity on demulsification rate; they report that the demulsification rate is proportional to the (-3.2) power of the oil phase viscosity.

2-2) Effect of crude oil compositions on stabilization of water-in-oil emulsions

Crude oil is a complex mixture of hydrocarbons. It also contains small amounts of sulfur, oxygen, nitrogen, and various metallic constituents such as vanadium, nickel, iron and copper. A common practice in the petroleum industry is to separate the crude oil into four chemically distinct fractions: saturates, aromatics, resins, and asphaltene (SARA) (Burya et al., 2001). Asphaltenes, resins, and naphthenic acids can accumulate at the water-oil interface and act as a barrier for the separation of phases. It is believed that asphaltenes are the major material stabilizing emulsions (Yan and Masliyah, 1996).

Water-in-oil emulsions are undesirable in most cases because of their large volume and high viscosity. A particular challenge for the oil industry is to develop an environmentally friendly, cost effective treatment method to destabilize these emulsions. In order to protect the environment, the oil content has to be minimized by breaking up the solids-stabilized oil droplets. The first point to understand is that these emulsions are stabilized through the formation of a film with elastic or viscous properties, a rigid protective film that encapsulates the water droplets (Yarranton et. al., 2000). The properties of this film play an important role in determining the efficiency of oil recovery. It is believed this film consists of a cross-linked network of asphaltenic molecules, which aggregate through lateral intermolecular forces to form primary aggregates or micelles at the oil-water interface (Sjoblom et al., 2003). Changing the fluid particle and particle-particle interactions can decrease the stability of the emulsions (Yan and Masliyah, 1996); this stability is closely related to the rheological properties both of the emulsion and of the crude oil comprising the dispersion medium (Puskas et al., 1996).

Besides asphaltenes, solid particles such as waxes, clays, inorganic materials, or naphthenates present in crude oil can increase the strength of the film. In most cases, the presence of an adsorbed layer of a polar surface-active material from crude oil, particularly asphaltenes on finely divided solids can alter the wettability and other characteristics of these solids, enabling them to adsorb on the emulsion interface and strongly stabilize water-in-oil emulsions. The concentration of the solids and, hence, their packing at the interface are important to the stability of the emulsions (Menon and Wasan, 1986). The removal of these solids can decrease emulsion stability significantly (Gafonova and Yarranton, 2001). Solid particle size is another important factor in stabilizing the emulsion. As the size of the solid particle decreases, its surface area per unit mass increases dramatically, so more surface-active materials such as asphaltene is adsorbed on the particle (Ali and Alqam, 2000; Sullivan and Kilpatrick, 2002).

This rigid film is a physical barrier; sufficient energy is needed to break that barrier and enhance collisions between droplets (Sjoblom et al., 2003). Levin et al. (1989) believe that the energy needed to remove a particle from an oil-water interface is approximately 10^6 times the thermal energy of the particles due to Brownian motion. All other types of potential energy (energy due to electric double layer, Vander Waals attraction, capillary interaction energy among the particles) are orders of magnitude smaller. Thus, solids-stabilized emulsions are stable from a thermodynamic point of view.

2-2-1) Asphaltene

Boussingault invented the word asphaltene in 1983. After examining the constituents of some bitumens found at that time in eastern France and in Peru, he described the

asphaltene as the fraction of distillation residue that was insoluble in alcohol and soluble in essence of turpentine. The strong interest in a better understanding of asphaltenes comes from their impact on the production, transportation, refining, and utilization of petroleum. Asphaltenes are the heaviest, non-volatile, polar fraction of crude oil (Sjoblom et al., 2003); changes in temperature, pressure, and oil composition can cause asphaltenes to precipitate (Ali and Alqam, 2000).

Asphaltenes are characterized by fused ring aromaticity, small aliphatic side chains, and other elements such as sulfur, oxygen, nitrogen, and metals such as vanadium and nickel. The heteroatoms in the asphaltene molecule account for a variety of polar groups such as aldehyde, carbonyl, carboxylic acid, and amid. Figure 2-4 shows a suggested asphaltene structure (Sjoblom et al., 2003).

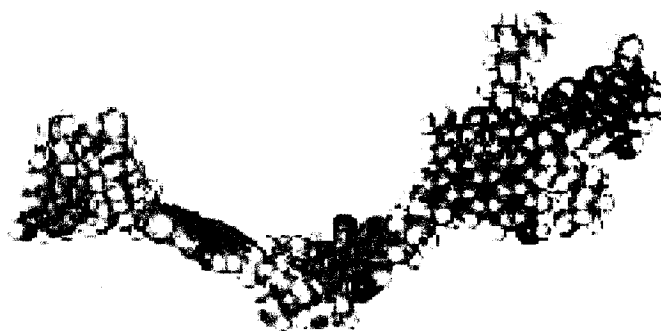


Figure 2-4 Hypothetical molecular structures of the asphaltenes (Sjoblom et al., 2003)

Asphaltenes are responsible for several problems related to the recovery and refining of petroleum. It has been shown that asphaltene particles may self-associate and form aggregates in the presence of aromatic hydrocarbons. Different ideas prevail on the accurate description of asphaltene self-association, but it is assumed that the aggregation

can occur through hydrogen bonding. Both micelles and colloids are used in reference to asphaltenes.

Asphaltenes tend to adsorb at water-in-crude oil interfaces to form a rigid film surrounding the water droplet, thereby protecting the interfacial film from rupturing during droplet-droplet collisions, and enhancing the formation of extremely stable water-in-crude oil emulsions. Asphaltene adsorbs on mineral and wax particles, thus contributing significantly to emulsion stability (Sjoblom et al., 2003). Other factors that influence the stability are the amount of asphaltenes, the degree of aging of asphaltenes and resins, and the ratio of asphaltenes to resins (Eow et al., 2001).

It has been found that, as the asphaltene bulk concentration increases, asphaltene surface coverage increases until a limiting value is achieved. Surprisingly, it has been seen that the stability of the emulsions decreases as asphaltene surface coverage increases. This unexpected behavior challenges the idea that the accumulation of asphaltenes on the interface creates a stronger, thicker interfacial barrier that increases emulsion stability. This change in stability could be related to the changes in the asphaltene configuration on the interface (Gafonova and Yarranton, 2001).

At low asphaltene concentrations and consequently, low surface coverage, molecules may be spread out on the interface, with many points of attachment, as shown in Fig. 2-5a. At high asphaltene concentrations, the molecules may adsorb in a more “vertical” position on the interface so that they become attached at one or only a few points per molecule. Lateral interaction between the asphaltenes may preserve this configuration. In the vertical position, much more material can be attached to a given surface area (Fig. 2-5b). When molecules are attached to the interface at only one point, they are extended

more into the continuous phase and may be more mobile than when they are attached at several points. This more mobile interface may not present a strong barrier to coalescence. When molecules are attached at several points to the interface, the produced emulsion is more stable (Gafonova and Yarranton, 2001).

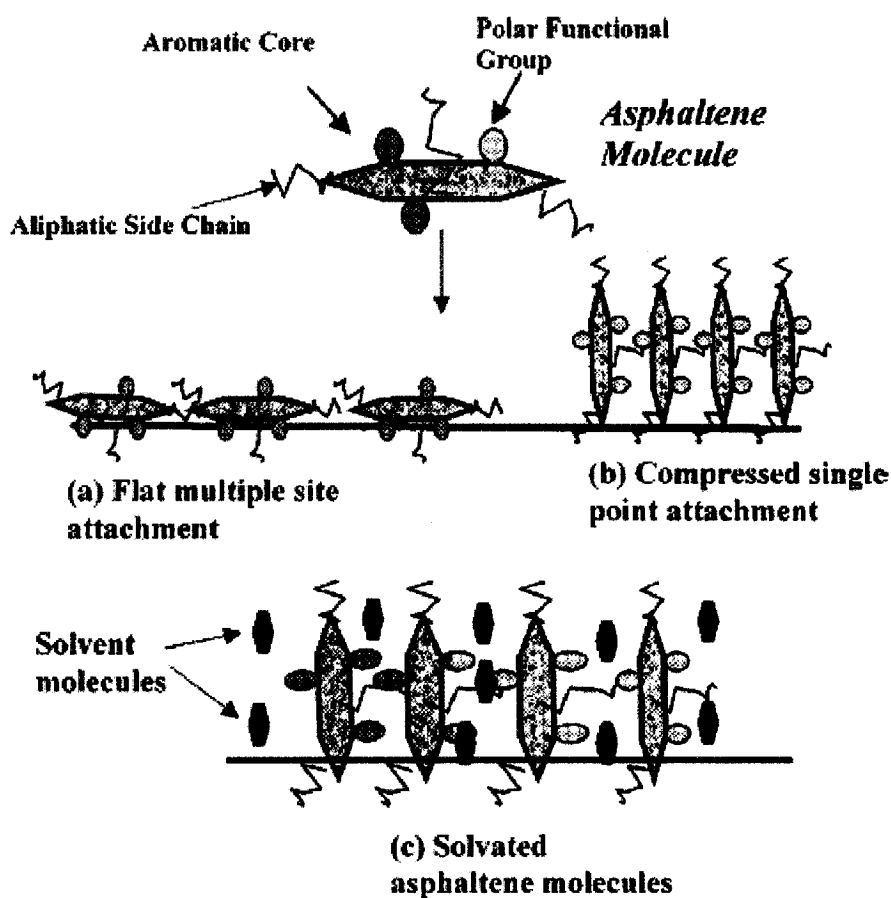


Figure 2-5 Possible configurations of asphaltene molecules on the emulsion interface (Gafonova and Yarranton, 2001)

The value of the zeta potential appears to increase slowly with increasing amount of asphaltenes. This increase is due to the ionization of some of the polar groups in the asphaltenes, which are amphoteric in nature (Menon and Wasan, 1986).

2-2-2) Resins

Resin molecules are structurally similar to asphaltenes but have lower molecular weight, higher hydrogen to carbon ratio, and lower heteroatom content. Asphaltenes and resins both have a largely hydrophobic hydrocarbon structure containing some hydrophilic functional groups and, consequently, are surface-active; therefore both asphaltenes and resins have the potential to accumulate on the water-oil interface.

Resins increase the solubility of asphaltene in the crude oil, thus minimizing the asphaltene interaction with water droplets. It is believed that the emulsion stability in a crude oil system is mainly controlled by the separated asphaltene fraction. Resins alone are not capable of stabilizing the emulsion, although the resin fraction might be even more interfacially active than are the asphaltenes (Eow et al., 2001).

2-2-3) Waxes

The waxes found in crude oil are mixtures of different types of paraffins such as normal paraffins, branched paraffins or isoparaffins, and cycloparaffins. Wax crystals can play an important role in the formation of water-in-oil emulsions because they slow down the coalescence of colliding water droplets by forming a rigid layer around water droplets. This phenomenon can occur if the polar molecules, such as asphaltenes, alter their wettability by being adsorbed on their surface. Their surface wettability should alter from complete hydrophobic to intermediate wettability.

The size distribution of the paraffin particles, their number per unit volume, and the interactions between them are important in determining the rheological properties of crude oil emulsions (Puskas et al., 1996). The type of the wax crystals, as well as their quantity, plays a key role on the stabilization process. Nucleation of the wax crystallinities

by asphaltene and resins at the interface adds to the thickness of the oil-water interfacial film and, hence, increases the stability of the emulsion.

2-3) Oily sludge

Oily sludge is a waste dumped by petroleum refineries (Kuriakose and Manjooran, 2001). Oily sludge is one of the major industrial wastes that require treatment in the petroleum refinery and petrochemical industries. Refineries generate approximately 30,000 tons of waste oily sludges per year per refinery (EPA, 1991). The hydrocarbon residue is collected in various ways, such as from clean-up operations of oil tankers, barges, and petroleum storage vessels; from oil pipelines, and from other clean-up operations at refineries (Burbridge et al., 2001).

Oily sludge contains almost 70 % hydrocarbons (mostly paraffines and asphaltenes), together with clay, sand, inorganic matter, heavy metals, water, etc. (Kuriakose and Manjooran, 2001). Oily sludge is a water slurry that contains a high level of oil and grease, corrosion products, and sulfur (Mukarji, 2000). Handling, treatment, and disposal of these sludges have received considerable attention from refineries and technology suppliers.

At present, there is no a technique or combination of techniques that provides a complete solution that is economically viable. The difficulty in solving this problem springs from a number of factors. The variable composition of the waste petroleum has a high impact on the efficiency of the different steps of any technologies. Even in relatively homogeneous waste petroleum, the variability of composition is still sufficiently great to have an adverse effect on the efficiency of separation of impurities from the waste petroleum (Ripley et al, 1998).

Oily sludge contains a large amount of combustible material having high heating values (Shie et al, 2000, Kuriakose and Manjooran, 2001). The sludge comes from several sources, such as:

- Cleaning of crude oil, asphalt, LSHS (Low Sulfur Heavy Stock), furnace oil, and intermediate storage tanks.
- Biological sludge
- Dissolved Air Floatation (DAF) scum
- American Petroleum Institute (API) separator sludge
- Cleaning of accidental heavy oil spillage on the ground.
- Cleaning of surge ponds in wastewater treatment plant.
- Chemical sludge

Oily sludge contains approximately (Table 2-1) (Kuriakose and Manjooran, 2001)

25 %	water
5 %	inorganic sediments like sand, clay, scales, etc
70 %	hydrocarbons (7.8 % asphaltene content and 4.8 % ash content)

The percentage weight of the different metals in the ash is as follows: Fe = 23.49, Al = 10.57, Ca = 1.64, Na = 0.57, K = 0.46, Ni = 0.12, V = 0.23, Mg = 0.65, Zn = 0.21, Ti = 0.53, and Mn = 0.10 %.

The solids in refining sludge consist of granular sands, so the oil is easily separated from the solid fraction; but the petroleum sludge has much higher oil content than the refining sludge has, and the solids exhibit a clay-like consistency (Marks et al, 1992). The sludges vary from slurry-like to mud-like to clay-like, with different specific gravities. Generally, the waste petroleum contains 2 to 50 weight percent solids. The

solids content varies with the source of the waste petroleum. Water, which is tightly bound to the solids, forms stable emulsions with petroleum, which are difficult to break (Ripley et al., 1998).

Table 2-1 Characteristics of purified refinery sludge (hydrocarbon fraction)
(Kuriakose and Manjooran, 2001)

Parameter	
Density @ 15C (g ml)	0.9573
Pour point (°C)	+ 42
Wax (% wt.)	6.0
Asphaltenes (% wt.)	7.8
Acidity (mg KOH /g)	4.3
Flash Point (°C)	>200
Kinematic viscosity @ 100 °C (cS)	30.33
Total sulfur (% wt.)	3.43
Ash content (% wt.)	4.8

Crude oil and refined oil contain some settleable matter. Whenever an oil product is stored, pollutants tend to settle as sludge at the bottom of the tank. However the sludge also contains rust originating from the wall and bottom of tanks and transport pipelines. The amount of sludge generated from the crude oil tanks is usually high (around 500 m tons per cleaning session) whereas the quantity from product tanks is comparatively small (ETPI, 2000). Residual sludges are inherent in petroleum storage tanks. Depending upon the source, the crude oil may contain various non-refinable contaminants, typically silt, salt, sulfur, and metals such as lead. The crude oil contains small quantities of fine solids, which can settle in the bottom of storage tanks. They are so tightly bound to

hydrocarbons that they resist conventional physical separation processes such as filtration and centrifugation (Conaway, 1999).

In tar-like sludges, there are appreciable levels of volatile fraction constituents such as benzene, toluene, styrene, and the dominant compounds being ethylbenzene and xylenes. The oily sludge contains crude oil, water, and petroleum solid particles in various proportions depending on its origin (Petrisor et al., 2001).

Although oil and water do not mix well, water will emulsify especially if the oil contains polar compounds that may form as the oil ages (U.S. Army Manual, 1999). An emulsion is composed of two phases. One phase exists as tiny droplets (the dispersed or internal phase) dispersed within the outer (external or continuous) phase. The thicker the emulsion, the more stable (physically) it will be. For viscous and stable water-in-oil emulsions, the motion of emulsions in the horizontal direction is slow (Fang and Lai, 1995). Oily sludge is generally a water-in-oil emulsion, with relative stability determined by the presence of mineral particles along with the oil and reservoir water (Petrisor et al., 2001).

The removal and treatment of sludge, on the bottom of crude oil storage tanks pose a problem. Heavy crude oil often contains 3% to 5% by volume in the globular form, which can settle to the bottom of the storage tank and produce a thick layer of settled globular oil. This settled material is commonly referred to as crude oil sludge or crude oil tank bottoms. Most refineries periodically take the storage tanks out of service and remove the bottoms. The residual solids are usually disposed of in a landfill, or they are incinerated (Miyasaki, 1998).

Table 2-2 shows the typical composition of API and DAF sludges. These wastes are black sludges with high viscosity and contain oil, water, and finely divided solids. With centrifugation alone, only limited separation of oil and water can be achieved, and a large volume of waste remains as secondary emulsion.

Table 2-2 Analysis of Typical API and DAF Float Sludges from Petroleum Refining
(Silva et al., 1998)

Content	Wt %
Oil	10 - 20
Solids	5 - 7
Water	75 - 85
Ash	2

Wastewater treatment produces unwanted semisolid, odoriferous residual sludge, which is difficult to manage. The ultimate disposal of the sludge to the environment usually requires some treatments such as thickening, stabilization, conditioning, dewatering, and disposal (Tay and Jeyaseelan, 1993). The main wastewater stream could be influenced by factors, such as rain-floods, and accidental spill at the production units (Galil and Rebhun, 1992). Table 2-3 shows typical characteristics of wastewater treatment sludge from Bedok Wastewater Treatment Plant. The oil content of sludge ranges from 1.8 % to 8.0 %, with an average of 3.0 % (Tay and Jeyaseelan, 1993).

Table 2-3 Characteristics of wastewater treatment sludge in Bedok Plant
(Tay and Jeyaseelan, 1993)

Parameter	Range	Typical
Total solids content	3.2 - 4.4 %	3.8 %
Oil content	1.8 - 8.0 %	3.0 %
Capillary suction time (s)	80 - 150	140
Specific gravity of dry solids	1.4 - 1.7	1.6

2-4) Effects on environment

Production of a product that is environmentally safe is an important consideration part of the solution for a cleaner world. The wastes generated in a production process must also be considered when evaluating impact.

Every day, large quantities of organic and inorganic compounds are released into the environment as a result of human activities. Many of these compounds are toxic and persistent and can contaminate soil, surface water, and groundwater. Oily sludge, as a mixture of hazardous hydrocarbons, is one of the contaminants. For treatment and disposal purposes, it should be remembered that these sludges may contain high amounts of toxic contaminants in the form of bioaccumulated heavy metals, metal precipitates, and sorbed organics (Dold, 1989). The chances of contamination of groundwater and soil are high at petroleum industries. This problem occurs mainly because of spills, leakage

from pipes and tanks, dumping of oily sludge, and the like. The dumping of oily sludge is the most potential threat to soil and ground water quality.

Numerous sources produce oily sludges as by-products. Because of environmental regulations, there is an increased tendency to treat oily sludges in the most economically feasible manner (Miyasaki, 1998).

1. Oily sludge generated from wastewater treatment plants has been classified as hazardous waste by many countries. The oil residues create a tar-like substance with high acid content, which creates a very bad odor.
2. Certain types of crude oil and certain types of petroleum-based products contain a hydrocarbon component that, over time, settles in storage tanks and other vessels. This component is typically in the form of a waxy or wax-like solid material and is very difficult to remove or recover. These kinds of storage tanks and vessels are commonly found on ships, at terminals, and at refineries.
3. After removing hydrocarbon residues from storage tanks, the residues are often disposed of into a waste stream rather than recycling them into a usable refinery product. This type of disposal of hydrocarbon residue in waste streams has the potential for contaminating land or water environments (Burbridge et al, 2001).
4. When the oily sludge runs off to surface water, the heavier hydrocarbon fraction sinks and accumulates as bottom muck, killing plants and bottom-dwelling animal life. Dissolved or emulsified fractions deplete the oxygen content of water bodies. Floating fractions cause fire hazards, as well as coat riverbanks and boat hulls. For example, residues and oily sludge from ship bunker tanks cause injury and death to some 350 penguins at Australia's Phillip Island each year (CSIRD, 1999).

Disposal of sludge from different storage tanks is indeed a major environmental problem for refineries. Generally, sludge is disposed of in open ground. In some countries, such as Pakistan, no measures are taken to avoid soil contamination or spreading of the waste sludge. Also, no special provisions are made for separating liquid oil from this waste sludge. The leakage to surrounding soil is also not monitored (ETPI, 2000). An area of 70,000 square meters in Bahrain is loaded with black petroleum residues dumped by a refinery in 1938 – 1942. Over the years, natural forces have induced some changes such as dusting over by desert sands, evaporation by heat, and deposition of rain water and migrated sea water. “Bahrain pitch” is one of thousands sites that has been a serious environmental problem for all these years. Depositing the waste petroleum in landfills by refineries results in groundwater contamination. Singapore’s authorities bagged the sludges as a containment measure, but eventually the bags were damaged and petroleum leaked out (Ripley et al., 1998). Hardly a country can be found which is exempt from similar problems. Unfortunately, many refineries refuse to acknowledge their waste petroleum problems while others have made only limited attempts to deal with them.

2-5) Wastes in refinery

Almost every refining operation from primary distillation to thermal cracking generates a waste flow. The term “ refinery waste” means the collective residuals of all petroleum acquisition, transportation, storing and refining operations; it includes sludges, bottoms, waxes, oils, greases, contaminated soil, and so on (Conaway, 1999). The

refining waste composition is classified in terms of the oil and grease content, and the size of oil droplets (Figure 2-6) in the oil-water mixture (Dold, 1989).

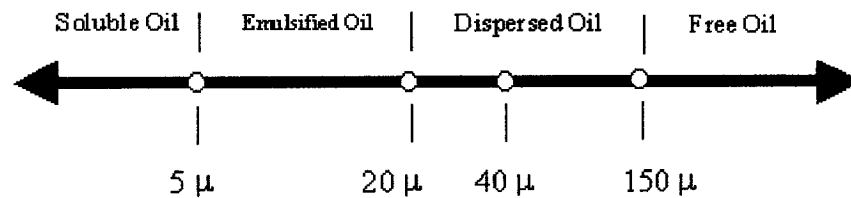


Figure 2-6 Oil droplet size distribution and classification

There are four kinds of wastes that are generated during petroleum refining:

- 1- Sludges
- 2- Spent catalysts
- 3- Spent chemicals
- 4- Various solids and sediments

Some of these wastes are indigenous to the crude oil; the others come from different stages of processing. Oily sludges may result from:

- Storage tank sediment
- Crude oil desalters
- Sewer cleaning
- Oil-water separator
- Floatation units
- Lube oil processing
- Alkylation

Sources of non-oily sludges include:

- Storm sewer cleaning
- Cooling towers
- Water treatment

Biological sludge is produced by biological wastewater treatment plants. Spent chemicals are generated during refining processes. Spent catalysts are generated as a result of catalyst replacement. In a refinery, there are other wastes such as empty drums (some of which contain hazardous materials), soil and debris from spills, spent filter media, scrap metal, and trash and construction debris.

RCRA lists six wastes associated with petroleum processing as hazardous (Spearman and Zagula, 1992):

- 1- Dissolved air floatation float (K048)
- 2- Slop oil emulsion solids (K049)
- 3- Heat exchange bundle cleaning solids (K050)
- 4- API oil-water separator sludge (K051)
- 5- Leaded tank bottoms (K052)
- 6- Primary oil-water separation sludges (F037, F038)

Identification of various sources of refinery waste helps engineers reduce the quantity and level of toxicity in these materials through source control, recycling, and treatment (Spearman and Zagula, 1992).

2-6) Methods for treating of oily sludges

Oil refineries need a well-planned oily sludge management strategy. At present, there is no established method in many refineries for disposing this oily sludge. Transferring

accumulated sludge from various collection systems, surge ponds, pitch, and so on into lagoons and quarries is the only option for most refineries. This dumping is hazardous, allowing the volatile hydrocarbons to escape into the atmosphere. New restrict regulations now obligate these industries to undertake the task of effective treatment and safe disposal of the waste. The oil component in oily sludge poses a challenge with respect to the treatment. Different technologies to treat oily sludge have been introduced, but none of them are quite successful: some of them have operational problems while others are too expensive.

Factors such as sludge characteristics, location of sludge (whether in an open pit or in a storage tank), age, source, quantity, quality of end results, and process duration required are all important in choosing the best technology (Abdulwahed, 1998). Local regulatory concerns economic viability and optional benefits will influence the development or treatment and disposal options.

Methodology ranges from simple single-step in situ chemical treatment for oil recovery to multi-step physical, chemical, biological and thermal treatment to meet standards for land disposal (Lal et. al., 2000).

Most refineries for treating their oily sludges that are listed as hazardous wastes use decanting through gravity separation. Some sites use a combination of thermal and gravity treatments that involve heating the hazardous wastes in a tank to around 120 °C (248 °F) combined with gravity separation over a period of weeks. Depending on the waste, sometimes de-emulsifying chemicals as well as filtration are used. Other treatment methods are also, such as incineration, solvent extraction, and thermal distillation. Table 2-4 shows processes used for separation and waste minimization.

Refiners are permitted by regulations to treat petroleum sludge wastes so long as the oil is recycled and the water treated at the on-site wastewater treatment facilities. However, the residual solids must be disposed of off-site subject to EPA treatment requirements.

Table 2-4 Processes used for separation and waste minimization

Process	Centrifugation	Solvent Extraction	Evaporation, Drying, or Low Temperature Desorption	High Temperature Desorption
Propane solvent extraction		X		
Craver-Greenfield	X	X	X	
Ohsol	X		X	
Retec/Tetra				X
Sarex	X		X	X
Soiltech				X
Waste-Tech			X	X
Scaltech	X		X	
TaBoRR			X	X
Centech	X			

Several treatment alternatives for hazardous oily waste and sludge streams are available:

1. Incineration

2. Coking
3. Biological treatment
4. Land farming
5. Propane Solvent Extraction
6. Carber-Greenfield process
7. Ohsol process
8. Retech/Tetral process
9. Sarex process
10. SoilTech process
11. Waste-Tech process
12. Sealtech process
13. TaBoRR process
14. Centech process
15. Hydrothermal processing

The three following factors must be studied and analyzed carefully to select the optimum technology (Abdulwahed, 1998):

- Economic benefits
- Time saving
- Environmental benefits

2-6-1) Incineration

In this method, oily sludge generated in refineries, machinery factories, or marine vessels is collected and incinerated. Combustion of oily sludge or waste solvents in an incinerator is a valuable source of energy, which is used to drive steam turbines and as a

heat source in a waste oil reclaiming factory. After dust removal with an electrostatic precipitator, and with hydrochloric and sulfuric acid scrubber, flue gas is discharged to the air. Ash is disposed to a landfill.

One incinerator that is used mainly to incinerate oily sludge is the rotary-kiln type. This is a multipurpose incinerator and promotes good firing and burning.

However, this management method is expensive (residue incineration costs more than \$800/t) and there is problem with public acceptance of incineration. Typically, an incineration system contains a variable incline rotary kiln to provide efficient combustion for a wide range of water-oil-solids mixtures. Combustion temperatures in the kiln are around 850 °C (1562 °F) (Silva et al., 1998). This method requires fuel as energy input.

2-6-2) Coking

There is a petroleum coke exception under 40CFR 261.6, and a refinery with a Coker can use that exception. By this exception, refinery hazardous waste that contains oil can be used as feed to stoke a Coker. But the rule applies only to wastes generated at the facility where the Coker is located, and provided the resulting coke does not have a hazardous characteristic.

Normally, the oil wastes that a Coker can receive include:

- DAF float (K048)
- Slop oil emulsion solids (K049)
- API separator sludge (K051)
- Tank bottom sludge
- Bio-sludge

This method is relatively expensive and is currently used in the industry. The process has been shown to be effective for recycling the above-mentioned wastes (Leeman, 1988). Metal removal is not considered in this method.

2-6-3) Biological treatment

Biological treatment has been shown to be successful for API separator sludge and DAF float from refinery operations. The treated residue can be disposed of in a RCRA permitted landfill because it meets EPA's Best Demonstrated Available Technology (BDAT) standards. The importance of this process is that the residue is land-filled, not incinerated, so it can reduce cost; however, metals can act as inhibitor for biological activities.

In this method, the sludge is first processed through a decanter / centrifuge. After this step, most of the oil can be returned to the refinery and most of the water after separation can be sent to the wastewater treatment system.

Bioprocessing of the residue from the decanter requires redilution with water. This produces a vent gas stream, which may require further treatment. Following the biotreatment comes a chemical treatment for the stabilization of the solids. Finally, the residue is dewatered and disposed in a landfill.

With this method, it costs more than \$400/t to treat and dispose residues at an installation processing 9000t/year of dilute waste (10 % solids, 30 % oil and grease). This total cost includes about \$120/t of operating costs and a unitized capital cost of \$280/t (Silva et al., 1998).

2-6-4) Land farming

Land farming is a bioremediation treatment process performed in the upper soil zone or in biotreatment cells. Contaminated soils, sediments, or sludges are incorporated into the soil surface and periodically turned over or tilled to aerate the mixture. This technique has been successfully used for years in the management and disposal of oily sludge and other petroleum refinery wastes. In situ systems have been used to treat near surface soil contamination for hydrocarbons and pesticides. The equipment employed in land farming is typical of that used in agricultural operations. These land farming activities cultivate and enhance microbial degradation of hazardous compounds. As a rule of thumb, the higher the molecular weight (i.e., the more rings within a polycyclic aromatic hydrocarbon), the slower the degradation rate. Also, the more chlorinated or nitrated the compound, the more difficult it is to degrade (Cookson, 1995; EPA, 1996).

Factors that can limit or otherwise affect the applicability and effectiveness of the process include: (1) space requirements; (2) the conditions advantageous to biological degradation of contaminants are largely uncontrolled, which increases the length of time needed to complete remediation, particularly for recalcitrant compounds; (3) inorganic contaminants are not biodegraded; (4) the potential for large amounts of particulate matter being released by operations; and (5) the presence of metal ions may be toxic to microbes and may leach from the contaminated soil into the groundwater (EPA, 1996). Typical costs for land farming range from \$45 to \$105 per cubic meter (Cookson, 1995).

2-6-5) Propane solvent extraction

EPA has recognized the propane solvent extraction method (Figure 2-2) as the BAT standard for refinery hazardous wastes K048 - K052. This process has certain advantages: These advantages are:

- The volume of residue for disposal can be reduced
- The oil can be recovered and recycled
- The water can be charged to wastewater system
- The extraction system is closed, so there is no emission to the atmosphere

However, the disadvantages of the process are higher initial capital investment, problem of propane availability, and transportation. The process temperature lies between 30 °C (86 °F) and 50 °C (122 °F) at $2 \times 10^6 \text{ N/m}^2$ (290 psig).

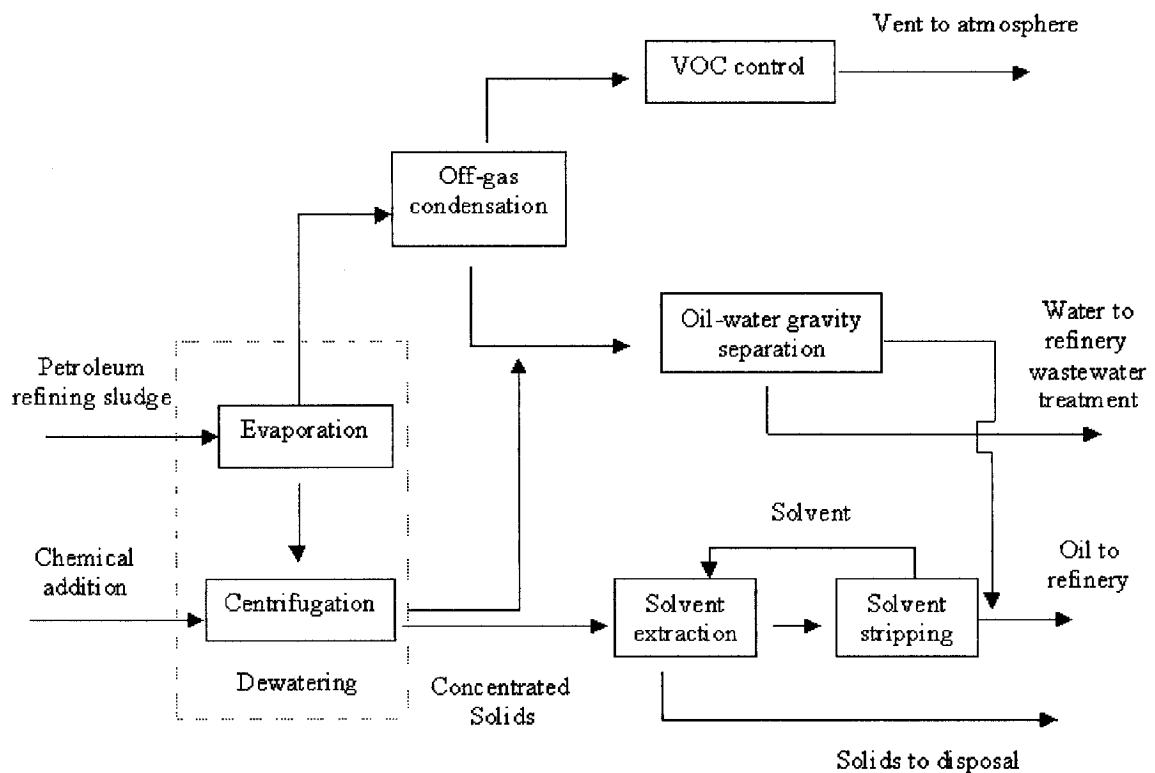


Figure 2-7 Flow diagram of solvent extraction (Silva et al., 1998)

Propane solvent extraction is a multistage extraction and decanting process. Liquid propane is the solvent used in this method. Mixing of solvent and sludge takes place in a stirred vessel. The solvent and oil has overhead to a solvent recovery flash unit. Recovered oil can be recycled to the refinery and the propane can be reused after recompression. From the bottom of the extractor, water and solids pass to a filter. Water is sent to the wastewater treatment and filtered solids are disposed of because they confirm BDAT standards (Filippi and Markiewicz, 1991).

2-6-6) Carver-Greenfield process

This method, which is a series of processes, is a combination of evaporation, centrifugal separation and solvent extraction. The method was developed by Charles Greenfield and has been used in many industries from food processing wastes to petroleum sludges.

The method uses steam, solvents, and evaporation equipment to remove all the water from wet oily sludge and can produce completely dry material free of hydrocarbons. The dry material can often be disposed of as non-hazardous wastes.

The solvent (usually fuel oil) is added at the beginning of the process. This will allow the complete evaporation of water from the sludge without producing an unpumpable residue. Another effect of using solvent relates to extracting the petroleum out of the solids into the liquid phase.

The type of evaporator depends on the specific composition of the sludge. For sludges with high water content, multi-effect evaporators are more efficient for water removal. For sludges with high water content of up to 30 %, a single-stage evaporator is used. The next stage is the condensing of the evaporated water and light distillate; after

condensation, these are separated by gravity. Water that has low levels of contaminants is sent to a water treatment system. A centrifuge separates the solvent and oil from solids. The final step consists of heating the solids and purging them with steam or an inert gas, such as nitrogen to remove residual oil from the solids. The oil removed in this step is combined with the recovered oil in the centrifuge and sent to a distillation tower for recovery of fuel oil solvent (Schindler, 1992). This method is complicated and expensive with high energy consumption; metal removal is also not considered.

2-6-7) Ohsol process

This method was developed by Uni Pure Corporation. The Ohsol process uses a combination of evaporation and centrifugation to treat refinery wastes. The first step is the adding of a surfactant to the waste to promote emulsion. The next step involves heating and pressurizing the wastes to about 150 °C (302 °F) and 10^6 N/m^2 (145 psig), and then rapidly flashing the wastes to break the emulsion and evaporate water and some light oils. The remaining waste is separated in a three-phase centrifuge (Rhodes, 1994). This method consumes high amounts of energy and it does not consider metal removal.

2-6-8) Retech / Tetral

The Retech/Tetral process is based primarily on high temperature thermal desorption. The first step entails dewatering the sludges to whatever extent possible. The second step entails heating to 500 °C (932 °F) to 600 °C (1112 °F) in a rotary kiln heated indirectly by a heat transfer fluid. To prevent the combustion of oil, a nitrogen purge gas is applied. The next step involves condensation and separation of the desorbed oil and water; then the oil is recycled, and the off-gas recovery system is used for treatment of the uncondensed portion of the vapor. The treated solids are cooled, and then disposed

(Abrishamian et al., 1992). This thermal process is expensive due to high energy consumption.

2-6-9) Sarex process

The Sarex process uses centrifugation, low temperature drying, and high temperature thermal desorption. This method is offered commercially by Separation and Recovery Systems, Inc. The first step in the process is to indirectly preheat sludges to about 65 °C (149 °F) with steam, and then centrifuge. Sometimes adding chemicals to assist with de-emulsifying the waste is needed. The mixture of oil and water from the centrifuge is returned to the wastewater treatment plant for separation and recovery of the oil. An enclosed screw conveyor carries the solids from the centrifuge. The next step is to dry the solids at 80 °C (176 °F) to 300 °C (572 °F) to remove water and light hydrocarbons. After that, the water and organic vapor are condensed, separated, and recovered separately.

For the final removal of hydrocarbons, the remaining solids are conveyed to a thermal desorber operating at 300 °C (572 °F) to 500 °C (937 °F). The hydrocarbons from the dryer and desorber are collected on granular activated carbons for disposal (Miller et al., 1994). This method is very expensive, incurring high capital cost.

2-6-10) SoilTech process

SoilTech has developed a thermal desorption system, a method that can be used for both contaminated soil and petroleum sludges. This process has been used primarily for contaminated soil. It includes some treatment steps for hazardous organics such as PCBs, that are not commonly found in petroleum refinery sludges (Silva, 1998).

2-6-11) Waste-Tech process

Waste-Tech Services Inc.'s desorption and recovery unit is a two-stage thermal desorption system. The first-stage heater, which dries the sludge at about 300 °C (572 °F), is a thermal screw process that removes water and light oils. The volatiles from this stage are condensed. Solids from the first-stage are discharged by gravity into the second-stage.

The second-stage features a paddle mixer with a high surface area that can be heated by electric heaters in the sealed, molten salt-filled hollow paddles. The second-stage temperature is about 500 °C (932 °F), which volatilizes the remaining hydrocarbons that are then separately condensed. The two condensing systems recycle the oil to the refinery. The condensed water is sent to the refinery's wastewater treatment system. The uncondensed vapor is oxidized or treated before releasing. At the end, the remaining solids are cooled and then disposed of (Rasmussen, 1994). This thermal process is complex and expensive, and consumes high amounts of energy.

2-6-12) Scaltech process

Scaltech Inc. offers a combination of centrifuge and drying processes to produce a cement kiln fuel from sludge. The type of the centrifuge may be either vertical or horizontal, depending on the sludge properties; it removes the water and oil. The water is sent to the wastewater treatment plant and the oil will be sent to the refinery. Then the concentrated sludge is processed in a high energy mixing tank. In this tank, the recovered oil is remixed with the solids in the correct proportion to produce the kiln fuel.

The next step is to dry the homogenized slurry in an agitated tank. This tank is equipped with steam coils, and it will reduce the water amount of slurry to less than 10

%. Final blending is then used to meet the specification of the particular kiln customer. Gravity separates evaporated water and oil. The oil is recycled and water is sent to the wastewater treatment facilities (Bishop, 1995). This method needs high amount of energy.

2-6-13) TaBoRR process

The TaBoRR process is offered by the Western Research Institute. The process, which follows standards for tank bottom recovery and remediation, is more often used for tank bottoms from oil-field production than refinery K-listed wastes. The first step is to concentrate solids by vaporizing inherent water and light hydrocarbons. After that, they are separately condensed and settled by gravity. The concentrated tank bottoms are then fed to a screw conveyor, where the sludge is exposed to a hot stripping gas generated in a furnace that uses fuel oil for combustion. Most of the hydrocarbons are transferred to the hot stripping gas and condensed separately. The next step is to heat the remaining solid streams to about 550 °C (1022 °F) in a pyrolysis reactor to crack any remaining hydrocarbon material. Finally, the solid residue is collected and cooled (Johnson et al., 1993). This method is not suitable for small facilities; high energy consumption limits its application.

2-6-14) Centech process

This method, a three-phase centrifugation process, is offered by Centech Inc. The method also is used mostly for tank bottoms from oil-field production (Silva et al., 1998). This method consumes high amounts of energy, and it does not consider metal removal.

2-6-15) Hydrothermal processing

Several hydrothermal technologies are available for separation of petroleum sludges.

Figure 2-8 shows a generalized process flow diagram of a hydrothermal sludge treatment process.

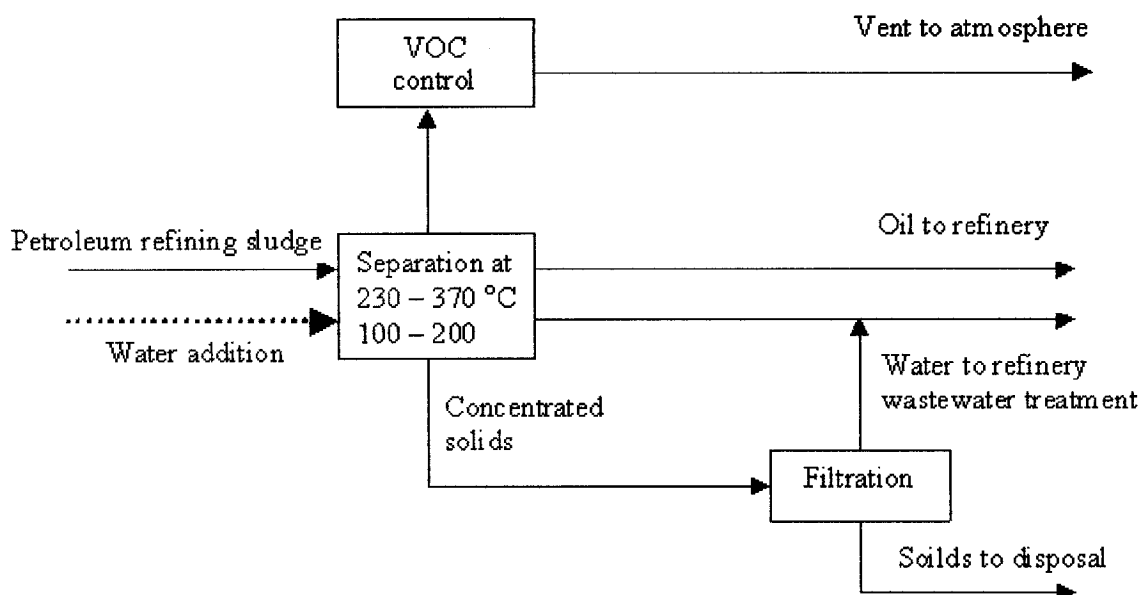


Figure 2-8 Process flow diagram of hydrothermal treatment (Silva et al., 1998)

One of these methods is an emulsion breaking process that includes heating the emulsion under autogenous pressure to temperatures of from 230 °C (446 °F) to 370 °C (698 °F). By cooling the mixture, four phases are found; these can be separated. The produced gas is vented, the oil is decanted, and the solids can be filtered from the water.

Another method is to heat the emulsion to at least 400 °C (752 °F) at a pressure of 2.1×10^7 N/m² (3045 psig) to 4.5×10^7 N/m² (6525 psig). At these conditions, a supercritical fluid can be removed from the vessel, which can then be cooled, depressurized and

separated by gravity into oil and water streams. The solids can be removed from the pressurized reactor.

Another process entails de-oiling and dewatering of refinery sludges, where sludges are diluted with recycled oil and then pumped into a distillation column. Steam is injected to the column to distill the oil and water, while dry solids are collected at the bottom of the distillation column. The oil and water are recovered above the distillation column and after cooling, are separated by gravity. Further separation of oil and water is achieved by steam stripping.

The Petroleum Sludge Treatment process is a hydrothermal method that separates emulsions into three distinct layers: oil, water, and solids. In this method the temperature is adjusted to 300 °C (572 °F) to 350 °C (662 °F), and pressure to 10^7 N/m² (1450 psig) to 2×10^7 N/m² (2900 psig). The pressure must be sufficient to prevent vaporization of the water and oil. The most important factor in achieving efficient separation of highly stable oil-in-water emulsion is the simultaneous separation and individual removal of the distinct phases at process conditions. Continuous process operation in this method allows recovery of most of the heat input required in a liquid-liquid heat exchanger. Separation time varies from a few minutes to hours.

By this method, more than 97 % of the oil can be recovered for recycling in the refinery. The water phase contains no visible oil but, due to dissolved organics, the chemical oxygen demand (COD) reaches to 5000 mg/L. This water can be treated in the refinery wastewater treatment plant.

Moisture in the wet solids is about 50 %; oil, 1-2 wt %. Preliminary tests have indicated that the solids meet EPA's BDAT standard requirements for land disposal. One

of the advantages of this process is that separation occurs in a single vessel (Silva et al, 1998), but it requires further treatment of wastewater. Hydrothermal processes consume high energy and time, and they incur high capital cost.

2-6-16) Conclusion

Reported costs for treatment of K and F wastes with these technologies, in 1998, ranged from \$100 to \$800 per tonne of sludge processed. Incinerating any sludge or other form of waste petroleum is not cost-effective or environmentally acceptable because of the necessity of dealing with emissions of NO_x, SO_x, heavy metals (Ripley et al., 1998), CO₂, CO, etc. The gases mentioned here have already caused the GHG effect and acid rain, resulting in great damage to Canadian, English, and Scottish forests (Santos, 1999).

Various centrifugal separators and filtration systems can be used to separate liquid components, including water and oils, for return to the refinery. However, to achieve good filter separation, diatomaceous earth is being used, which produces, after filtering a cake with high petroleum content. In centrifugal decanter centrifuges, polymers are added ahead of the decanter to flocculate solids for easier settling. Solvents or “cutter stock” also may be added to reduce the viscosity of heavier fractions, improving separation. The separated solid and cake, which can be disposed in landfill, contain a high amount of hydrocarbon (Conaway, 1999).

“Land farming”, which is natural degradation of petroleum waste is slow, expensive, demanding of space, requires complicated mechanisms of control. This method can fail to meet the requirements for reduction of high molecular weight hydrocarbons (Conaway,

1999). Landfill of petroleum sludge is hazardous to health since its components can leach into the water table below (Santos, 1999).

The incineration method is too expensive to meet air pollution regulations. Bioconversion is a simple and effective method but its success depends on the choice of

- a) The right type of microorganism
- b) The right type of biosurfactant formation
- c) The right quantity of additives
- d) The correct incubation period
- e) The right temperature profile

Even a tiny variation in these parameters makes the operation ineffective (Kuriakose and Manjooran, 2001).

From the literature review, therefore, it can be concluded that the high-temperature thermal desorption processes produces the highest quality solids, but has the highest range of costs. Processes that rely primarily on non-thermal methods, have a lower range of costs, but the solids quality in these cases is poorer than thermal desorption. These costs include labor cost, capital recovery, and disposal costs for the residual solids (Silva et al., 1998).

2-7) Electrokinetic method

“Electrokinetics” generally refers to the relative motions of charged species in an electric field. The movements could be as a result of charged, dispersed species or of the continuous phase, and the electric field could be due to an externally applied field or generated by movements of the dispersed or continuous phases.

Electrokinetics is a developing technology used to separate and extract heavy metals, radionuclides, and organic contaminants from soils. Recently, the application of electrokinetic processes has been increased. The goal of the electrokinetic technique is migration of contaminants in an imposed electric field via electroosmosis and/or electrophoresis. The process may be enhanced through the use of surfactants or reagents to increase the contaminant removal rates at the electrodes. In electrokinetics, a low-intensity direct current is applied through the region between the electrodes. The current creates a low-pH region at the anode area and a high pH region at the cathode area (Kim et al., 2000).

The research group at Concordia University has performed investigations for several years on phase separation in oil sludge by applying an electrical field. These investigations considered different emulsion components (Jahanbakhshi, 1996; Elektorowicz et al., 1995), different devices (Rizakos, 1994; Elektorowicz and Hatim, 1997) and various conditioning liquids (Jesien, 1995 and 1996; Yellamraju, 1995 and 1996; Norssair 1995; Elektorowicz and Hatim, 1999). The investigations concluded that electrokinetic phenomena, generated upon the application of electrical field, take an active part in phase separation in diesel fuel soil suspensions (Norssair, 1996a and 1996b; Elektorowicz et al., 1995; Chifrina and Elektorowicz, 1998).

Electrokinetics can be applied for the following contaminants:

- Heavy metals (Lageman, 1989; Pamukcu and Wittle, 1992; Shiba et al., 2000)
- Radioactive species (Buehler et al., 1994)
- Toxic anions (nitrates, sulfates) (Chew and Zhang, 1998)

- Dense non-aqueous phase liquids (DNAPLs) (Kokal et al., 1995; Elektorowicz et al., 1995)
- Cyanides (Podol'skaya et al., 2001)
- Petroleum hydrocarbons (Bhattacharya et al., 1996; Elektorowicz and Hatim, 2000)
- Explosives (Hilmi et al., 1999)
- Mixed organic/ionic contaminants (Hilmi et al., 1999; Hakimpour, 2001)
- Halogenated hydrocarbons (Wall et al., 2002)
- Polynuclear aromatic hydrocarbons (Maini et al., 2000)

Concentrations compatible with this method, range from a few ppm to tens of thousands ppm. Moisture content is important to the effectiveness of the process, especially when the moisture content is less than 10 percent. Acidic conditions may help to remove metals. To prevent corrosion of the electrodes, inert electrodes made from, for example carbon, graphite or platinum should be used (Rizakos, 1994).

According to Evans and Wennertrom (1994), four important electrokinetic phenomena pertain to colloid science (Table 2-5). In electrophoresis and sedimentation, charged particles move in quiescent liquid. In streaming potential and electro-osmosis, the flow of fluid passes a stationary charged surface. These phenomena can be classified in terms of driving force and response. In electrophoresis, applied electrical field, forces particles to flow and in electro-osmosis the applied electrical field, forces the fluid to flow. In sedimentation potential or streaming potential experiments, an imposed external pressure gradient or an acceleration force generates electrical potential. Figure 2-9 shows the scheme of the four different electrokinetic phenomena.

Table 2-5 Summary of electrokinetic effect (Evans and Wennertrom, 1994)

Potential	Stationary (wall)	Moving (colloid particles)
Applied	Electro-osmosis	electrophoresis
Induced	Streaming potential	Sedimentation potential

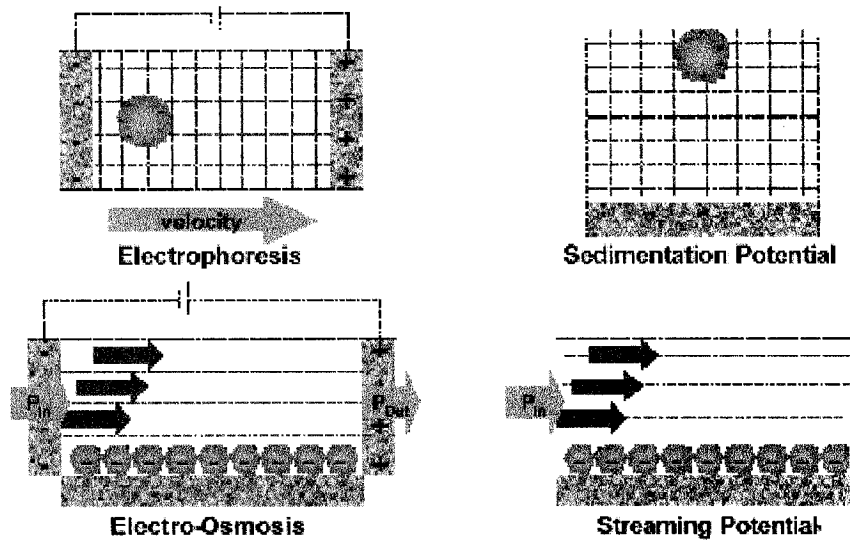


Figure 2-9 Electrokinetic phenomena (Pelton, 2003)

2-7-1) Electrokinetic effect

The assessment of the effective potential (or charge) might be expressed as a potential (or charge) of the diffuse part of the double layer (Fig 2-10). The charge (or potential) should be measured at some distance away from the surface of the particle, outside the layer of strongly adsorbed ions on the surface. It is desired to determine the electrostatic potential at the beginning of the diffuse part of the double layer, but it can be approximated by measuring the electrokinetic or zeta potential (ξ) (Hunter, 1993).

Different processes are referred to as the electrokinetic effects by which the zeta potential can be determined. When there is a charge at the boundary between the two phases and one phase moves with respect to the other, the electrokinetic effects occur. Electrokinetics in colloidal suspension can occur when the particles settle under gravity or in a centrifuge. If the particles carry an electric charge, when they settle, they produce a potential difference called the sedimentation potential (Fig 2-11).

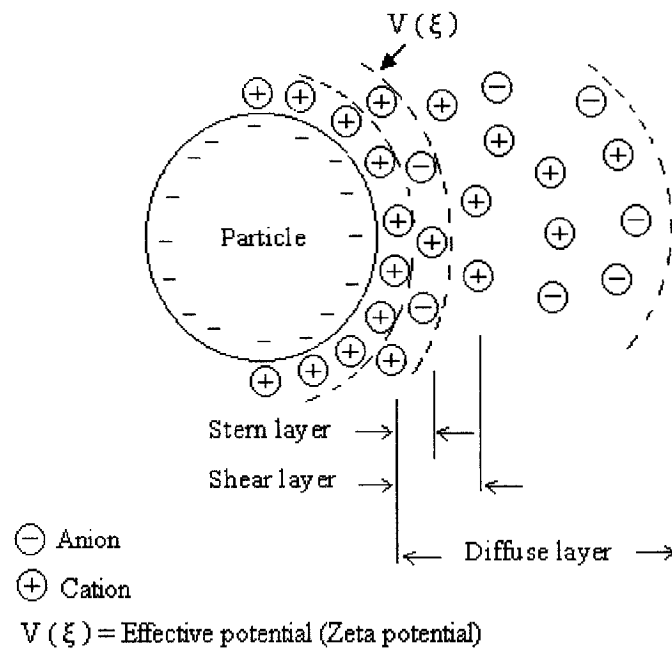


Figure 2-10 Double layer charge distribution (Carberry and Englande, 1983)

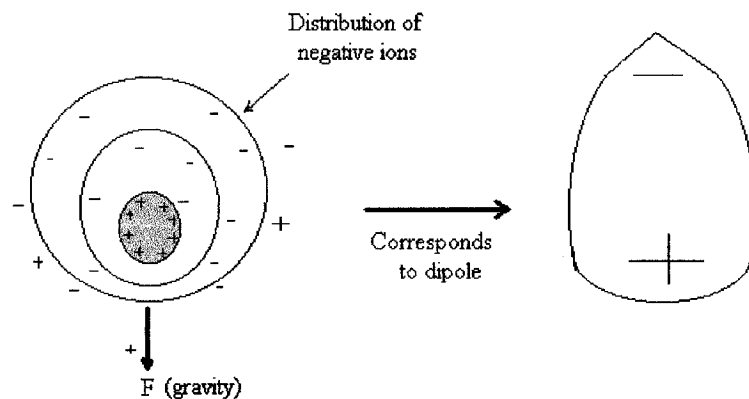


Figure 2-11 The generation of a sedimentations potential (Hunter, 1993)

The negative ions try to keep up as the positive ions move downward, causing a slight distortion of diffuse double layer and a tiny dipole is formed around each particle. The sum of the dipoles is a measurable electrical potential, which makes the bottom of the suspension positive with respect to the top. By measuring that potential difference, the zeta potential of the settled particles can be calculated (Hunter, 1993).

Electrophoresis is another phenomenon that permits obtaining zeta potential by applying an electric field to a suspension and measuring the mobility of the particles, and the specific capacitance. For a colloidal suspension, the motion of each particle can be followed using a suitable microscopic technique.

Another electrokinetic process is electro-osmosis, which is movement of liquid in a solid phase due to the application of an electric field. The most widely accepted theory for this phenomenon is that water surrounding the ions is dragged along via friction forces during movement of cations to the cathode and anions to the anode (Eykhardt & Daniel, 1994). The movement of counterions in electrical field drags the liquid along with them. The volume of liquid transported by a known electric field per unit time can be used to calculate the zeta potential of the system.

Sometimes the particles in the system are larger than colloidal size (1 μm or more). In that case, the applied electrical field cannot move them so it is the liquid that moves. If the liquid is forced through the system instead of applying electrical field, a potential is generated, called; streaming potential and this can be used to determine the zeta potential (Hunter, 1993).

2-7-2) Electroosmosis

Electroosmosis is defined as the mass flux of a fluid containing ions through a stationary porous medium caused by the application of an electrical potential. The fluid moves through the voids in the porous medium (e.g. soil), called pores, where the pore walls have at least a slight electrical charge, either positive or negative. Under the influence of a DC electric field, the thin layer of charged fluid moves in a direction parallel to the electrical field. Bulk liquid might be transported along with the thin layer of charged fluid carrying as well as other species within the liquid. Since there are cations more than anions in the electric double layer (EDL), the flow of water is toward the cathode (Choudhury, 1998).

It was Von Smolvchowskis who first gave the theory of the electro-osmotic effect in its present form. He considered the movement of the liquid near a large, flat, charged surface in a known electrical field, applied parallel to the surface. If the surface is negative, a net excess of positive ions in the liquid near the surface will be mobilized within electrical field, and the liquid will be dragged along with them. The electro-osmotic mobility, u_{eo} , can be measured by the following equation:

$$u_{eo} = v_{eo} / E_z = - \epsilon \xi / \eta \quad (2.1)$$

Where,

v_{eo} is the electro-osmotic velocity of the liquid (m/s)

E_z is the electrical field strength (volt)

ϵ is the permittivity ($C^2/J.m$) , [C is Coulomb]

ξ is the zeta potential (volt)

η is the viscosity of the liquid (Pa . s)

This equation assumes that both η and ε retain their bulk values all through the double layer. The negative sign indicates that when ξ is negative, liquid flows from bottom to top between electrodes because the space charge is positive (Hunter, 1993).

2-7-3) Electrophoresis

In an electrophoresis experiment, by imposing an electrical field across a colloidal solution, the electrophoretic velocity of the colloidal particle can be measured (Evans and Wennertrom, 1994). Smoluchwski considered the liquid to be a fixed medium so the solid particles would move with the same velocity of electroosmosis but in the opposite direction (Hunter, 1993):

$$u_E = -u_{eo} = \varepsilon \xi / \eta \quad (2.2)$$

where, u_E is electrophoretic mobility. This relation has limitations and is valid only when the double layer around the particle is very thin compared to its radius ($ka \gg 1$, where $1/k$ is thickness of double layer and a is radius of the particle). When the double layer is very thick compared with the particle radius ($ka \ll 1$), the electrical forces acting on the double layer can be ignored because they are not transmitted to the particle. The only considered forces acting on particles are

- 1) The direct electrical force
- 2) The viscosity drag of the liquid

In the early 1920s, Huckel proposed the equation for electrophoretic mobility with thick double layer as follows:

$$u_E = 2 \varepsilon \xi / 3 \eta \quad (2.3)$$

Henry, in the 1930s, showed that by considering the effect of the particle shape and size on the electrical field, equations (2.2) and (2.3) could be combined to the following:

$$u_E = (2 \varepsilon \xi / 3 \eta) f(ka) \quad (2.4)$$

where f is a function that varies from 1 to 1.5 as ka varies from 0 to ∞ .

Electrophoresis involves migration of charged particles towards the electrical poles in an electrical field, based on their charges. In an identical environment, the most highly charged particles move farthest. Inside the electrical field matrix, molecules with the same size and charge all move the same distance, whereas different-size molecules move different distances. This concept applies to all electrically charged particles such as colloid clay particles in pore solution, organic particles, and droplets. These particles transfer the electrical charges and affect the electrical conductivity and the electroosmotic movement (Hunter, 1993).

Electrophoresis is an important mechanism in electrokinetic soil remediation when surfactant is added into the fluid to form micelles (charged particles) (Pamukcu and Wittle, 1992).

Electrophoresis movement can contribute to the transport of contaminants in the form of colloidal electrolytes or ionic micelles. Ionic micelles often carry a high charge and exhibit a high conductance in dilution. By increasing the concentration of surfactants, a build-up of charge occurs due to further aggregation and, as a result, the conductance increases (Pamukcu et al., 1995).

2-8) Coagulation

Colloidal coagulation is a complex process. It is governed by a number of factors such as colloid type, particle concentration, pH, coagulant concentration, particle size distribution, surface area, surface charge, interfacial reactions and collisions between suspended particles (Gregory, 1993).

From a mechanistic point of view, coagulation depends on two effects:

- a) Particles must move in such a way that collision occurs
- b) Interaction between colliding particles must be such that permanent contacts can be formed

The earliest, and still the only, quantitative analysis of colloid stability is the DLVO theory, developed independently by Derjaguin and Landau (1941) and Verwey and Overbeek (1948). Essentially, they combine the Van der Waals attraction (caused by dipole moments in the constituent molecules of two approaching colloidal particles) and the electrical double layer repulsion to give the total energy of interaction between particles as a function of the separation distance. All other types of interactions are ignored.

The attraction between colloidal particles can occur in any suspension medium. Molecules that have permanent dipoles attract one another strongly because the dipoles tend to align themselves. Even molecules with no permanent dipole are able to attract one another by London dispersion interaction. The fluctuating electron distribution around one atom or molecule produces a temporary dipole (Figure 2-12). The first dipole induces a dipole in the second atom (neighboring atom or molecule), which is oriented in exactly the same direction as itself. The first atom dipole generates and establishes an electric field through the surrounding space at the speed of light. Because of that field, the responding atom becomes slightly polarized and radiates a dipole field back to the first atom. The interaction of that field with the first atom produces the attraction. The strength of the attraction depends on the second field, on the way back to the first atom, finding it

has the same dipole orientation. If, in the meantime, the orientation of the dipole of the first atom has changed significantly, the interaction will be diminished (Hunter, 1993).

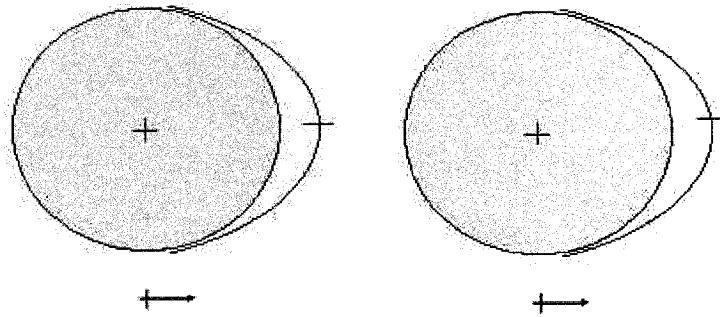


Figure 2-12 Temporary dipoles of atoms (Hunter, 1993)

There are two different coagulation rates, rapid and slow. When a colloid particle under goes rapid coagulation, the result is a very loose aggregate that contains a great deal of entrapped solvent. The flocs settle fairly quickly, and the volume of the sediment is very large. On the other hand, if the colloid particle under goes slow coagulation, the resulting flocs are denser. They settle more slowly and the volume of the sediment is much smaller.

When the colloid under goes coagulation, there is no repulsion between the particles and they attract one another very easily. In slow coagulation, two particles approach by a diffuse process and only if they are persistent enough can they overcome the potential energy barrier. Increasing the attractive force can enhance this process. Surmounting the energy barrier is easier for a particle when it moves in a direction that can interact with two particles at the same time, because the attractive forces are additive but the repulsive force is not much influenced by the other particle. The shape of the particles is also important; non-spherical particles can produce more dense flocs.

2-8-1) Fractal approach

The loose open structure of a colloidal floc can be explained using the mathematical concept of fractal. This term coined by Mandelbrot in 1975, is useful in a wide variety of areas. It promotes a deeper understanding of complex and disordered systems that have resisted conventional geometrical attempts to model them (Bushell et al., 2002). Fractal geometry is applied to many real systems and is used for the understanding of many physical phenomena (Namer and Ganczarczyk, 1994).

Fractal geometry can be applied as a measure for characterizing the structure of fine particles. The expression, which represents the concept of the fractal structure of aggregates, is as follows:

$$M \propto L^{D_f} \quad (2.5)$$

where M is the mass of particles, L is a linear measure of size, and D_f is the mass fractal dimension. The mass dimension is a useful method for estimating the fractal dimension of a given object (Barnsley et al., 1988). Fractal dimension is an important parameter in understanding the properties of colloidal aggregates. It is expected that the magnitude of the fractal dimension may be useful for estimating the history of aggregate formation (Namer and Ganczarczyk, 1994).

Particles produced through aggregation are highly amorphous, non-spherical and fractal, and have three-dimensional fractal dimensions that span a range of ~ 1.1 to the maximum of 3 (Bushell et al., 2002). A completely dense two-dimensional pattern would have a fractal dimension of 2. A lower fractal dimension means a more open aggregate structure. As the coagulation of solid particles proceeds, fluid is incorporated into pores in the new aggregates. Therefore, as the process continues, the aggregate density

decreases, and total aggregate volume increases. The result is that the collision diameters of the aggregates increase, and the rates of interparticle contact by Brownian diffusion, fluid shear, and differential sedimentation, increases (Hunter, 1993).

2-9) Surfactant

Synthetic surfactants are the largest class of anthropogenic organic compounds. Surfactants has been enhanced the recovery of oils from rocks. There are four mechanisms that may explain how the surfactants enhance the oil recovery: 1) the production of low interfacial tension between the oil and aqueous solution; 2) the spontaneous emulsification of the trapped oil; 3) the reduction of the rheological properties of the interfacial interface of the oil and aqueous solution; 4) control of the rock pores wettability to optimize oil displacement (Myers, 1992). The recovery of oil from petroleum wastes can be more effective when surfactant is used (Omar et al., 2002). Surfactants are able to enhance the removal of oil by means of two mechanisms: solubilization and mobilization.

The use of surfactants with electrokinetics in soil remediation is a new concept. The application of surfactant through electrokinetic technology probably takes advantage of electrophoretic flow in addition to electroosmotic flow (Elektorowicz and Hatim, 1999).

Properties of surfactants reflect their nature as amphiphilic chemicals. Surfactant molecules contain both strongly hydrophobic and strongly hydrophilic functions. The hydrophobic group is generally a hydrocarbon radical, and the hydrophilic portion can be an ionized or non-ionized entry, all resulting in the existence of anionic, cationic, amphoteric and nonionic surfactants.

When the concentration is low, surfactant molecules exist in the monomeric state in aqueous solution. As the concentration increases, they begin to associate, and eventually they reach the critical micelle concentration (CMC). The formation of this new phase enhances the solubilization of nonpolar organic solutes. This is the reason why surfactants can be used to clean up contaminated soil (Scamehorn and Harwell, 1988).

2-9-1) Anionic surfactants

Anionic surfactants carry a negative charge with the hydrophilic group. Most of them are high-foaming, but because they are sensitive to hard water, substances are added to them to complex calcium and magnesium ions (i.e., detergent builders) (Schmitt, 2001).

2-9-2) Nonionic surfactants

Nonionic surfactants contain a hydrophilic group without charge. Generally, the tolerance of nonionic surfactants to water hardness is more than that of anionic ones. The two types have different applications, such as being emulsifiers and detergents. Most of them are low-foaming products and are soluble in cold water. Their critical micelle concentration (CMC) is low, so they are effective at low concentration. They are also more common in industrial applications than are anionics (Schmitt, 2001).

2-9-3) Cationic surfactants

Cationic surfactants carry a positive charge with the hydrophilic group. Cationic surfactants are used as fabric softeners, corrosion inhibitors, and antimicrobial agents. They cannot provide effective cleaning at neutral pH, so they are not used in general purpose detergents. In pesticides and pharmaceuticals, only nitrogen-based compounds are used as cationic surfactants (Schmitt, 2001).

2-9-4) Amphoteric surfactants

Depending on the pH of the system, amphoteric surfactants can function either as anionic or cationic agents. Amphoteric surfactants have both anionic and cationic functions in one molecule. They are largely used in personal care products and their irritation is less than other materials. Amphoteric surfactants are less volatile than other surfactants (Schmitt, 2001). There are two main groups of amphoteric surfactants: betaines and real amphoteric surfactants based on fatty alkyl imidazolines. Their key functional groups are the more or less quaternized nitrogen and the carboxylic group.

Betaines are primarily used in personal care products, like, hair shampoos, liquid soaps, and cleansing lotions, other uses include all-purpose cleaning agents, hand dishwashing agents, and special textile detergents. Betaines are used for oil recovery of crude oil (Wagner, 1981) and enhanced petroleum recovery by flooding with betaine or amidobetaine microemulsions has been also described (Lomax, 1996). All betaines are characterized by a fully quaternized nitrogen. In alkyl betaines, one of the methyl groups in the 'betaine' structure (*N,N,N*-trimethylglycine) is replaced by a linear alkyl chain. Betaines are almost 100% biodegradable (Thalasso et al., 1999).

Choosing a surfactant requires following certain criteria, summarized as follow:

2-9-5) Solubility

The most important property of a surfactant is having water-soluble and oil-soluble groups in its molecule. Surfactant lipophile can be dispersed in non-polar or low-polar media because the bonding between the lipophiles is very similar to that in surfactants intermolecular bonding (Cain, 1994).

Solubility in polar media, especially water, depends on the similarity of intermolecular bonding between surfactant polar and nonionic hydrophils and between molecules of polar media or water. In water, hydrogen bonding is a critical factor.

Water solubility depends on the presence of ionic or nonionic water-soluble groups in the molecule. Nonionic groups will solubilize over essentially the entire pH range because they do not require counter-ions: hydrogen bonding between the hydrophilic and water molecules causes the solubility. Nonionic surfactants lose their solubility at high and low pH, and at high electrolyte levels because the electrolyte competes with the ethoxylate chain for hydrogen-bonded water. Amphoteric by having both anionic and cationic groups are soluble over a wide pH range, even wider than for nonionics (Figure 2-13).

pH	1	2	3	4	5	6	7	8	9	10	11	12	13	14
Anionic														
Nonionic														
Cationic (weak)														
Cationic (quat)														
Amphoteric														

Figure 2-13 Typical solubility ranges of surfactant types (Lomax, 1996)

The solubility of amphoteric, which have ionic groups, is not as limited. Amphoteric in their isoelectric (equal charge) areas have minimum solubility because of “tail-biting”

between their ionic groups (Figure 2-14). Depending on the relative strengths of the anionic and cationic groups, the pH of the isoelectric area may be as high as 9 or as low as 2 (Lomax, 1996).

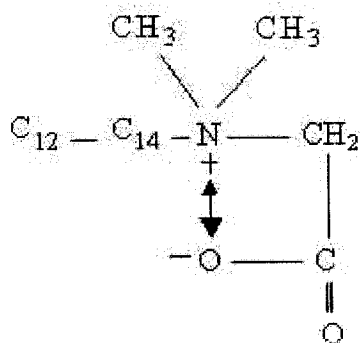


Figure 2-14 “Tail-biting “ in the isoelectric area

2-9-6) Adsorption

Because of the existence of both water-soluble and water-insoluble groups, surfactants tend to adsorb at interfaces like air-water, oil-water, and solid-liquid. This adsorption decreases the surface tension (or interfacial tension) until the interface is saturated with molecules. The surfactant tension of amphotericics varies with pH (Lomax, 1996).

2-9-7) Micelle formation

In Figure 2-15, the large unshaded area shows the ionic head group, and the small shaded area shows the hydrocarbon chain. If hydrophilic repulsion is smaller than hydrophobic attraction, then the CMC is low.

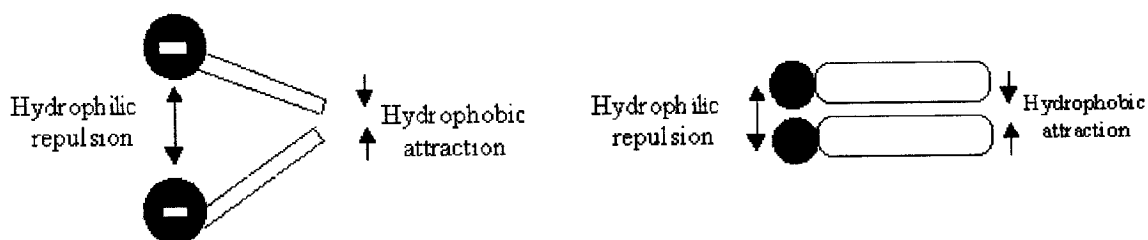


Figure 2-15 Relative sizes of hydrophilic and hydrophobic groups (Lomax, 1996)

The first micelles that form from ionic surfactants are spherical, with a diameter roughly twice that of the hydrocarbon chain length, and are formed at high CMCs. The reduction in repulsive forces between hydrophiles increases in the number of molecules in the micelle. This can cause closer packing of molecules within a spherical micelle that may follow a sphere-to-rod transition (Figure 2-16).

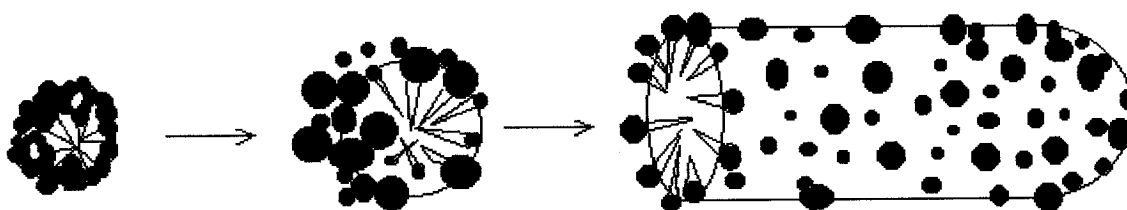


Figure 2-16 Schematic diagram of sphere-to-rod transition (Lomax, 1996)

Hydrophilic repulsion can be reduced in different ways such as by the effect of pH. At low pH, the hydrophilic repulsion decreases and the molecules aggregate more easily.

Sphere-to-rod transitions can cause considerable increase in viscosity (Figure 2-17). At higher concentrations, rods may adopt hexagonal packing. As the viscosity increases, eventually lamellar phases are formed and viscosity decreases again (Lomax, 1996).

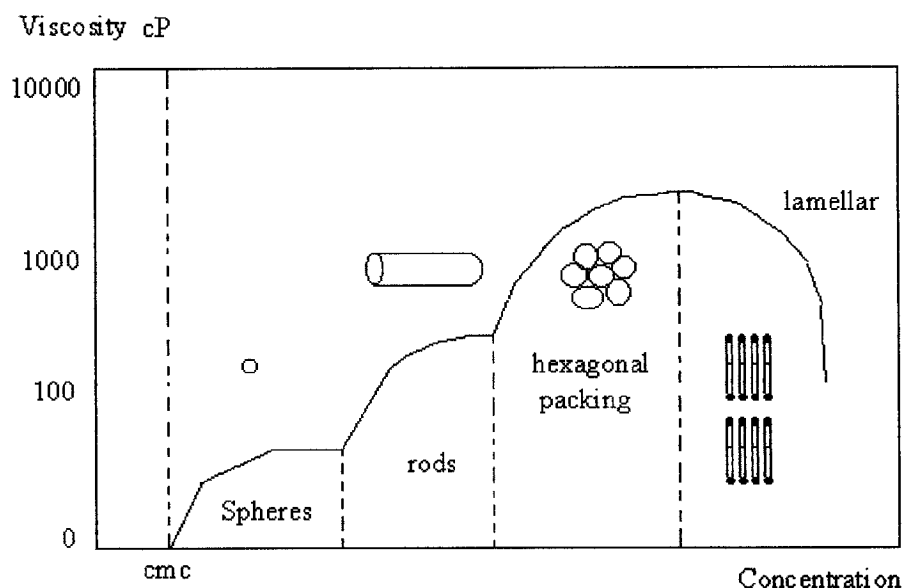


Figure 2-17 Viscosity vs. surfactant concentration, indicating micellar structures (Lomax, 1996)

2-9-8) Critical micelle concentration

Any factor, which increases hydrophilic repulsion, will increase the CMC. The lower the CMC, the less surfactant is needed. There is a close connection between CMC and solubility.

In amphoteric surfactants, the pH influences the solubility (Figure 2-18). At high pH, amphoteric surfactant acts as an anionic one with a cationic group that has negligible effect. As the pH decreases, the cationic group becomes more effective, and the influence of the anionic group weakens. The isoelectric area has the lowest solubility; below the isoelectric area the cationic group becomes powerful and CMC rises again (Lomax, 1996).

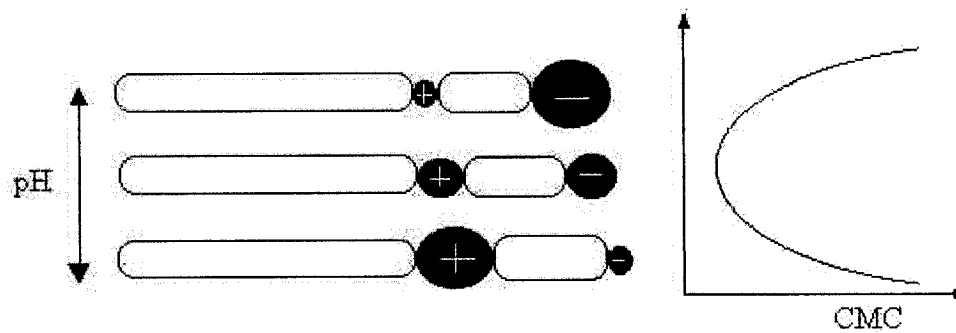


Figure 2-18 Schematic diagram of CMC vs. pH for an amphoteric surfactant (Lomax, 1996)

2-9-9) Electrokinetic transport

Under an electric gradient cationic micelles move in the same direction as the electroosmotic flow; the anionic micelles migrate in the opposite direction to the electroosmotic flow. Nonionic micelles will be transferred due to electroosmosis (Taha, 1996). By applying an electric field and creating a pH gradient, the amphoteric micelles migrate according to the polarity and their charges, until they reach the isoelectric point (Lomax, 1996).

Chapter 3

Experimental methodology

Figure 3-1 illustrates the experimental methods applied in this research. Each method of measurement will be discussed in detail. As mentioned in the literature review, electrokinetic phenomena have been used for phase separation in contaminated soil with diesel fuel (Norssair, 1996a and 1996b; Elektorowicz et al., 1995; Chifrina and Elektorowicz, 1998). In these investigations, the optimal concentration of 0.005 M was found for amphoteric surfactant. In the current experiment, the same surfactant with the same concentration was added to three cells to investigate its effect on the new system.

As mentioned in the literature review, betaines (a type of amphoteric surfactant) are useful in oil recovery. To study the effect of this type of additive under the effect of an electrical field, it was added to three cells. Two cells that contained only surfactant solution were intended to evaluate the characteristics of the solution under different electrical potential. Based on several investigations of electrokinetic remediation of contaminated soil, 0.5 Volt/cm potential was considered as the lowest electrical potential applied in the current experiment. To find out the effect of higher voltage, a 1.5 Volt/cm electrical potential was also applied. Two control cells without connection to DC current were also considered. The behaviors of sludge and a mixture of sludge and additive under the electric field were compared with those of the control cells during the experiment to find the impact of electrokinetics phenomena.

Oily sludges in refineries are collected in rectangular pools for further treatment or disposal. The same rectangular shape cell was designed as an electrokinetics cell for this experiment. In the refinery, using these pools as the electrokinetics cell could save

considerable amount of money. To increase the strength of the electric field, stainless steel sheet was used as electrodes.

The cap of each cell had a special design. For measuring the pH between electrodes, five holes were designed on the cap of each cell; these holes were also used for sampling. Two of the holes were located along the probe electrodes, which were used to measure the resistance changes within the cell. Using the same points for sampling and analysis increased the accuracy of the results, providing a better understanding the thermodynamics of the process.

Considering the above-mentioned factors, eight cells were used in this experiment. The cells differed in voltage and amount of surfactant. Table 3-1 provides a summary of each cell in this experiment.

Table 3-1 Summary of cells

Cell No.	Symbol	Volt / cm	Cell content
1	S	-	Sludge (control cell)
2	SA	-	Sludge + Surfactant (control cell)
3	AE(1.5)	1.5	Surfactant
4	SE(1.5)	1.5	Sludge
5	SAE(1.5)	1.5	Sludge + Surfactant
6	AE(0.5)	0.5	Surfactant
7	SE(0.5)	0.5	Sludge
8	SAE(0.5)	0.5	Sludge + Surfactant

3-1) Experimental installation and cell configuration

To provide a correct analysis of the distribution of the electrical and chemical properties in the space between the electrodes, all cells had the same dimensions of $l = 25$ cm, $w = 14.5$ cm and $h = 10.5$ cm. Chemical resistance of cell material to sludge components, simplicity, and accuracy of sludge sampling during the experiment were all considered when designing the cell. Cells made of rigid polyethylene were subsequently used. To obtain a uniform distribution of electrical field in different sections of cell, two plates of $12 \times 10 \times 0.2$ cm (stainless steel 304) were used as electrodes. The distance between adjacent electrodes was 19.5 cm.

Five holes were cut in the cap of each cell for sampling and pH measurement. To study continuous changes in sludge physical properties during the electrokinetic phase separation, the cells were equipped with probe electrodes. Therefore, 10 silver probe-electrodes in two vertical lines, 6.5 cm from electrodes, were installed. The distance between two probe-electrodes in each line was 1.5 cm. Each probe electrode was inserted 2.75 cm inside the cell. Figure 3-2 illustrates the sketch of the cells. The electrical parameters were measured along those two vertical lines between anode and cathode. The voltage distribution between the electrodes was monitored by direct measurements of the electrical potential difference between the electrodes and each probe-electrode. In addition, the configuration of the cell cap permitted measurement of the electrical parameters in the same section as the pH was measured.

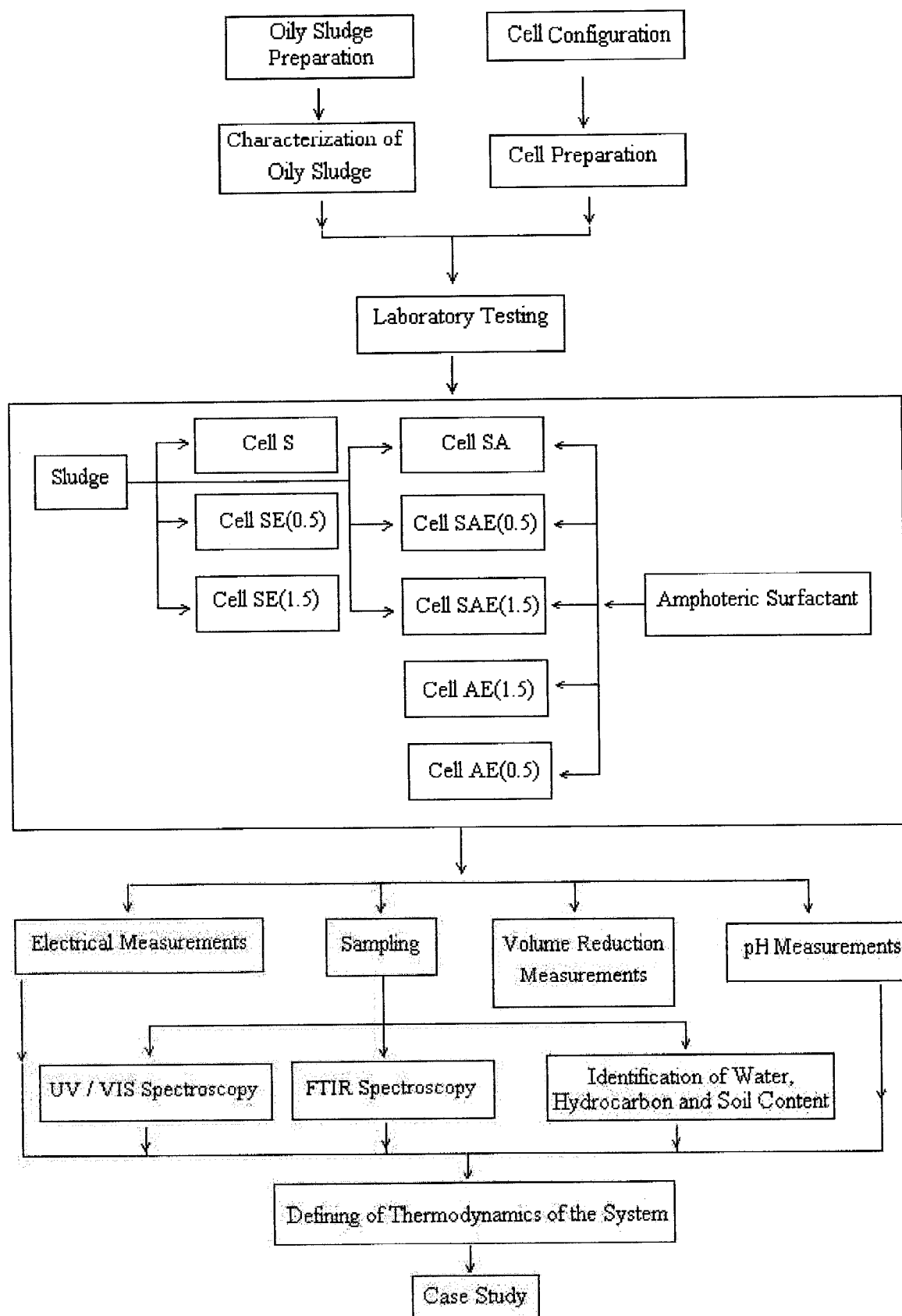


Figure 3-1 Experimental methodology

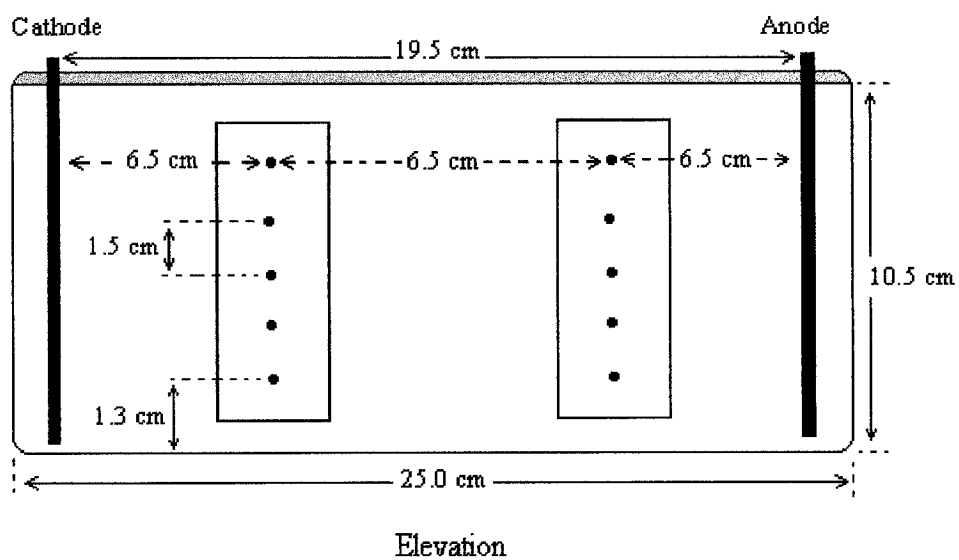
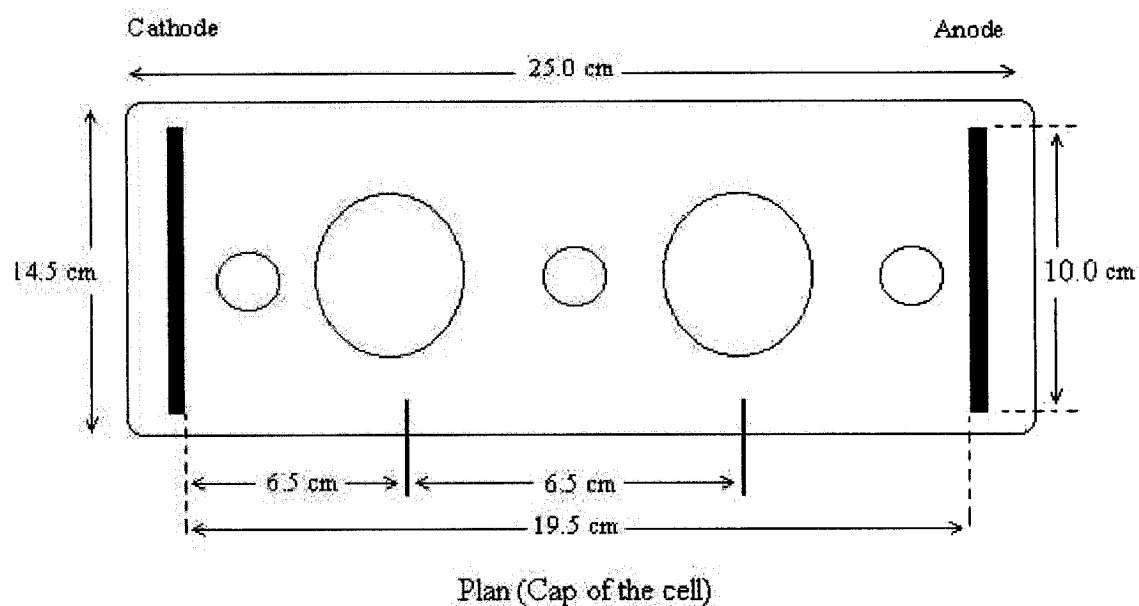


Figure3-2 Configuration of electrokinetic cell

3-2) Apparatus, reagents and equipment

This section provides a summary of installations and equipment used in the experiment and analysis.

❖ Apparatus and Experimental Setup

- 16 stainless steel (304) plate electrodes (12 x10 x 0.2 cm)
- 80 silver probe electrodes (D = 0.1 cm)
- 1500 of 20 ml glass vials
- DC power supply (ANATEK, 25-2D)
- Digital multimeter (Mastercraft)
- Glass container
- Heater (Fisher stirring hotplate)
- Reflux condenser
- Glass receiver
- Graduated glass trap

❖ Reagent

- 0.005 M surfactant (prepared from C12-C14-Alkyl-Dimethyl-Betain with
CMC = 0.009 M)
- Hexane
- Benzene

❖ Measurements and Analysis

- Mechanical shaker (AROS 160)
- pH meter (Fisher scientific, AR25)
- Dry keeper (SANPLA)

- UV/ VIS Spectrometer (Perkin Elmer, Lambda 40)
- FTIR (Nagna, Nicolet)

3-2-1) Initial oily sludge

The initial oily sludge for this experiment was supplied by Shell Canada Refinery in Montreal. It was taken from the bottom of a crude oil storage tank.

3-3) Characteristics of oily sludge before and after the experiment

3-3-1) Parameters measured

As mentioned in the litterateur review, oily sludge is a mixture of different kinds of hydrocarbons (aliphatic and aromatic), light and heavy fractions, water, soil, and suspended materials including minerals, metals, and the like. The sludge used in this experiment came from the bottom of the crude oil storage tank, and it was not in contact with air so it was expected to contain a significant amount of light hydrocarbons. The following fractions were assessed for the sludge:

- Water content
- Volatile hydrocarbons content
- Non-volatile hydrocarbons content
- Solids content

3-3-2) Water content

Standard method ASTM D95 was used for measuring the water content of the oily sludge. This distillation method determines water content in the range from 0 to 25 % volume in petroleum products, tars, and other bituminous materials.

The apparatus, Figure 3-3, comprises a glass container, a heater, a reflux condenser, a receiver, and a graduated glass trap. The connections between the glass container, trap and receiver were leak-proofed.

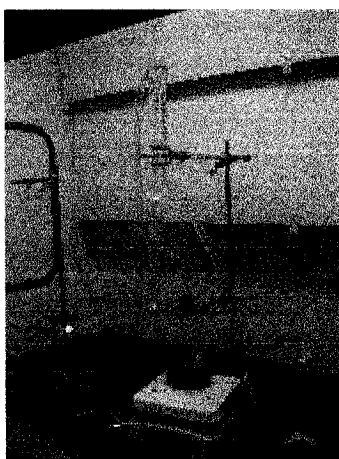


Figure 3-3 Distillation apparatus

The oily sludge was heated with benzene as solvent, which co-distilled with the water in the sample; condensed solvent and water were continuously separated in a trap, the water settling as the bottom layer.

Around 25 g of sample were placed in the glass container, and 25 milliliter of benzene was added. The container was agitated for 2 minutes and then connected to the system, as shown in Figure 3-3. The mixture was heated to the boiling point. The rate of boiling was adjusted so that the condensed distillate discharged from the condenser at the rate of two to five drops per second. Heating was continued until no more condensation was

observed. The system was cooled to room temperature and any drops of water adhering to the sides of the trap were dislodged and transferred to the water layer.

The condensed liquid containing water and hydrocarbons was transferred to a graduated cylinder; the water, being the more dense settled to the bottom. The volume of the water was used to calculate the weight-percent water content of the sample as follows assuming a water density of 1g/cm^3 .

Water % w =

$$\{[\text{Weight of water in trap} - \text{Weight of water in benzene}]/(\text{Weight of tested sample})\} \times 100\%$$

3-3-3) Light hydrocarbon content

To find the amount of light hydrocarbons in the oily sludge, a weighed sample was heated in a ventilated oven at $105\text{ }^{\circ}\text{C}$ for 24 hours. The loss in weight indicated the moisture and light hydrocarbon content of the sludge. Because the water content was measured before heating, the light hydrocarbon content was calculated as follows:

Light hydrocarbon % w =

$$\{[(\text{Change in weight}) / (\text{Weight of tested sample})] \times 100\% - (\text{water content, \%w})\}$$

3-3-4) Solids content

Dried samples ($105\text{ }^{\circ}\text{C}$) were heated in a furnace at $550\text{ }^{\circ}\text{C}$ for half an hour. The residue represented the solids content of the sludge as weight percent:

Solid % w =

$$[(\text{Residue remaining after } 550\text{ }^{\circ}\text{C, g}) / (\text{Weight of tested sample, g})] \times 100\%$$

3-3-5) Non-volatile hydrocarbon content

After measuring the water content, light hydrocarbon content, and solid content, the non-volatile hydrocarbon content was calculated as weight percent as follows:

Non-Volatile hydrocarbon % w =

$$100 \% - (\text{Light hydrocarbon, \% w} + \text{Solid, \% w} + \text{Water content, \%w})$$

3-4) Surfactant preparation

In this experiment, C12-C14-Alkyl-Dimethyl-Betain (Gen) was used; this is an amphoteric surfactant with a molecular weight of 327 g/mol and a density of 1.05 g/l. To prepare 0.005 M surfactant, 4.905 g of the surfactant and 3 liters of tap water were transferred to a 4-liter glass container and shaken for 4 hours.

3-5) Cell preparation procedures

This section shows the preparation of each cell as defined in the following:

Cell S (Sludge): 1.5 liter of initial oily sludge was poured into cell S without initial preparation. This cell had no electrical connection.

Cell SA (Sludge, Amphoteric Surfactant): The mixture of 1 liter of sludge and 500 ml of 0.005 M Gen (Amphoteric Surfactant) was shaken for 4 hours at 75 rpm. This mixture was poured into Cell SA. This cell had no electrical connection.

Cell AE (1.5), (Amphoteric Surfactant, 1.5 Volt / cm): This cell contained 1.5 liter of 0.005 M Gen without sludge. The applied voltage gradient for this cell was 1.5 Volt per cm.

Cell SE (1.5), (Sludge, 1.5 Volt / cm): This cell contained 1.5 liter of initial sludge without surfactant. The voltage was 1.5 volt per cm.

Cell SAE (1.5), (Sludge, Amphoteric Surfactant, 1.5 Volt / cm): 1 liter of sludge plus 500 ml of 0.005 M Gen was shaken for 4 hours at 75 rpm and was poured in this cell. The applied voltage was 1.5 Volt per cm.

Cell AE (0.5), (Amphoteric Surfactant, 0.5 Volt / cm): This cell contained 1.5 liter of 0.005 M Gen without sludge. The applied voltage for this cell was 0.5 Volt per cm.

Cell SE (0.5), (Sludge, 0.5 Volt / cm): This cell contained 1.5 liter of initial sludge without surfactant. The applied voltage was 0.5 Volt per cm.

Cell SAE (0.5), (Sludge, Amphoteric Surfactant, 0.5 Volt / cm): 1 liter of sludge plus 500 ml of 0.005 M Gen was shaken for 4 hours at 75 rpm and was poured in this cell. The applied voltage was 0.5 Volt per cm.

3-6) Duration of experiment

After the cells were prepared, six of them were connected to the electrical power supply. Two cells were considered as control cells (S, SA). After 32 days, the electricity was disconnected, but cells remained untouched for further observation of electrokinetic processes. After 75 days, the liquid phase and solid phase were separated in different containers and kept for future analysis.

3-7) pH measurement procedure

The pH value has a significant influence on surface tension and can indicate the characteristics of different components in the system. The pH of each cell was measured at five points, both top and bottom (Figure 3-2). During the experiment, the distance

between the top and bottom decreased due to evaporation and movement of particles between electrodes. Therefore, the volume of sludge changed, and it was different in each cell during the 75 days. During the first 24 hours the pH was measured twice; after that, it was measured once a day. After disconnecting the electric current, the pH was measured every two days. The pH of the control cells was measured once a week.

3-8) Electrical parameters

The electrical current (I) in each cell and the electrical potential (V) between cathode and each probe electrode were measured daily. The resistance was calculated from Ohm's formula:

$$R = V/I \quad (3.1)$$

where R = resistance (Ohm), V = electrical potential (V), and I = electrical current (A)

3-9) Sampling procedures during the experiment

Based on the results from daily pH and resistance measurements, sampling of sludge took place on certain days as summarized in Table 3-2.

Samples were taken from the top and the bottom of each cell through the five holes in the cap. Each sample was placed in a 20 ml vial. After measuring the weight of each sample, 8 ml of hexane was added, shaken manually for 1 min, and left standing for 24 hours. Then the liquid part was poured into another 20 ml vial. The remaining solid was air-dried in a fume hood for 48 hours. Then the caps were sealed and samples were kept for FTIR analysis. The liquid part was stored for UV/VIS analysis.

Table 3-2 Schedule of sampling

Cell	Sampling points top and bottom	Day of Sampling	Connection to DC	No. of samples
SE(1.5), SAE(1.5), AE(1.5) ,SE(0.5), SAE(0.5), AE(0.5)	2 x 5 points	24 th	On	60
S, SA	2 x 3 points	24 th	On	12
SE(1.5), SAE(1.5), AE(1.5) ,SE(0.5), SAE(0.5), AE(0.5)	2 x 5 points	32 nd	On	60
S, SA	2 x 3 points	32 nd	On	12
SE(1.5), SAE(1.5), AE(1.5) ,SE(0.5), SAE(0.5), AE(0.5)	2 x 5 points	39 th	Off	60
S, SA	2 x 1 points	39 th	Off	4
SE(1.5), SAE(1.5), AE(1.5) ,SE(0.5), SAE(0.5), AE(0.5)	2 x 5 points	46 th	Off	60
S, SA	2 x 1 points	46 th	Off	4
Total samples taken				274

3-10) UV/VIS analysis

As mentioned already, the liquid part was considered for aromatic hydrocarbon content by means of UV/VIS analysis. More hexane was used for dilution of each sample to achieve acceptable peaks between 500 nm and 190 nm, which were attributed to the aromatic hydrocarbons. For all samples, three different peaks were visible in this area. To

compare the hydrocarbon content between samples, the absorbance of the p⁺ peak at 224 nm was used.

The following equations were applied:

$$C = (W / L) * D \quad (3.2)$$

where:

W = weight of sample (g)

L = initial hexane volume that was added after sampling (8 ml)

D = dilution factor

C = concentration (mg/l)

$$A_{\lambda} = a_{\lambda} b C \quad (\text{The Beer-Lambert Law}) \quad (3.3)$$

where:

a_{λ} = absorptivity coefficient of wavelength λ

λ = wavelength (240 nm)

b = path length (1 cm)

C = concentration (mg/l)

A_{λ} = absorbance

“a” and “b” were equal for all samples so their multiplications were considered a constant (K).

$$K = a_{\lambda} b = A_{240} / C \quad (3.4)$$

3-11) FTIR analysis

This experiment has been used mostly for aliphatic hydrocarbon analysis. The solid part of each sample, after drying for 48 hours in the fume hood, was used for FTIR

analysis. A portion of dried sample was mixed with potassium bromide (KBr), and compacted under pressure (9 bar) for 6 min. This compacted sample was analyzed by FTIR spectrometer. Acceptable peaks were found by changing the amount of KBr. The area between 4000 cm^{-1} to 500 cm^{-1} was studied; different peaks were observed, and three peaks at 1635 cm^{-1} , 1462 cm^{-1} and 1034 cm^{-1} were considered. The peak at 1462 cm^{-1} was attributed to deformation vibrations of the CH bond in aliphatic components and the peak at 1034 cm^{-1} to Si-O stretch vibrations in soil. It is assumed that the absorbance of the second bond depends on the concentration of soil in the sample, so this bond can be used for normalization procedure. The peak at 1635 cm^{-1} was assigned to OH deformation vibrations. These peaks were used to compare the aliphatic hydrocarbon content between samples, according to the following equation.

$$A_{\nu} = a_{\nu} b C \quad (\text{The Beer-Lambert Law}) \quad (3.5)$$

where:

a_{ν} = absorptivity coefficient of wavelength ν

ν = wavelength (cm^{-1})

b = path length of the sample

C = concentration (mg/l)

A_{ν} = absorbance

$$K_1 = A_{1635} / A_{1034} \quad (3.6)$$

$$K_2 = A_{1462} / A_{1034} \quad (3.7)$$

K_1 was almost constant for all samples; an average amount of K_1 for all samples of each cell in each day of sampling was defined as follows:

$$K_{1-ave} = (K_{1-1} + K_{1-2} + \dots + K_{1-N}) / N \quad (3.8)$$

where:

N = number of samples

K_{1-ave} was used to find a correction factor for K_2

$$K'_1 = K_{1-ave} / K_1 \quad (3.9)$$

$$K'_2 = K_2 * K'_1 \quad (3.10)$$

K'_2 changes in each sample, and shows a comparison between aliphatic hydrocarbon content in solid phase in different points of each cell.

3-12) Fractal analysis

To determine the difference between the structures of the remaining solid phase, the fractal analysis for each cell was performed. 2-dimensional sampling was carried out using 1- ml glass pipette. Samples varied in height and weight with the same surface area. Sampling was performed after 75 days of the experiment. The following equation was used to calculate the fractal dimension.

$$M \propto L^{D_f} \quad (3.11)$$

where

M = mass of the sample

L = two-dimensional size of the sample

D_f = fractal dimension

Chapter 4

Results

This section deals with the presentation of results from this experiment. Results related to electrical, physical, and chemical parameters led to accurate conclusions. To assess the thermodynamics of the proposed process as well as quantification of the separated phases, several parameters were measured during the experiment, such as electrical values and pH. Changes in the resistance and pH along the system permitted the evaluation of the colloidal behavior in each cell in the top and bottom. By using FTIR and UV spectrometry, behaviors of aliphatic and aromatic hydrocarbons under the influence of an electrical field were assessed.

Both vertical and horizontal movements were observed within the experimental system. Break down of the colloidal aggregates occurred under the influence of the electrical field, so the process is called electro-demulsification. This action took place in the y-axis in the vertical direction. Colloidal particles of oily sludge and separated solid phase were moving toward the anode area as a result of electrophoresis forces, and the separated liquid phase, which consisted of water and hydrocarbon, flowed toward the cathode area as a result of electro-osmosis forces. These movements took place in the horizontal direction (Figure 4-1).

Following electro-demulsification, the separated solid phase, which consisted of heavy hydrocarbons like asphaltine, mineral particles and metals, started to aggregate near the anode area. This action is called electro-coagulation.

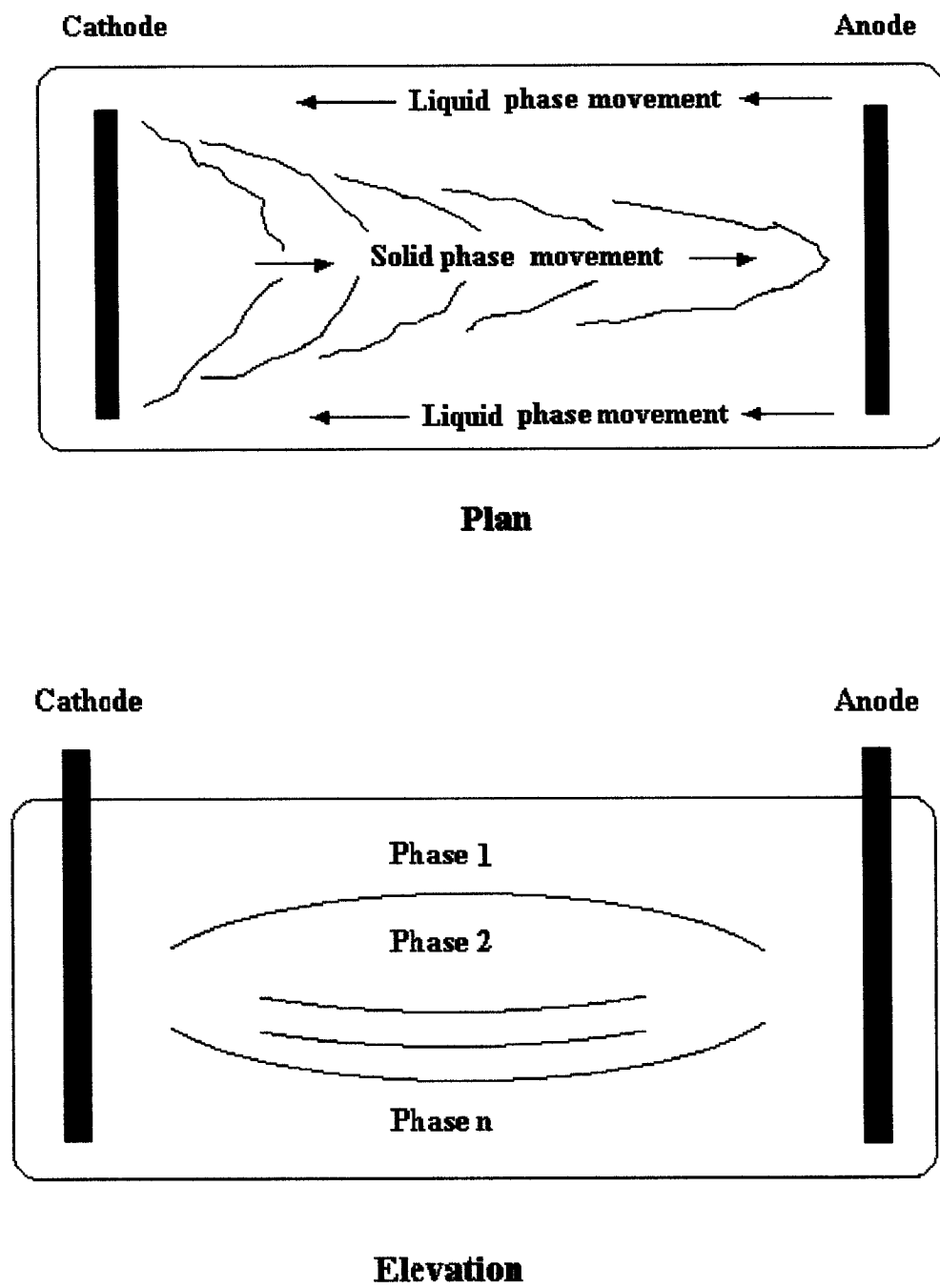


Figure 4-1 Different movements and creation of phases during the experiment

4-1) Different fractions in oily sludge

This test was performed on initial oily sludge before the experiment, and on the remaining solids after the experiment. After 75 days of the experiment, separated liquid and solid phases were stored individually in different containers. The samples for this test were taken from these containers. The results obtained from the test are summarized in Appendix A. Water content in the benzene (solvent) was negligible. Table 4-1 shows the description of samples that were characterized.

Table 4-1 Samples description

Sample #	Description
1	Initial oily sludge
2	Separated solid phase from cell SE (0.5)
3	Separated solid phase from cell SE (1.5)
4	Separated solid phase with amphoteric surfactant from cell SAE (0.5)
5	Separated solid phase with amphoteric surfactant from cell SAE (1.5)

The weight percentages of different fractions of the samples from Table 4-1 are presented in Figures 4-2 through 4-6. The results indicate that application of electrokinetics reduced the amount of water by almost 63 % and light hydrocarbon content by almost 43 % in the solid phase. Electrokinetics in combination with amphoteric surfactant achieved a 60 % reduction in water content and 50 % in light hydrocarbon in the solid phase. Variation of electrical potentials did not have a significant effect on the system.

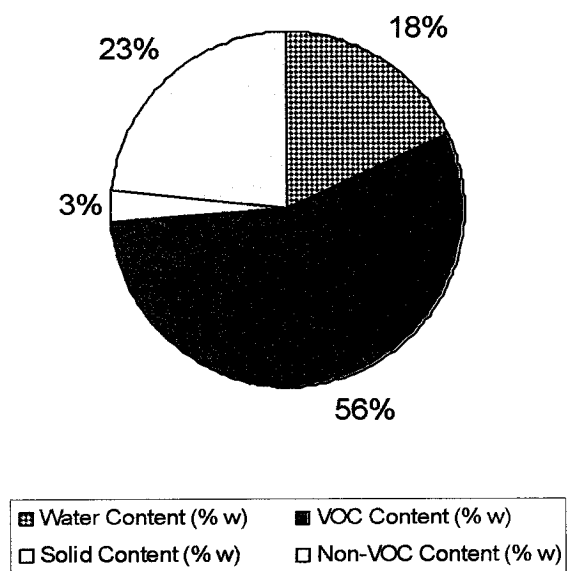


Figure 4-2 Initial sludge

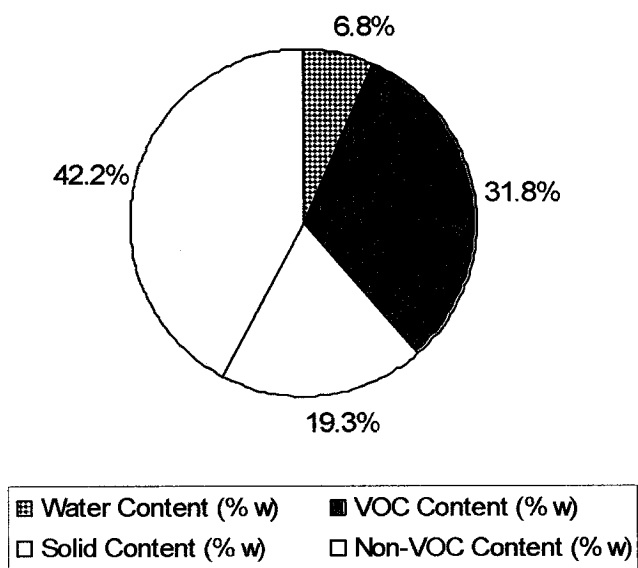


Figure 4-3 Electrokinetics separated solid phase - cell SE (0.5)

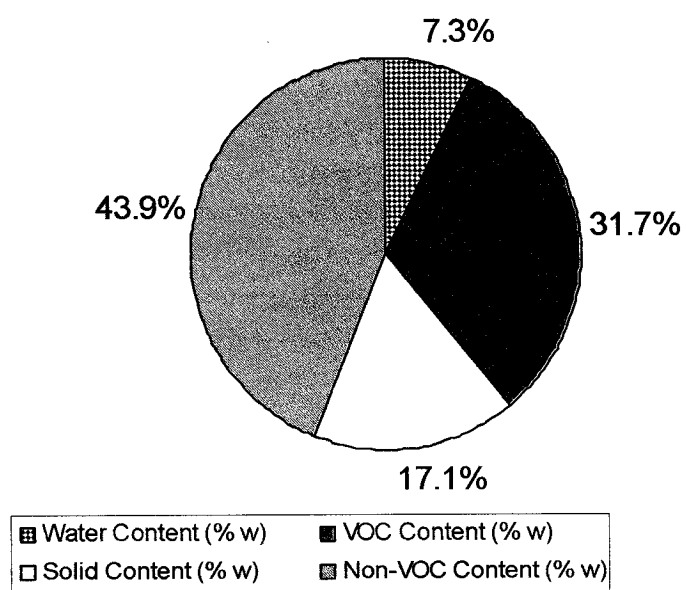


Figure 4-4 Electrokinetics separated solid phase - cell SE (1.5)

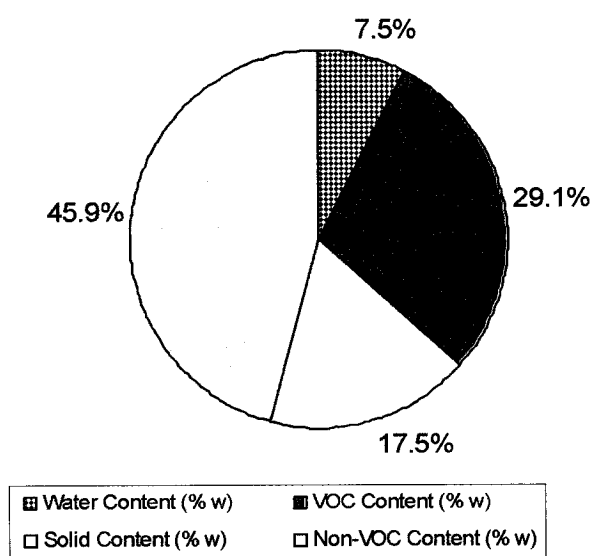


Figure 4-5 Electrokinetics separated solid phase with amphoteric surfactant
cell SAE (0.5)

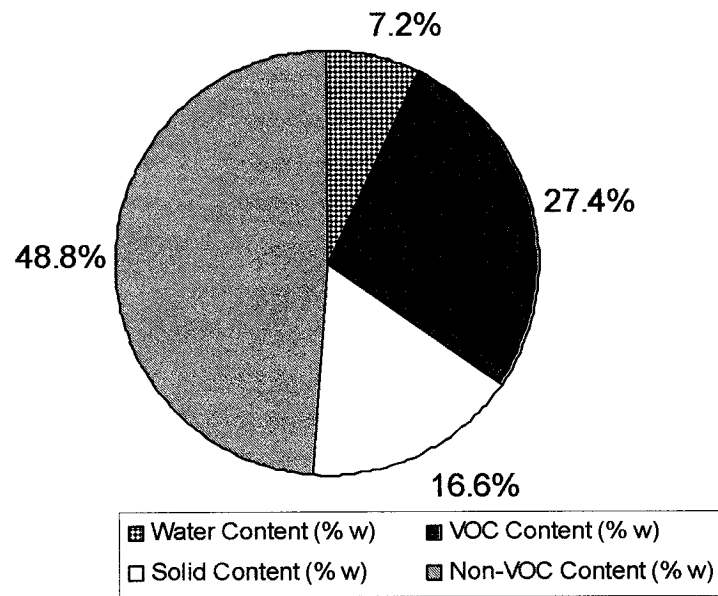


Figure 4-6 Electrokinetics separated solid phase with amphoteric surfactant
cell SAE (1.5)

4-2) Volume reductions in the cells

Changes within the volume were measured every two days during the experiment. In this respect, the sludge level changes were marked on the wall of electrokinetic cells and volume calculated. Table 4-2 shows the average volume reduction for each cell; this reduction could be as a result of separation of liquid and solid in the sludge due to electroosmotic and electrophoretic phenomena.

As mentioned already, probe-electrodes (Figure 3-2) were installed in two vertical lines in the middle cathode and the middle anode areas of each cell. Three probes were submerged in sludge, showing top, middle, and bottom electrical conditions. As time

progressed, the third probe came out of sludge (or liquid) due to evaporation and changes of volume. The rate of evaporation in each cell was found to be different.

Table 4-2 Volume reduction rate

Cell	Volume reduction rate (ml/day)
S	11.1
SA	9.3
SE (1.5)	22.2
SAE (1.5)	27.1
SE (0.5)	25.0
SAE (0.5)	24.0

4-3) Electrical parameters

The potential at each probe, and the electrical current supplied in each cell, were measured daily. The voltage between two electrodes in cells AE (1.5), SE (1.5), and SAE (1.5) was set at 29.2 Volt (1.5 Volt per cm distance between cathode and anode) and in cells AE (0.5), SE (0.5), and SAE (0.5) it was set at 9.7 Volt (0.5 Volt per cm distance between cathode and anode). The resistance and its variation for each probe versus time for different cells are displayed graphically in Figures 4-7 through 4-12.

4-3-1) Electrical changes in cells with surfactant only

4-3-1-1) Cell with higher voltage - AE (1.5)

Figure 4-7 shows the resistance changes in the cell without sludge with higher voltage - AE (1.5). The difference between the resistances near the cathode and the anode was

approximately the same, and notable changes in resistance did not occur in any of days. After day 25, small changes in resistance in both sides of the cell were observed, but mostly in the anode area. This could be as a result of the formation of Fe^{3+} because of electrolysis of electrodes in that area.

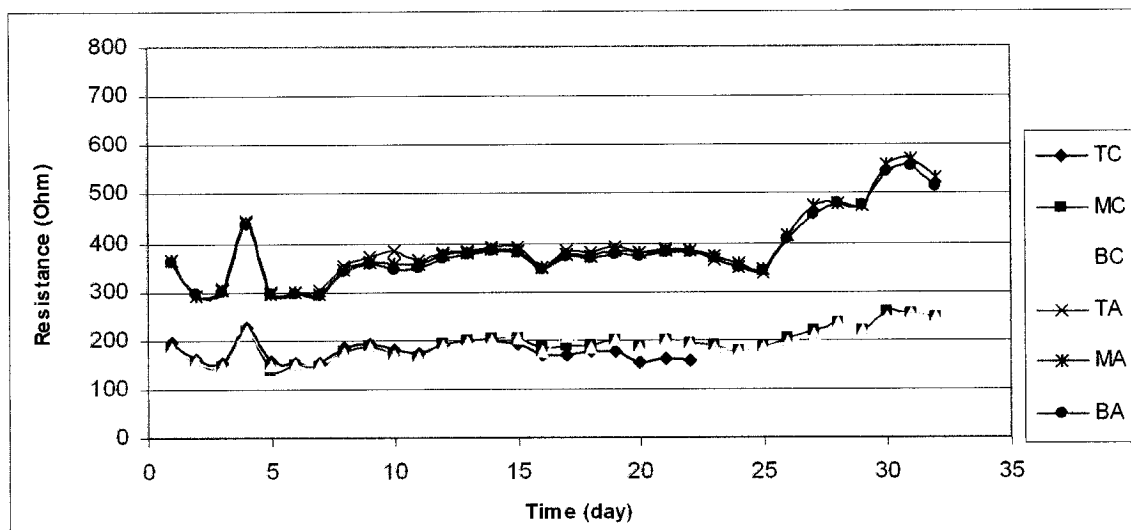


Figure 4-7 Resistance changes in cell AE (1.5)

*Note: TC= top of cathode area, MC = middle of cathode area, BC= bottom of cathode area, TA= top of anode area, MA= middle of anode area, BA= bottom of anode area.

4-3-1-2) Cell with lower voltage - AE (0.5)

Figure 4-8 shows the resistance changes in the cell without sludge and with lower voltage - AE (0.5). The difference between the cathode and the anode values was almost the same over 32 days of the experiment. Changes in resistance in the anode area were more than those in the cathode area, possibly the result of formation of Fe^{3+} in that area.

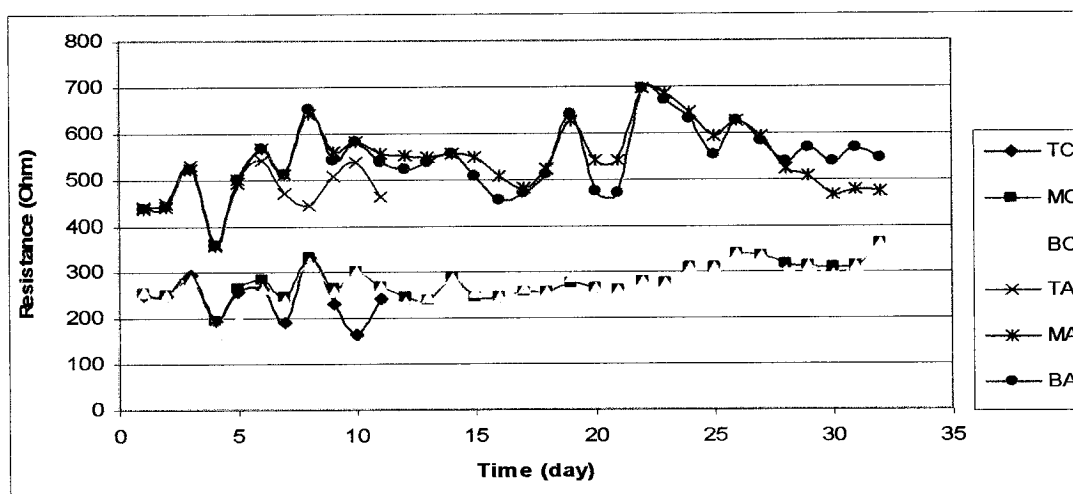


Figure 4-8 Resistance changes in cell AE (0.5)

*Note: TC= top of cathode area, MC = middle of cathode area, BC= bottom of cathode area, TA= top of anode area, MA= middle of anode area, BA= bottom of anode area.

4-3-2) Resistance changes in cells containing sludge

4-3-2-1) Cell with higher voltage - SAE (1.5)

Figure 4-9 illustrates the changes in resistance versus time in cell SAE (1.5). As a result of the surfactant existence, in the first 14 days, the changes in resistance between anode and cathode area in the cell were not remarkable. It could be assumed that the rate of vertical electro-separation was higher than the rate of horizontal forces. From day 14 onwards, solid particles began to accumulate near the anode, and rate of horizontal movements started to exceed vertical movements, so the resistance increased quickly (slope of 1: 0.714). There were few changes in resistance of the cathode area because, as a result of electrophoresis, particles moved toward the anode area and water and hydrocarbon accumulated in that area. After day 25, small increment in resistance was observed in the cathode area, perhaps the result of evaporation of the separated water phase. The highest resistance value in this cell -in the anode area- was almost 3100 Ω , the

highest value reported for all cells. The behavior in resistance in the anode area can be best described by equation (4.1)

$$R = 69.062 \exp (0.1174 t) \quad \text{with } r^2 = 0.95 \quad (4.1)$$

and in the cathode are by equation (4.2)

$$R = 26.685 \exp (0.1051 t) \quad \text{with } r^2 = 0.94 \quad (4.2)$$

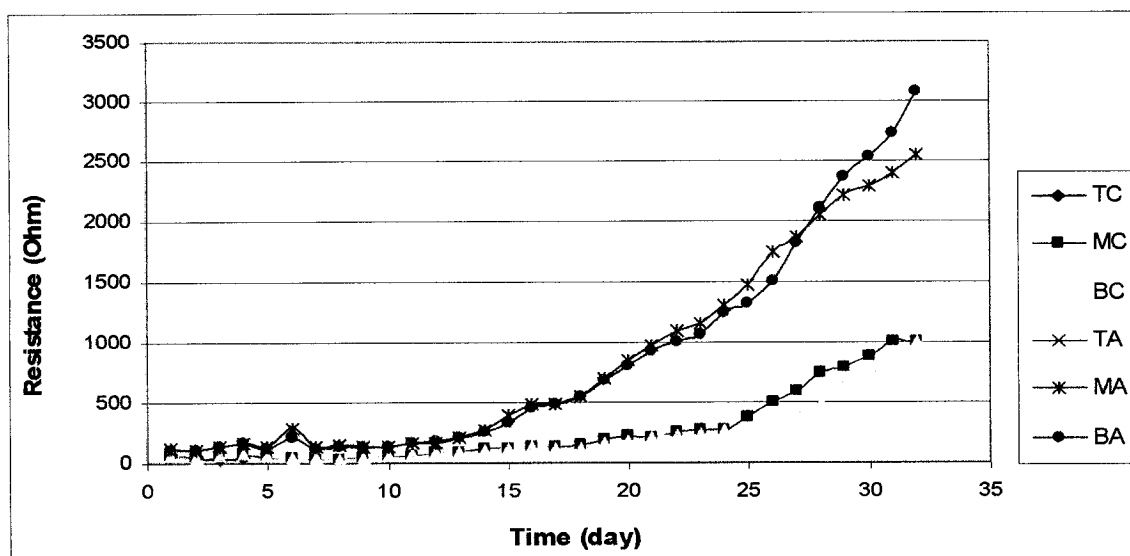


Figure 4-9 Resistance changes in cell SAE (1.5)

*Note: TC= top of cathode area, MC = middle of cathode area, BC= bottom of cathode area, TA= top of anode area, MA= middle of anode area, BA= bottom of anode area.

4-3-2-2) Cell with lower voltage - SAE (0.5)

Figure 4-10 shows the resistance changes in cell SAE (0.5) versus time. Over the first 22 days, the resistance in the anode area increased very slowly. Because of the low electrical potential and presence of surfactant, the rate of electro-separation during the 22 days was higher than horizontal movements. A lower electrical potential helped the system to separate the phases slowly and continually, so postponing the sharp increment

in resistance to day 22. After day 22, the resistance increment observed near the anode area was due to accumulation of solid particles in that area, as well as higher rate of horizontal movements. As illustrated in Figure 4-10, during most days, the resistance of the middle point of the anode area was higher than of the bottom points. It could be as a result of electro-osmotic movements of liquid phase from bottom of the cell. This higher quantity of liquid in the bottom decreased the viscosity and resistance of the bottom point compared with values at the top and middle points. In the anode area, resistance increased by a slope of 1: 0.88, while changes in resistance were not significant in the cathode area. Lower resistance in the cathode area can be attributed to the movement of liquid toward the cathode.

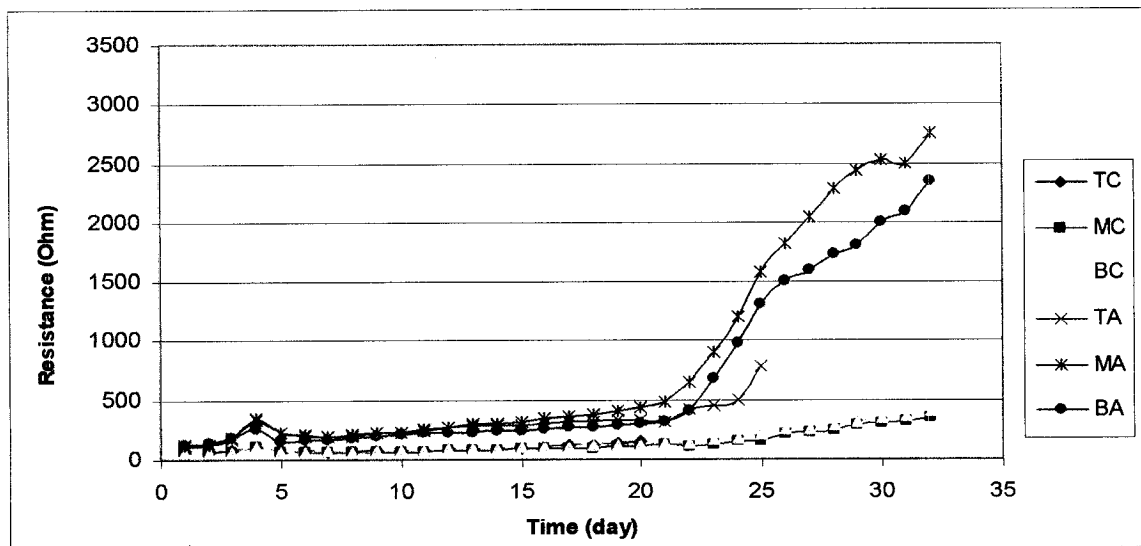


Figure 4-10 Resistance changes in cell SAE (0.5)

*Note: TC= top of cathode area, MC = middle of cathode area, BC= bottom of cathode area, TA= top of anode area, MA= middle of anode area, BA= bottom of anode area.

Behavior of the resistance in the anode area can be best described by equation (4.3)

$$R = 91.995 \exp(0.0955 t) \quad \text{with } r^2 = 0.87 \quad (4.3)$$

and in the cathode by equation (4.4)

$$R = 44.855 \exp (0.058 t) \quad \text{with } r^2 = 0.88 \quad (4.4)$$

4-3-2-3) Cell without addition of surfactant, higher voltage - SE (1.5)

Figure 4-11 shows the resistance changes in cell SE (1.5). Neither surfactant nor water was added to this cell, so the sludge was more viscous. From day 2 of the experiment, a solid phase formed near anode, so the resistance began to increase. The rate of this formation was slow until day 9; from then until day 19, this rate increased (slope 1: 0.81). Between days 4 and 9, the amount of liquid, which was separated by vertical forces, increased so no significant changes in resistance occurred in the anode area. At this time, rate of vertical movements was much faster than horizontal movements. After day 9, the rate of horizontal movement of separated liquids toward the cathode increased, so more liquid abandoned the anode area and the resistance there increased quickly. From day 20 to day 32, again near the anode, a vertical separation produced some liquids. If the electricity had not been disconnected, this amount of the liquid also could have moved toward the cathode. That is why, during the sampling and after disconnection, some liquids were detected near the anode. As illustrated in the Figure 4-10, the difference between anode and cathode values increased by the time because most of the solid parts had accumulated in the anode area and most of the liquid parts had accumulated in the cathode area. The highest value of the resistance in this cell was almost 1600 Ω , which was nearly 50 percent of the highest value in the cell SAE (1.5), which had the same voltage and contained amphoteric surfactant. Behavior of the resistance in the anode area can be best described by equation 4.5,

$$R = 73.292 t^{0.9348} \quad \text{with } r^2 = 0.93 \quad (4.5)$$

and in the cathode by equation 4.6.

$$R = 39.819 t^{0.6545} \quad \text{with } r^2 = 0.83 \quad (4.6)$$

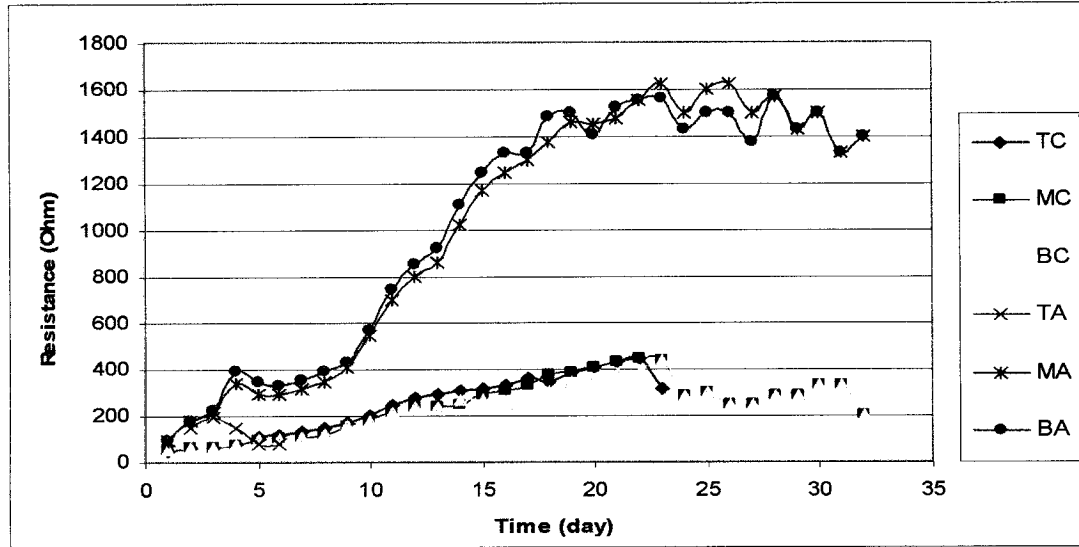


Figure 4-11 Resistance changes in cell SE (1.5)

*Note: TC= top of cathode area, MC = middle of cathode area, BC= bottom of cathode area, TA= top of anode area, MA= middle of anode area, BA= bottom of anode area.

4-3-2-4) Cell without addition of surfactant, lower voltage - SE (0.5)

Figure 4-12 shows the resistance changes in cell SE (0.5). This cell contained only oily sludge (without additive). Vertical separation and horizontal movements of phases between electrodes are clearly shown. The changes in resistance in the cathode area were not remarkable, but in the anode area the resistance was increasing and decreasing periodically.

During the first two days, vertical separation of phases occurred, so the resistance was almost constant. Separated water and liquid hydrocarbon moved toward the cathode by electro-osmotic phenomena, and separated particles moved toward the anode area by electrophoretic phenomena; therefore, near the anode the amount of solid increased until day 4, causing higher resistance in that area. From day 4 onwards, rate of liquid formation by vertical electro-separation increased, so the changes in resistance in the anode area was not remarkable until day 9. From day 10 to day 13, the amount of solid near the anode increased. From day 13 to day 20, the resistance near the anode decreased, possibly attributable to an increase in the liquid phase due to vertical electro-demulsification. From day 21 to day 25, the resistance near the anode was rising because of movement of liquid toward the cathode, so the solid phase near anode became more dense. From day 26 to day 30, vertical forces were separating more liquid, so more decrease in resistance was observed in the anode area. On day 32, the resistance increased; however, electrical power of the system was disconnected. These movements also could be described by resistance behavior in the cathode area. No noticeable changes in the resistance of the cathode area occurred because there was more liquid in that area and solids were moving toward the anode. Resistance in the cathode area was increasing slowly at this time as a result of evaporation of separated water and volatile organic carbon (VOC). This liquid was produced from the break-down of water-in-oil emulsions in the sludge. The highest resistance in this cell reached nearly 1100 Ω , which was less than the highest resistance in the other cells. Since the resistance changes in the anode was periodical, for comparison with the cell SE (1.5), only the 15 days of the experiment were considered when preparing equation 4.7. The equation for the cathode area covers

all days of the experiment. The behavior of the resistance in the anode area can be best described by equation 4.7,

$$R = 109.8 t^{0.5948} \quad \text{with } r^2 = 0.82 \quad (4.7)$$

and in the cathode by equation 4.8.

$$R = 27.313 t^{0.7263} \quad \text{with } r^2 = 0.84 \quad (4.8)$$

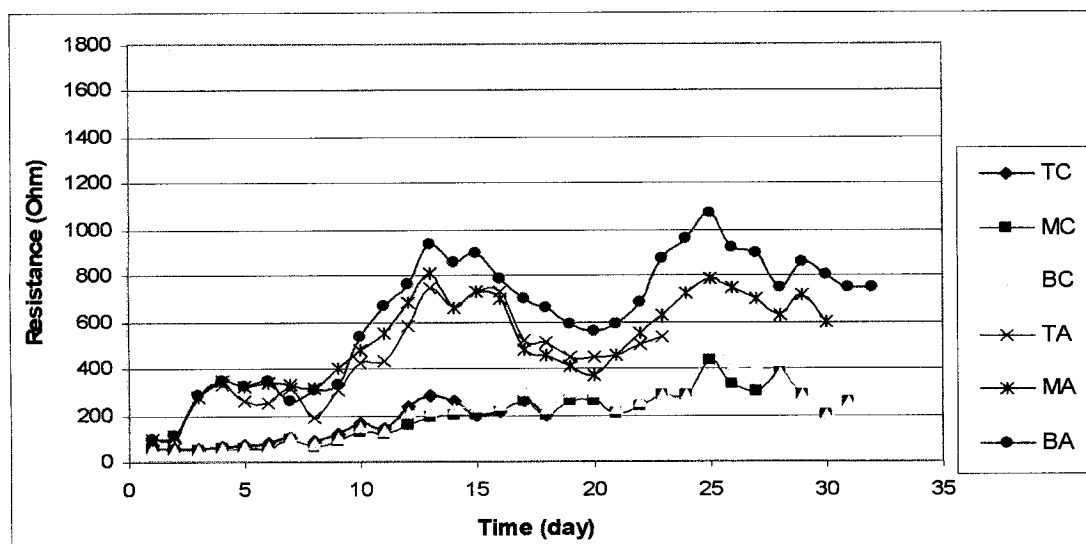


Figure 4-12 Resistance changes in cell SE (0.5)

*Note: TC= top of cathode area, MC = middle of cathode area, BC= bottom of cathode area, TA= top of anode area, MA= middle of anode area, BA= bottom of anode area.

4-4) pH measurements

The daily pH values for all cells are shown in Figures 4-13 to 4-42. The pH in cells S and SA (without electricity) was measured weekly; the pH was near neutral in both cells.

4-4-1) pH changes in cells with surfactant only

4-4-1-1) Cell with higher voltage - AE (1.5)

Figures 4-13 and 4-14 illustrate the pH values in cell AE (1.5) for the top and bottom of five points (section 3-7). Many changes in pH values were observed in all points in

the top and bottom, over the first 12 days; the values changed at the same rate. From day 13 to day 18, the pH at all points in the top and bottom, except the anode area, was around 10. The decrease in pH in the anode area can be attributed to the constant formation of hydrogen ions due to the oxidation of the anode. After day 18, the pH in the second point from anode (middle anode) also decreased but values in the cathode, middle cathode, and middle areas remained around pH 10 until day 32 (disconnection day). Between days 32 and 75, the pH values at all points had tendency to reach 9.

Figure 4-15 shows more clearly the difference between the pH values of the cathode and the anode areas after day 13. Figure 4-16 shows that from day 13 onwards, the middle and cathode points had the same pH, but the pH in the anode was less than these two points. Figure 4-17 shows that, until day 18, the pH in the middle cathode and the middle anode were almost the same. This figure shows more clearly the tendency of pH to reach 9 after the electricity was disconnected.

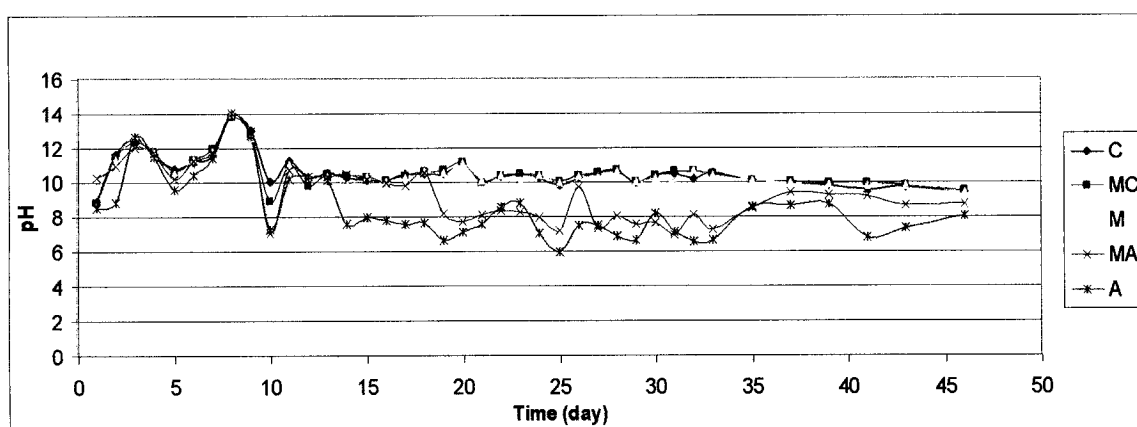


Figure 4-13 pH changes in the top level of cell AE (1.5)

*Note: C= cathode, MC = middle cathode, M= middle, MA= middle anode, and A= anode

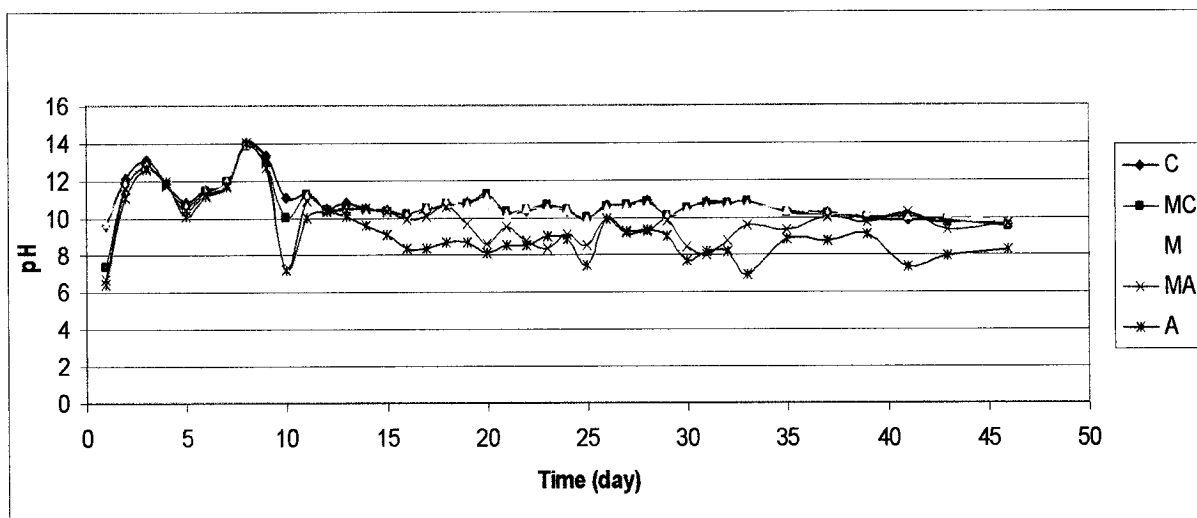


Figure 4-14 pH changes in the bottom level of cell AE (1.5)

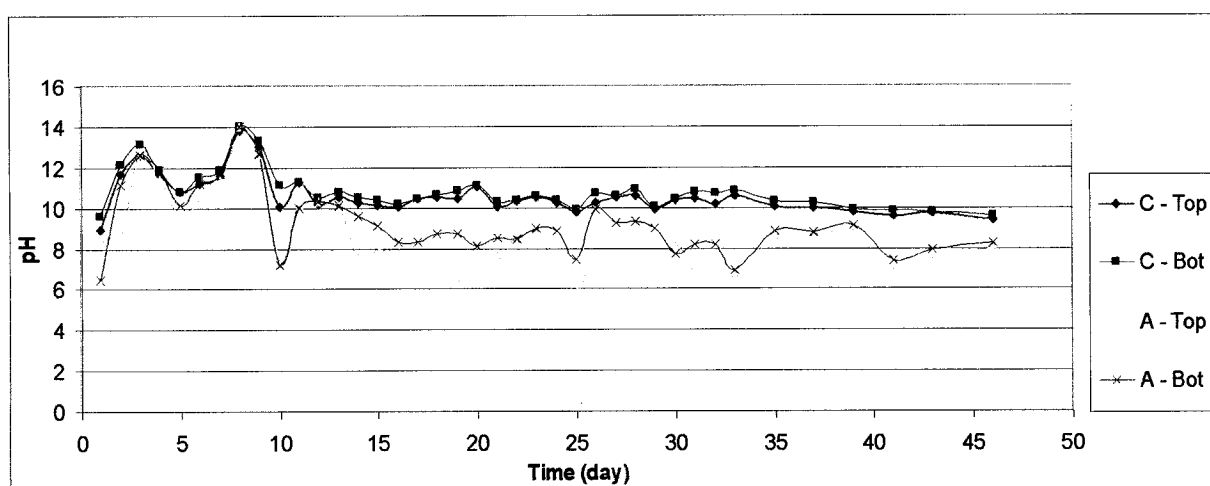


Figure 4-15 pH changes in the cathode and the anode areas of cell AE (1.5)

*Note: C= cathode, MC = middle cathode, M= middle, MA= middle anode, and A= anode

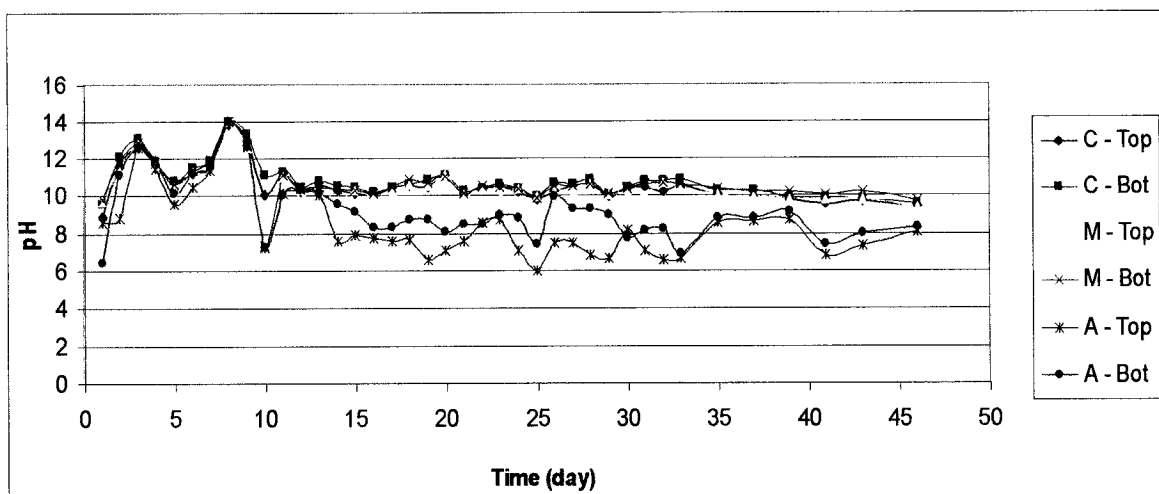


Figure 4-16 pH changes in the cathode, the middle and the anode areas of cell AE (1.5)

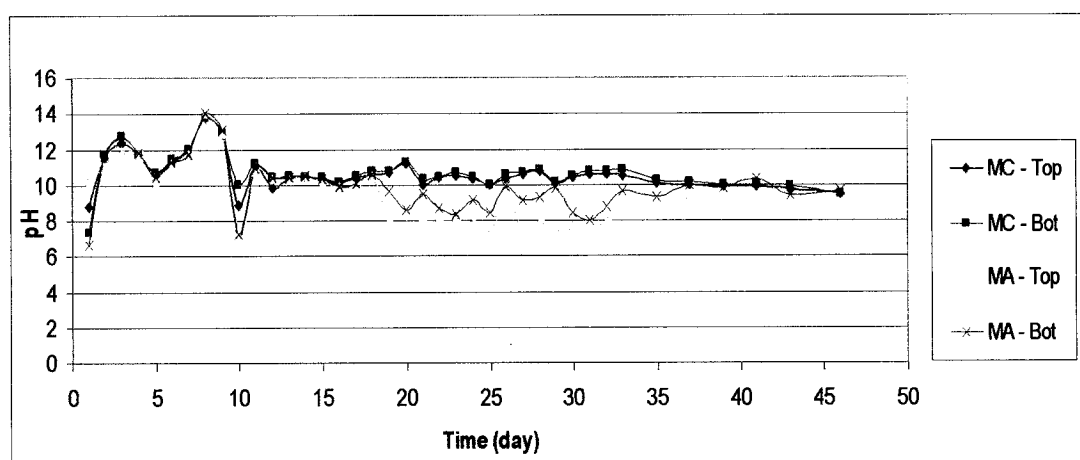


Figure 4-17 pH changes in the middle cathode and the middle anode areas of cell AE (1.5)

*Note: C= cathode, MC = middle cathode, M= middle, MA= middle anode, and A= anode

4-4-1-2) Cell with lower voltage - AE (0.5)

Figure 4-18 shows the pH values for the top points. Until day 17, the changes in all points were almost the same. From day 17 to day 32 (disconnection day), the anode area showed a lower value of pH. This could be as a result of the formation of hydrogen ions due to the oxidation of the anode. The pH values in the bottom were different (Figure 4-19). Over the first 6 days the cathode area had higher pH values than the other points. From day 7 to day 32, the anode had the lowest pH, but the other points showed about the same pH. After disconnection, all points tended to reach pH 9.

Figure 4-20 shows the pH values in the cathode and anode areas. During the first 11 days, there was great difference between pH values at the anode and cathode. In Figure 4-21, the differences between pH values in the bottom of the anode area and the other points were quite obvious. Figure 4-22 shows that between day 5 and 15 there were some differences between pH values in the middle cathode and the middle anode, but before and after those days, the pH values were nearly the same.

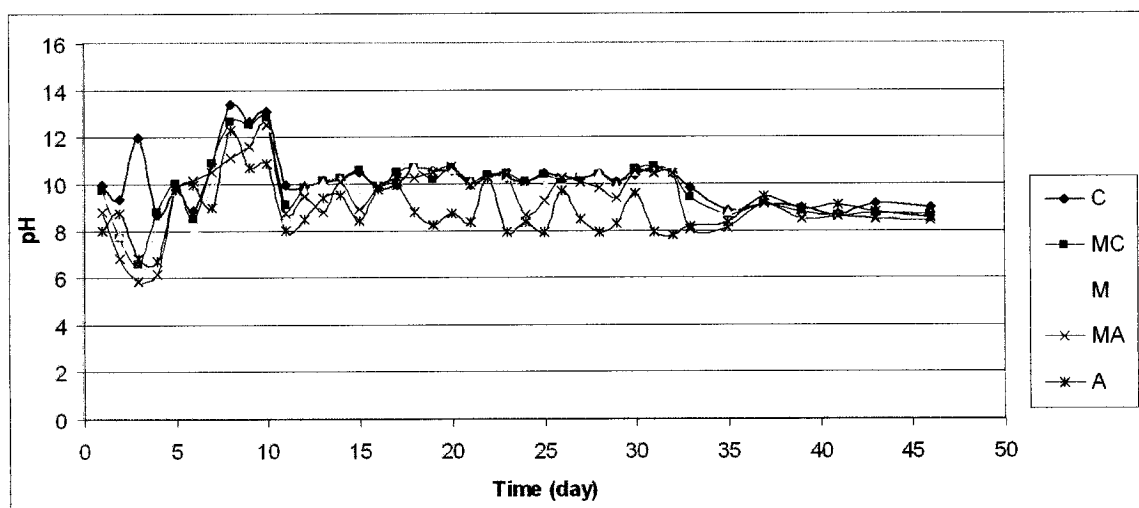


Figure 4-18 pH changes in the top level of cell AE (0.5)

*Note: C= cathode, MC = middle cathode, M= middle, MA= middle anode, and A= anode

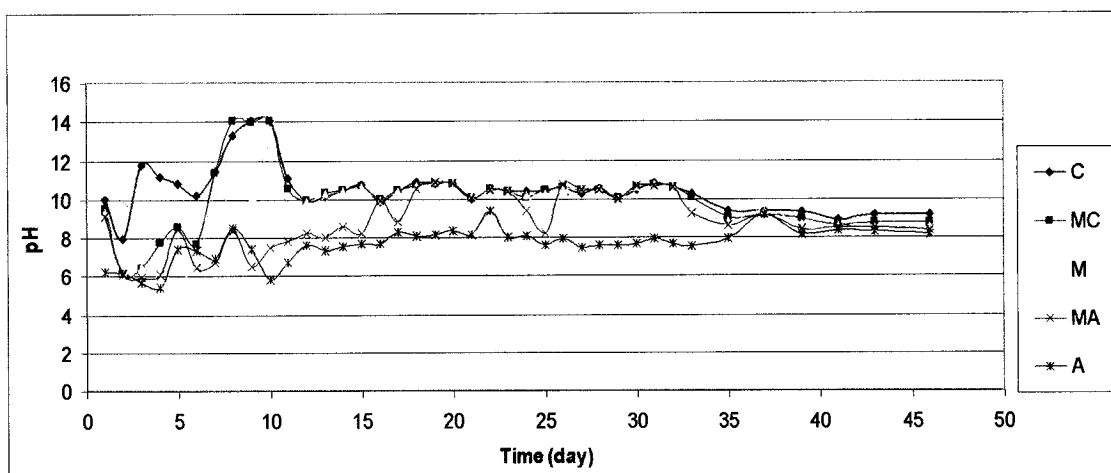


Figure 4-19 pH changes in the bottom level of cell AE (0.5)

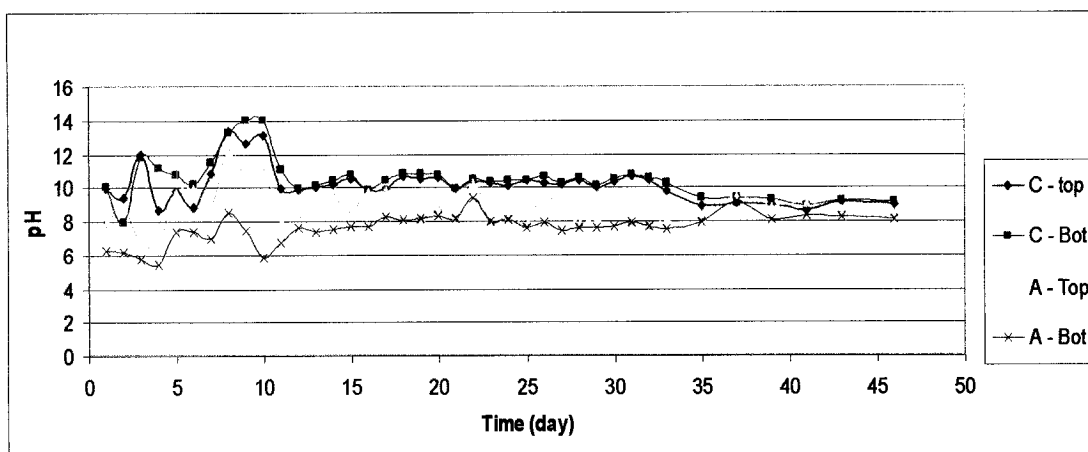


Figure 4-20 pH changes in the cathode and the anode areas of cell AE (0.5)

*Note: C= cathode, MC = middle cathode, M= middle, MA= middle anode, and A= anode

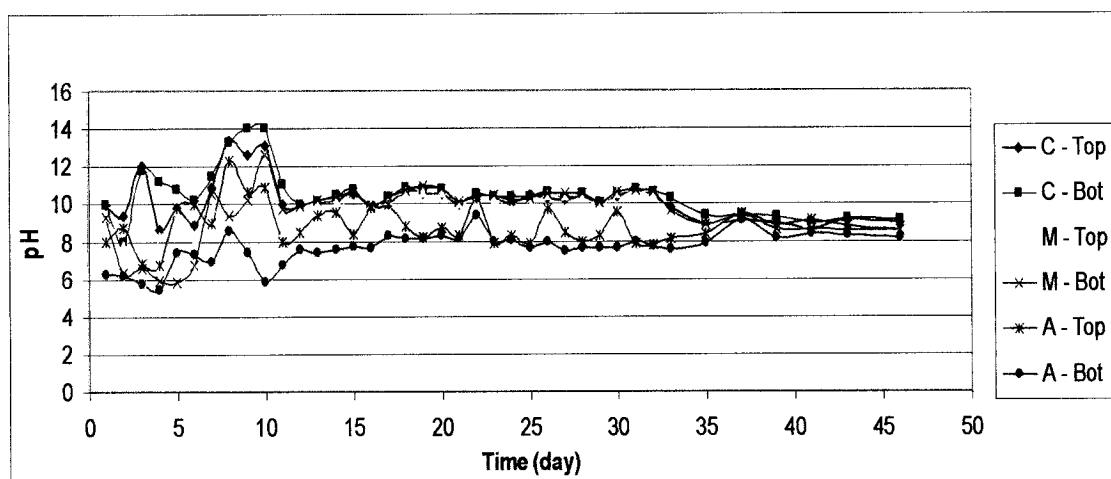


Figure 4-21 pH changes in the cathode, the middle, and the anode areas of cell AE (0.5)

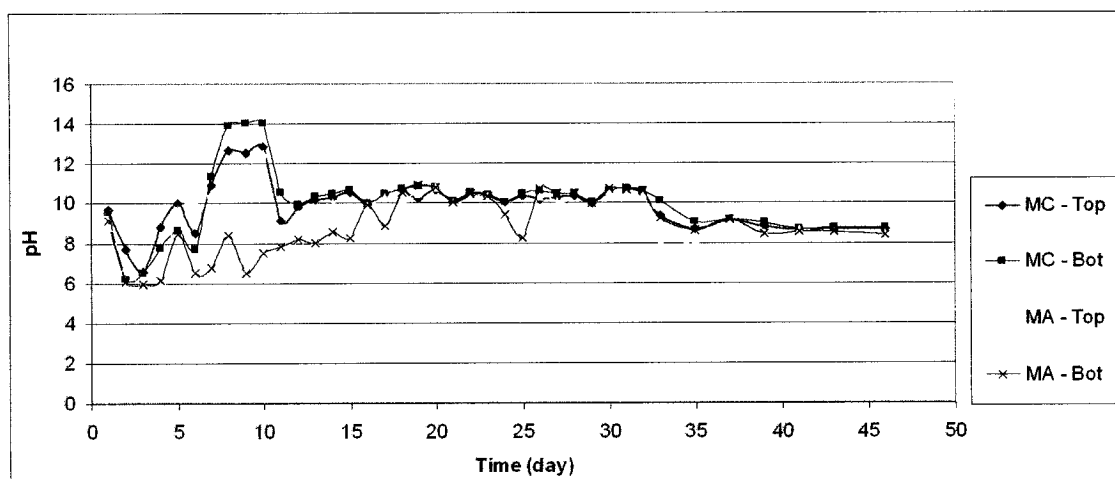


Figure 4-22 pH changes in the middle cathode and the middle anode areas of cell AE (0.5)

*Note: C= cathode, MC = middle cathode, M= middle, MA= middle anode, and A= anode

4-4-2) pH changes in cells containing sludge

4-4-2-1) Cell with higher voltage - SAE (1.5)

Figures 4-23 and 4-24 show the values of pH for the top and the bottom of all 5 points in cell SAE (1.5), respectively. In the first 11 days, pH values in top and bottom showed the highest variation. From day 12 to day 32 (disconnection day) changes occurred, but they were not the same as on the first 11 days. After day 32, the system moved close to pH 8. The highest difference between the pH values in the top points was 7.25, in day 3, which means the pH value near the cathode was 7.25 higher than that near the anode. The highest difference between cathode and anode (8.05) in the bottom of cell SAE (1.5) was also observed in day 3 of the experiment.

These differences in pH in the cathode and anode areas are more visible in Figure 4-25, showing the pH changes in the cathode and the anode. The graph illustrates that, after 12 hours, movements of particles from cathode to anode (electrophoresis) and movements of liquid from anode to cathode (electro-osmosis) started.

Figure 4-26 shows the pH values in the top and the bottom in cathode, anode, and middle areas of the cell. In the first 11 days, the pH of the middle point was more similar to that at the anode than at the cathode. This could be as a result of movements of solid toward the anode and accumulation of these particles in the middle point. From day 6 onward, in the middle point, the pH of the top was higher than the pH of the bottom because separated liquid phase was moving from the bottom of the cell toward cathode area. After day 11, the pH of the middle point increased. It shows that most of the solids passed from middle point to the anode area, so the middle point had more liquid than

solid. Figure 4-27 shows the pH values for the top and bottom of the middle cathode and middle anode areas.

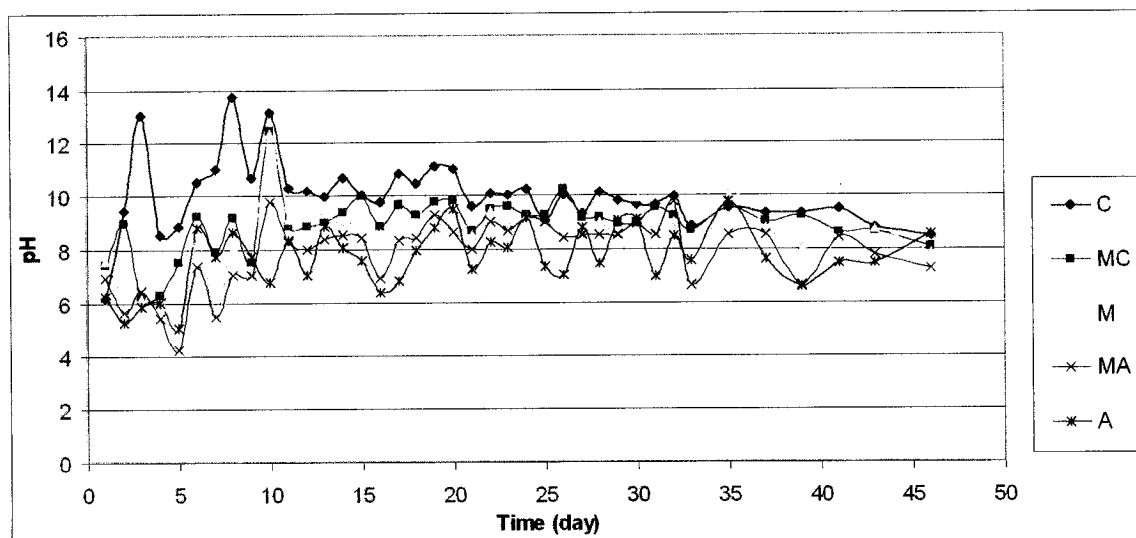


Figure 4-23 pH changes in the top level of cell SAE (1.5)

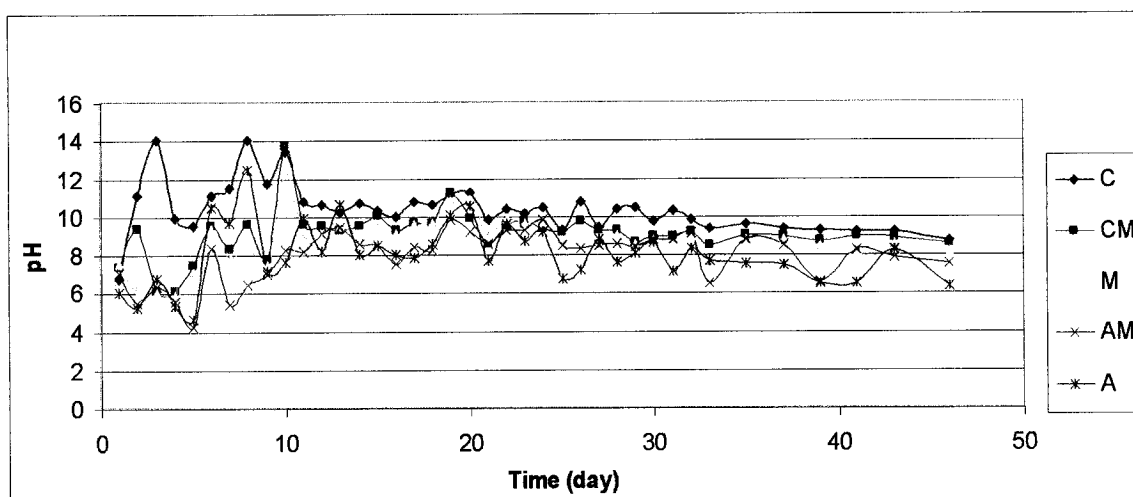


Figure 4-24 pH changes in the bottom level of cell SAE (1.5)

*Note: C= cathode, MC = middle cathode, M= middle, MA= middle anode, and A= anode

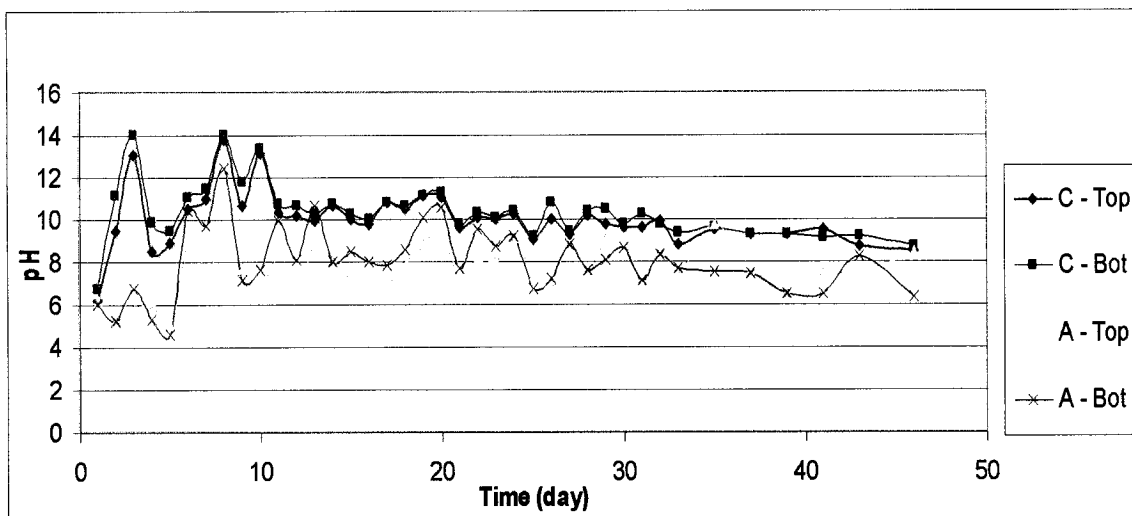


Figure 4-25 pH changes in the cathode and anode areas of cell SAE (1.5)

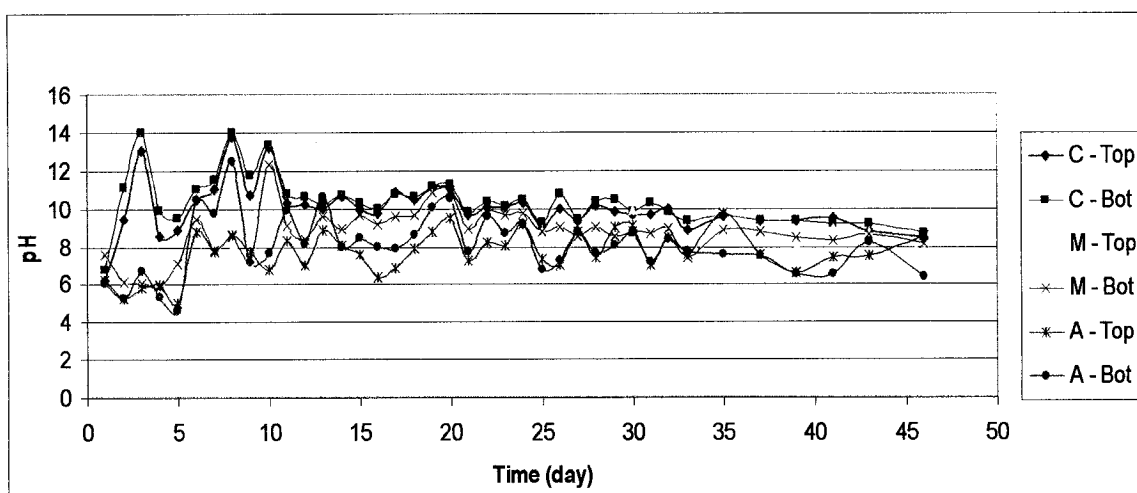


Figure 4-26 pH changes in the cathode, the middle and the anode areas of cell SAE (1.5)

*Note: C= cathode, MC = middle cathode, M= middle, MA= middle anode, and A= anode

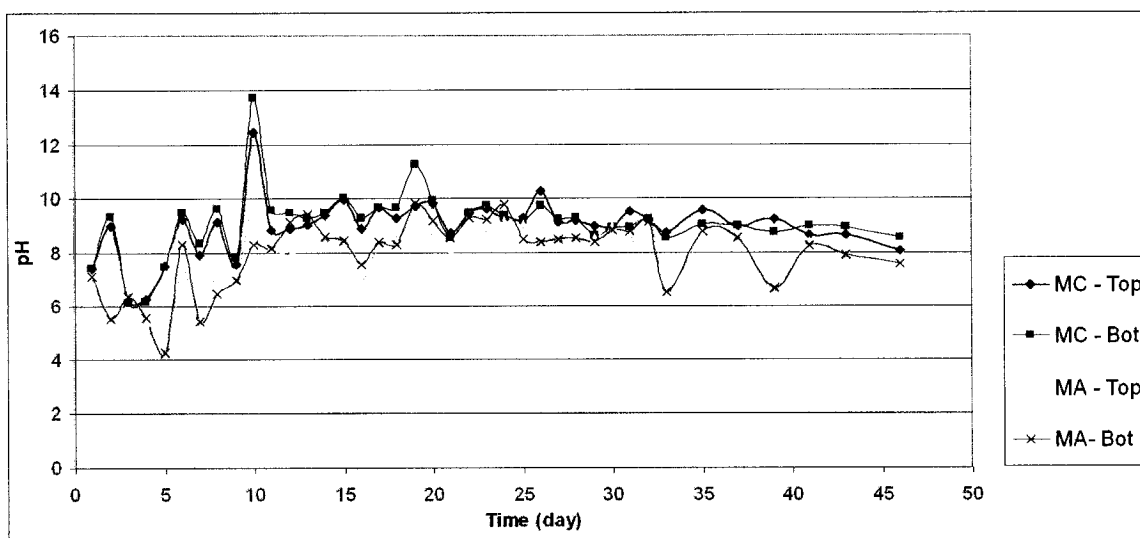


Figure 4-27 pH changes in the middle cathode and middle anode areas of cell SAE (1.5)

*Note: C= cathode, MC = middle cathode, M= middle, MA= middle anode, and A= anode

4-4-2-2) Cell with lower voltage - SAE (0.5)

Figure 4-28 shows the pH values for the top points of cell SAE (0.5). During the first 10 days, many changes in pH were observed. From day 2 to day 6, the pH difference between the cathode and the other four measuring points was very high. The highest difference (8.92) was measured on the third day. From day 11 to day 25, the pH variation in all points was almost the same. From days 25 to 32 (disconnection day) the pH value near the anode decreased, possibly as a result of formation of more solid phase in that area. After disconnection, the cathode, the middle cathode, and the middle points showed almost the same pH of around 9. The anode and the middle anode areas also moved slowly to this pH value.

Figure 4-29 shows the pH values of the bottom points in this cell. As at the top points, many changes in pH values were observed during first 11 days. The highest pH difference between cathode and anode areas in bottom points was on day 3. By day 22, the pH in the anode and the middle anode started to increase because of solid phase formation. After disconnection (day 32), the cathode, the middle cathode, and middle areas showed the same pH values, higher than those at the anode and the middle anode areas. It can be concluded that the first three points contained more liquid but the anode area contained more solids. The pH changes in the solid phase were slow.

Figure 4-30 illustrates the pH values of the cathode and anode areas. This figure shows three separate zones. Over the first 6 days, the pH differences between cathode and anode were high. This shows that movement of liquid toward the cathode and the movement of solid toward the anode started immediately after system connection to the electrical power, and grew faster after 12 hours. From day 7 to day 20, the pH values of the cathode and anode areas were almost equal. It seems that the vertical electro-demulsification effect was much stronger than horizontal movements in these days. After this period, the difference again started to increase. After disconnection day, all points tended toward reaching pH 9, but in the anode area the changes were slower than in the other points.

Figure 4-31 shows more clearly the movements of solid and liquid in the cathode, anode, and middle areas. Over the first 6 days, the pH values in the anode and the middle area were lower than in the cathode area, showing that the amount of solid phase was higher in the anode and the middle area. From day 7 to day 20, there was more viscose sludge in the middle than in the cathode and anode areas. After day 21 to day 32, the

solid phase moved toward the anode, and the pH value in the middle point started to increase around the pH value of the cathode area. After disconnection, the pH values in the cathode and the middle areas were almost equal, but near the anode area lower pH values were observed. The pH value in the anode area increased very slowly.

Figure 4-32 shows some differences in pH values between the middle cathode and the middle anode between day 6 and day 10. From day 17 to day 32, this gradient again started to increase until day 32, possibly as a result of formation of solid phase in the anode area. After disconnection, the pH values of both points moved toward pH 9.

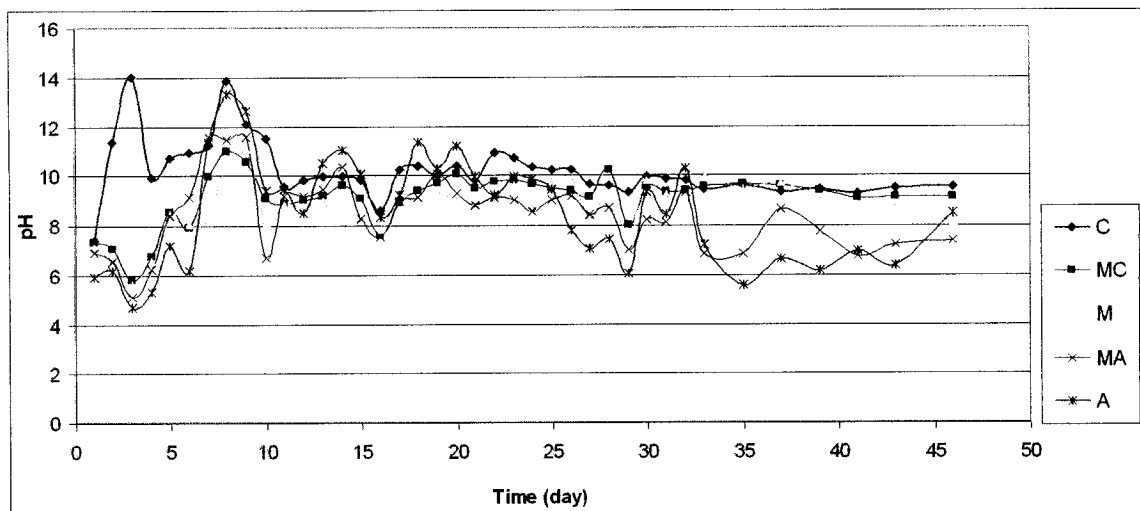


Figure 4-28 pH changes in the top level of cell SAE (0.5)

*Note: C= cathode, MC = middle cathode, M= middle, MA= middle anode, and A= anode

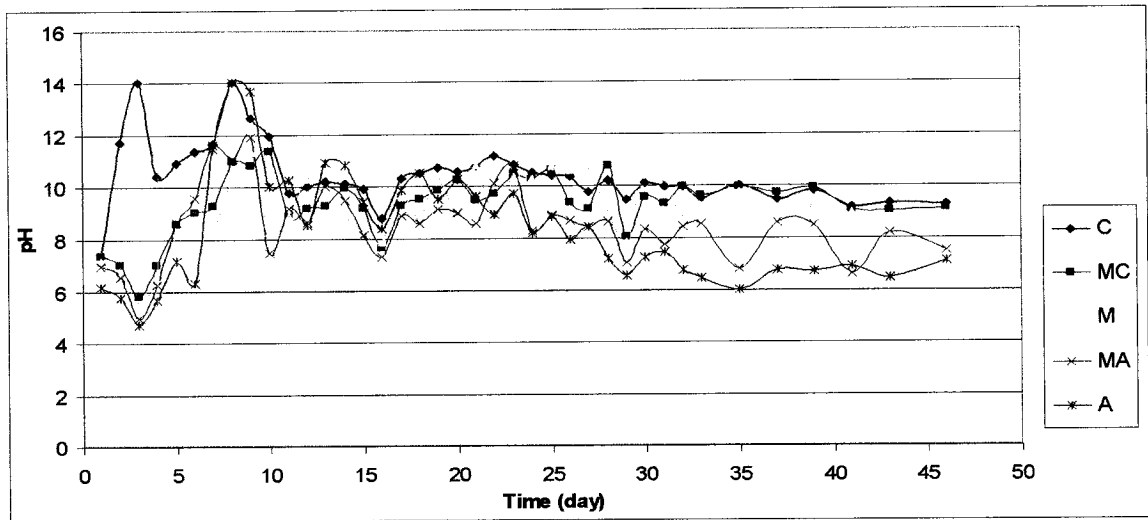


Figure 4-29 pH changes in the bottom level of cell SAE (0.5)

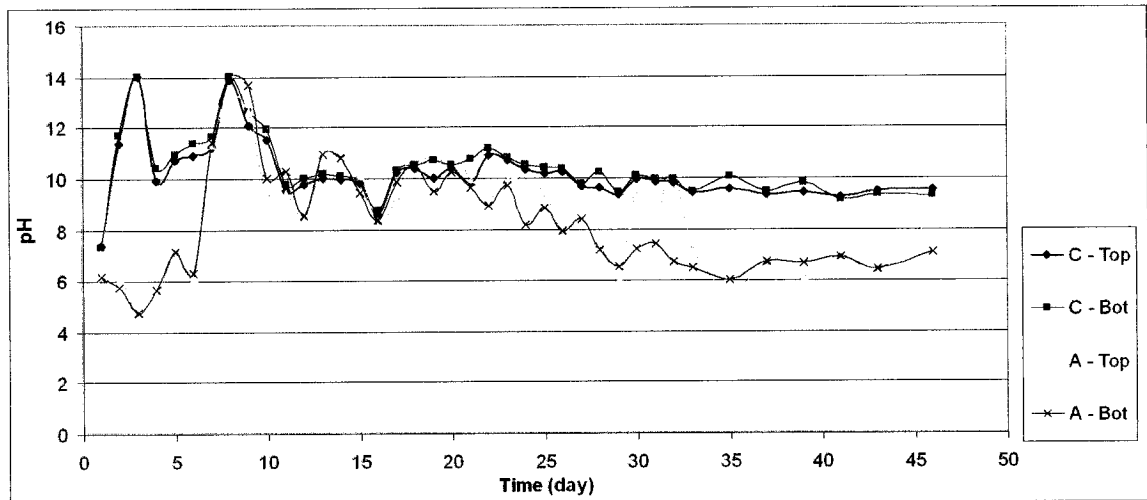


Figure 4-30 pH changes in the cathode and anode areas of cell SAE (0.5)

*Note: C= cathode, MC = middle cathode, M= middle, MA= middle anode, and A= anode

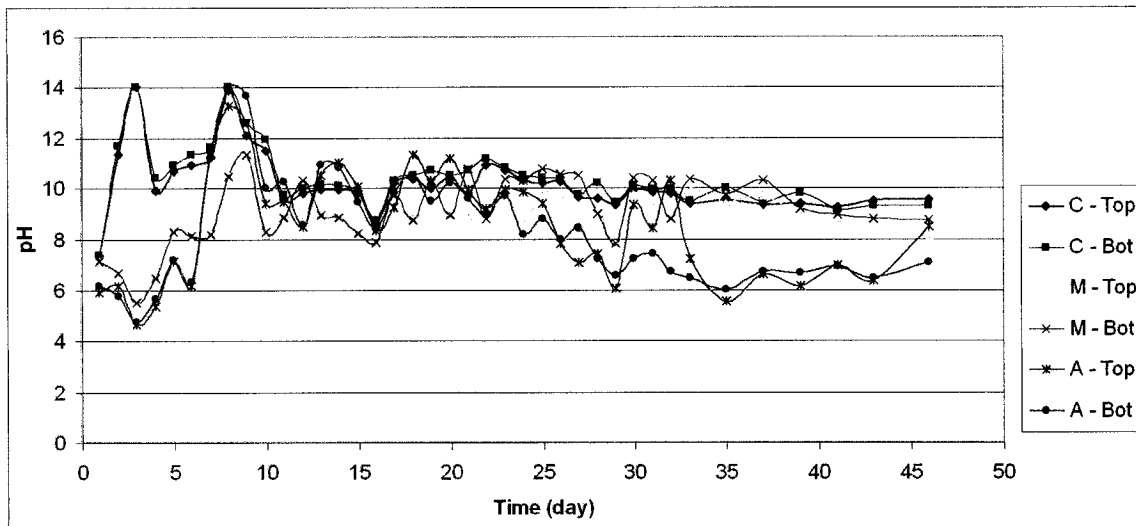


Figure 4-31 pH changes in the cathode, middle, and anode areas of cell SAE (0.5)

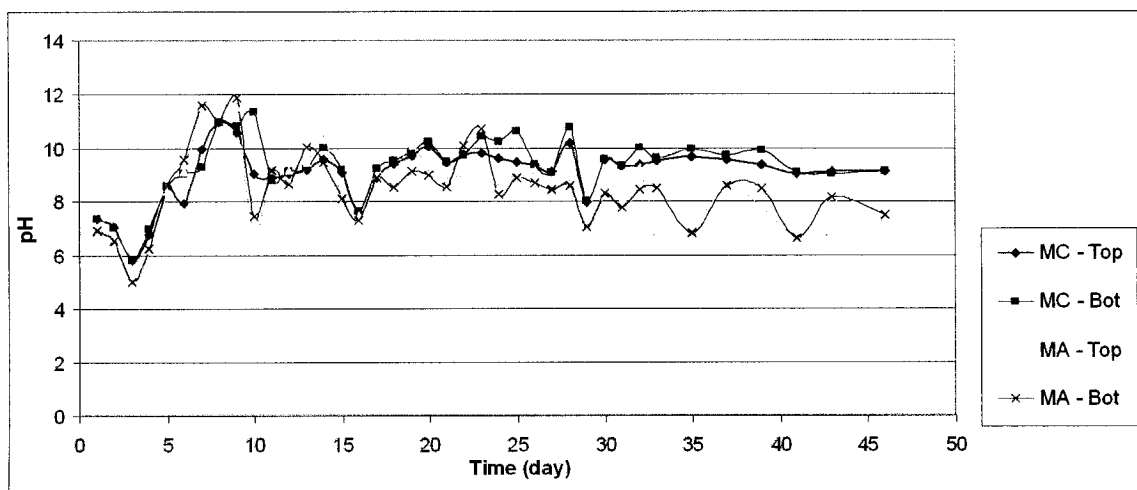


Figure 4-32 pH changes in the middle cathode and middle anode areas of cell SAE (0.5)

*Note: C= cathode, MC = middle cathode, M= middle, MA= middle anode, and A= anode

4-4-2-3) Cell without addition of surfactant, higher voltage - SE (1.5)

Figures 4-33 and 4-34 show the pH values in the top and bottom of cell SE (1.5), respectively. After 12 hours, the electroosmotic movement toward the cathode and electrophoretic movement toward the anode started. During the first 10 days of the experiment, there were high differences between pH in the cathode and the anode areas. From day 11 to day 32 (disconnection day), the variations of pH in different points were not noticeable in the top and the bottom areas, except in the anode area. From day 23, the pH of the anode area in the bottom decreased, a decrease that could be a result of accumulation of solid phase in that area. After day 33, pH values in all points were slowly reaching 9.

Figure 4-35 shows the pH changes in the cathode and the anode areas; it shows the starting time of electroosmotic and electrophoretic movements more clearly. Figure 4-36 shows the pH changes at three points: cathode, anode and middle areas. The pH of the middle point during the first 10 days of the experiment was close to the pH of the anode area. Between day 11 and 25, this value was approximately mid-way almost between pH values of cathode and anode areas, but after day 26, it increased to the pH value of the cathode area. This phenomenon could be explained by electrophoretic and electroosmotic movements as follows: In the first 10 days, the middle point contained more solid. Between days 11 and 26, the amount of liquid, which was moving toward the cathode, and the amount of solid, which was moving toward the anode were almost equal, so the pH value in middle area was between the values of anode and cathode. After day 26, most of the solids moved toward the anode and the middle point contained more liquid, so the pH value increased to near the pH value of the cathode area. After day 32

(disconnection day), due to lack of electrical potential, the pH value of the middle point returned to values between those of cathode and anode.

Figure 4-37 shows the pH changes in the middle cathode and the middle anode points; the changes are obvious in the first 11 days in both points. After day 12, the pH values slowly expressed a tendency to reach pH 9 and this trend continued after day 32 (disconnection day) until the end of the experiment.

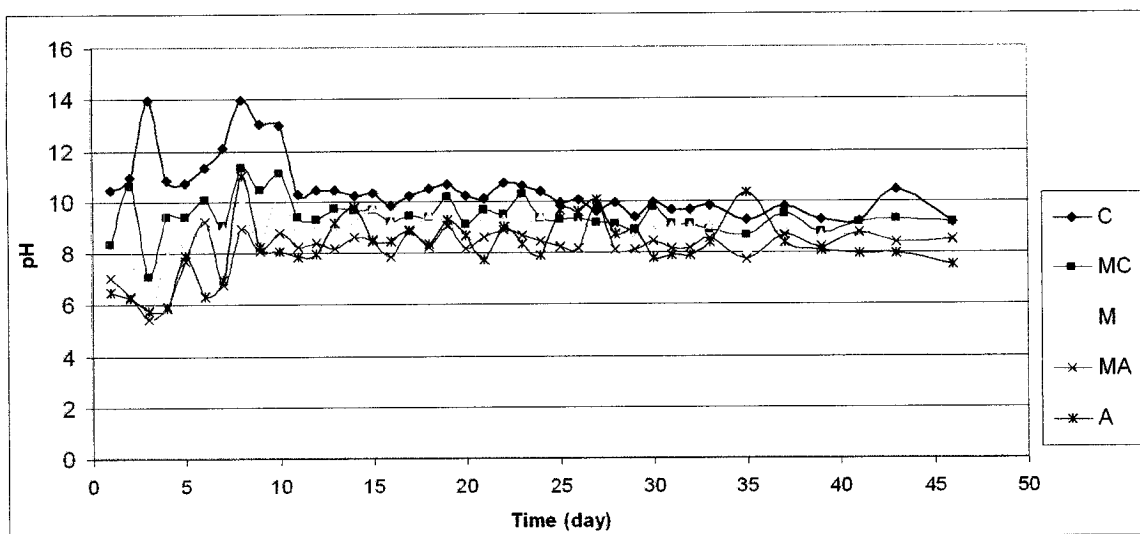


Figure 4-33 pH changes in the top level of cell SE (1.5)

*Note: C= cathode, MC = middle cathode, M= middle, MA= middle anode, and A= anode

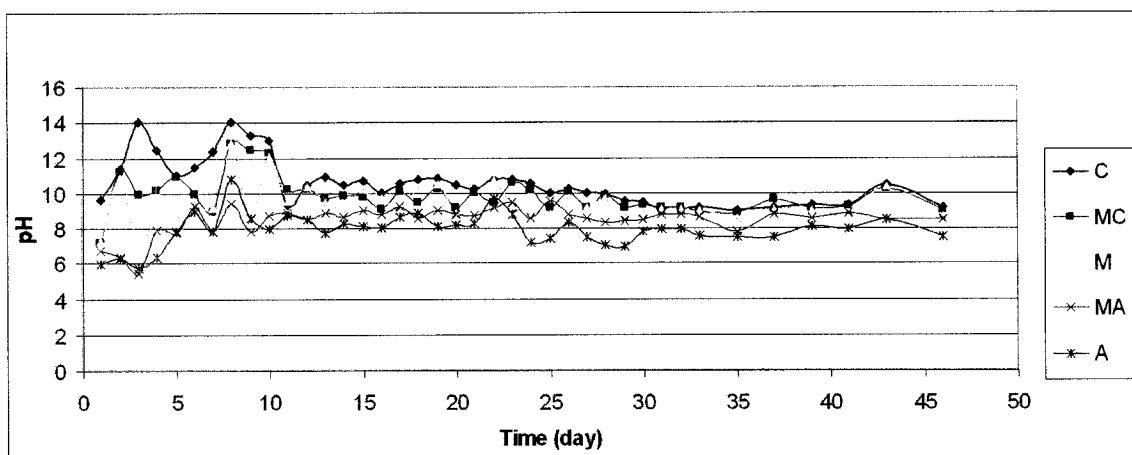


Figure 4-34 pH changes in the bottom level of cell SE (1.5)

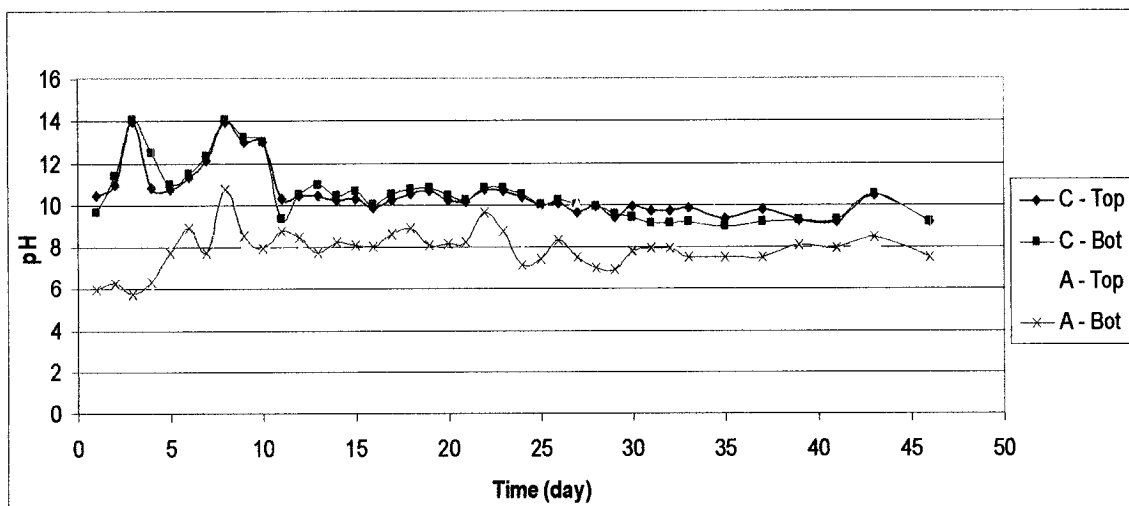


Figure 4-35 pH changes in the cathode and anode areas of cell SE (1.5)

*Note: C= cathode, M= middle, and A= anode

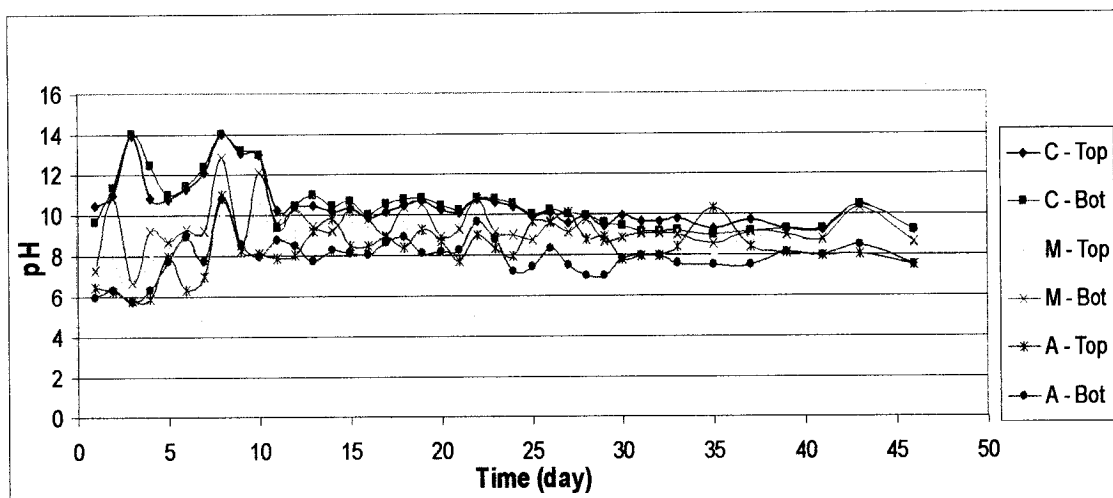


Figure 4-36 pH changes in the cathode, the middle, and anode areas of cell SE (1.5)

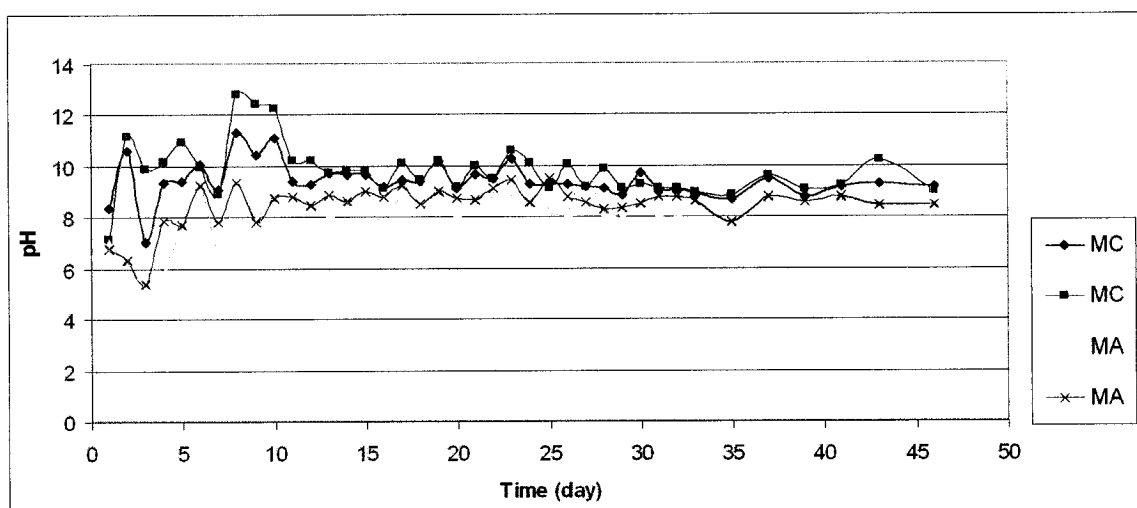


Figure 4-37 pH changes in the middle cathode and middle anode areas of cell SE (1.5)

*Note: C= cathode, MC = middle cathode, M= middle, MA= middle anode, and A= anode

4-4-2-4) Cell without addition of surfactant, lower voltage - SE (0.5)

Figure 4-38 shows the pH values in the top level of cell SE (0.5). The difference in pH between cathode and anode areas was very high during the first 9 days. From day 10 to day 32 (disconnection day), these differences decreased. After day 32, all points at the top level were reaching neutral pH; this tendency was faster in the cathode, middle cathode, and middle areas than in the anode and middle anode areas.

Figure 4-39 shows the pH values in the bottom of this cell for different days. During the first 15 days, a large pH difference existed between the cathode and the anode areas. From day 16 to day 27, this difference decreased except at the anode area. Because of the formation of the solid phase near the anode, this point had a very low pH value. Between day 28 and day 32, variations in pH values in both anode and middle anode areas were very low. After day 32, all points were reaching neutral pH, but this tendency was very slow in the anode area.

Figure 4-40 shows the pH distribution in the cathode and the anode areas. It illustrates that the movement of liquid toward the cathode and movement of particles toward the anode started on the third day of the experiment. In Figure 4-41, the pH value of the middle point is also shown in addition to pH values of the cathode and the anode areas. Over the first 15 days, there was a high difference between these points. From day 16 to day 27, the difference between the cathode and middle areas decreased. Because of formation of solid phase near the anode, this point had a very low pH value. From day 28 to day 32 (disconnection day), the amount of solid phase increased, so the pH value in that area decreased. After day 32, all points were nearing neutral pH, but this movement in the anode area was very slow.

This Figure illustrates that the rate of movement of liquid toward the cathode and movement of particles toward the anode increased from the third day of the experiment. After 6 days, the pH of the middle point increased, and became closer to the pH value of the cathode area. This shows that more liquid accumulated in the middle area. After day 29, the pH values of the middle and cathode areas were almost equal, and much higher than in the anode area, possibly as a result of formation of more solid phase in the anode area. Figure 4-42 shows the pH value of the middle cathode and the middle anode areas. From day 6, the electroosmotic and electrophoretic movements were more obvious in these points.

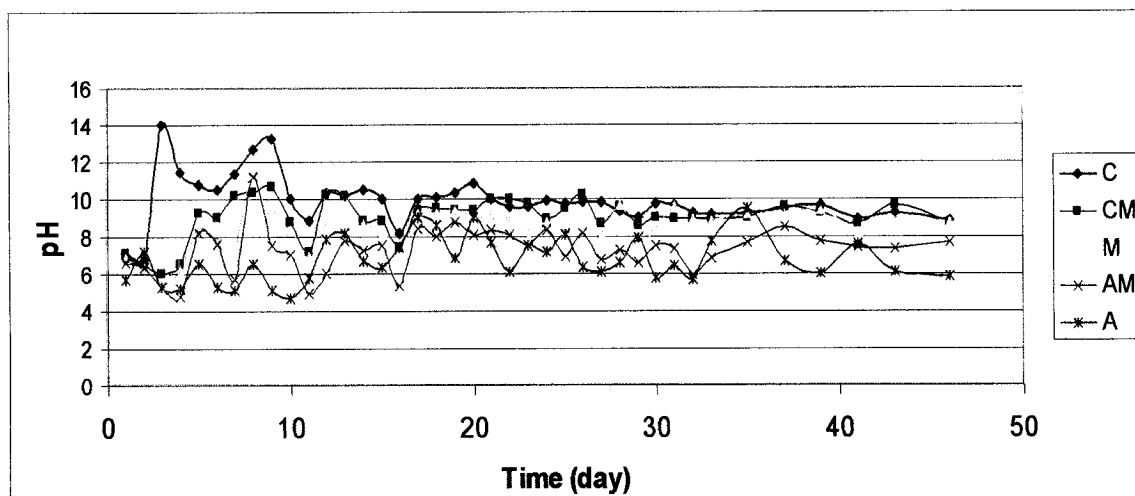


Figure 4-38 pH changes in the top level of cell SE (0.5)

*Note: C= cathode, MC = middle cathode, M= middle, MA= middle anode, and A= anode

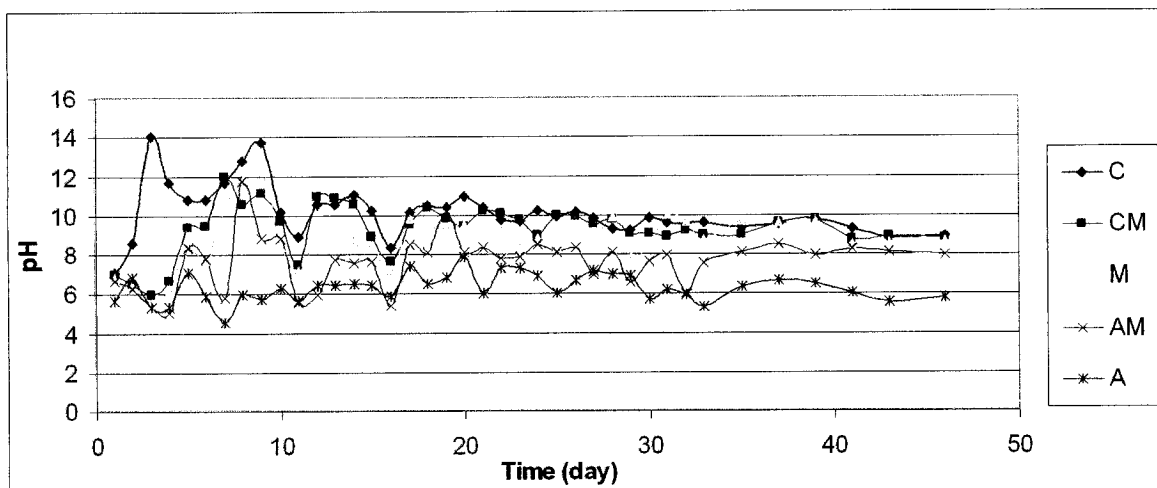


Figure 4-39 pH changes in the bottom level of cell SE (0.5)

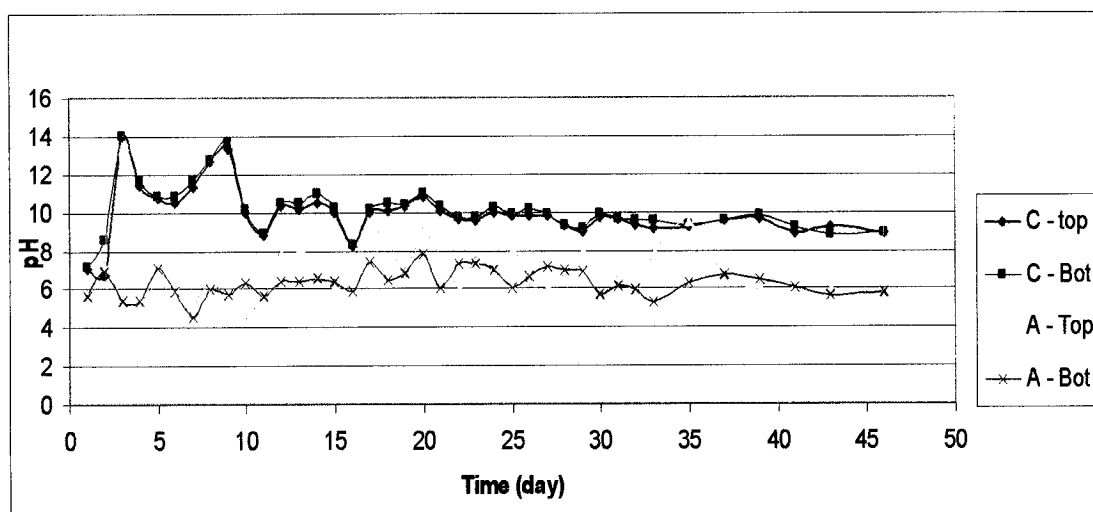


Figure 4-40 pH changes in the cathode and anode areas of cell SE (0.5)

*Note: C= cathode, M= middle, and A= anode

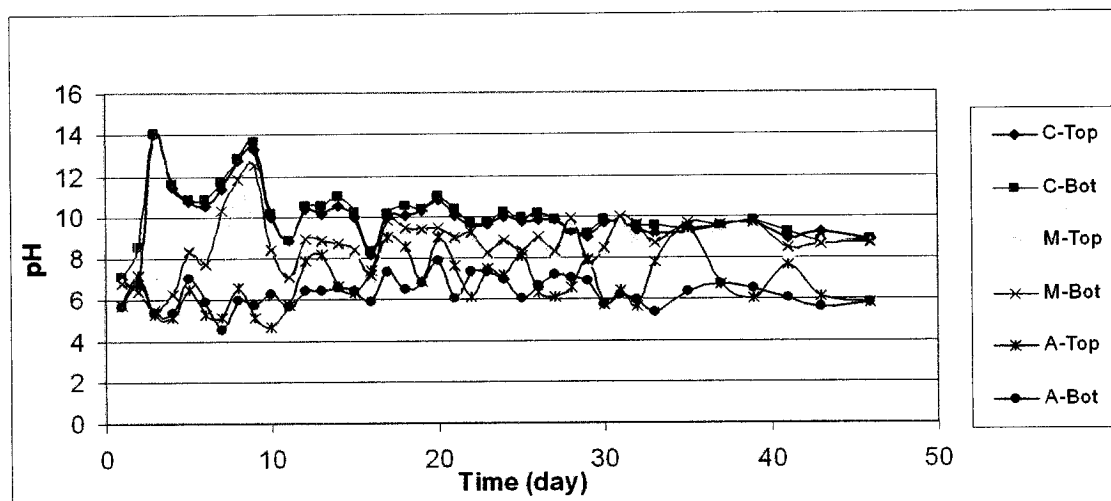


Figure 4-41 pH changes in the cathode, middle, and anode areas of cell SE (0.5)

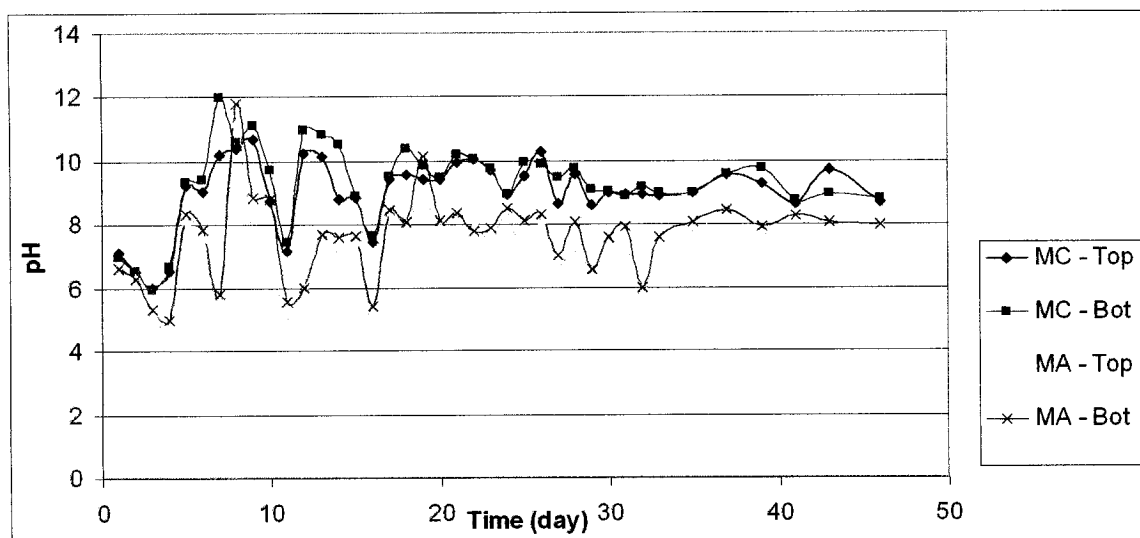


Figure 4-42 pH changes in the middle cathode and middle anode areas of cell SE (0.5)

*Note: C= cathode, MC = middle cathode, M= middle, MA= middle anode, and A= anode

4-5) Relative aromatic hydrocarbon content

This section deals with the results of the UV/VIS spectra test. As mentioned in Chapter 3, UV/VIS analysis was performed to assess the content of aromatic hydrocarbons in solid phase. Hexane was used for extraction of hydrocarbons from solid phase. Figures 4-43 to 4-48 show the comparison of aromatic hydrocarbon at the top and bottom of each cell in different points and on different days of the sampling.

Figure 4-43 shows the results for cell SAE (1.5). On day 25, the difference between the anode and the cathode in the top and the bottom was high. The difference between values at the cathode and anode areas shows the electroosmotic and electrophoretic movements, and the difference between top and bottom of each location shows the vertical separation of phases. On day 32 (disconnection day), the amount of aromatic hydrocarbon at the top was less than at the bottom, and the difference between cathode and anode was less than on day 25th. One week after disconnection (day 39), the cathode and the middle areas showed higher amounts of aromatic hydrocarbon in the bottom but in the middle anode and the anode areas this amount was higher in the top level. This Figure shows that rate of horizontal movement became very slow, but still, some vertical changes were observed. On day 46, the difference between top and bottom in this cell increased. This could be as a result of sedimentation phenomena.

Figure 4-44 shows the aromatic hydrocarbon content in cell SAE (0.5). The difference in values between the top and the bottom in this cell was higher than in cell SAE (1.5) on day 25. On day 32, the difference between the cathode and the anode values was more significant than in cell SAE (1.5). This difference was much more obvious on day 39. On day 46, both cells reached stable conditions, and two separate phases of liquid and solid

in the top and the bottom were observed. It could be concluded that horizontal movements in the cell with lower voltage were slower than in the cell with higher voltage. This caused more vertical separation of phases so the system, after disconnection was more stable.

Figure 4-45 shows the aromatic hydrocarbon content in cell SE (1.5). On day 25, the variation between the anode and the cathode values in the bottom was higher than in the top. As shown in the figure, the difference between the top and bottom values was insignificant in the cathode and middle cathode. The low amount of aromatic hydrocarbon in the cathode shows that there was a high amount of water in that area. On day 32, results for the cathode, middle cathode, and middle were almost equal, with less aromatic hydrocarbon in the top and bottom compared to day 25. Visual observation confirmed the above-mentioned conditions. From day 39 onward (one week after disconnection), the system reached nearly stable conditions. On day 39, the difference between the cathode and the anode values was very small, and on day 46, the system was almost stable with completely two separate phases in the top and bottom.

Figure 4-46 shows the aromatic hydrocarbon content in cell SE (0.5). On the first day of sampling, the difference between values in the cathode and the anode was higher in the bottom than in the top. In the cathode and middle cathode areas on day 32, the tendency to reach the same value in the top and the bottom was more obvious. However, even one week after disconnection there was still a large difference between the top and bottom values in the anode area, and also between the cathode and anode values. The liquid phase in the cathode, middle cathode, and middle areas had almost the same amount of aromatic hydrocarbon. On day 46, the system had reached nearly stable condition.

Because of lower voltage in this cell, horizontal movements were slower than for cell SE (1.5), but the amounts of liquid and solid that were separated were higher. In this cell, the system had enough time for more vertical separation to occur. Observations also confirmed that this cell had the highest amount of liquid phase separation from the sludge, and lower amount of residual solid phase.

Figure 4-47 shows that the amounts of aromatic hydrocarbon in control cell S were almost equal on different days and at different points in the top and bottom. Figure 4-48 shows corresponding amounts for control cell SA; the amount of aromatic hydrocarbon in the bottom was very low on the first three days of sampling, but on day 46 the amount was increased. The average error calculated for UV analysis was 11.7%.

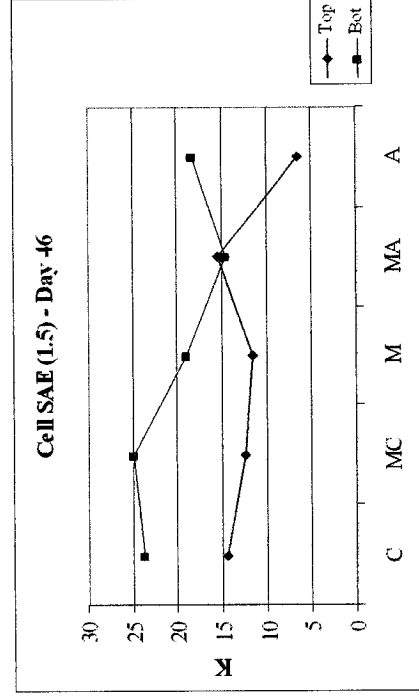
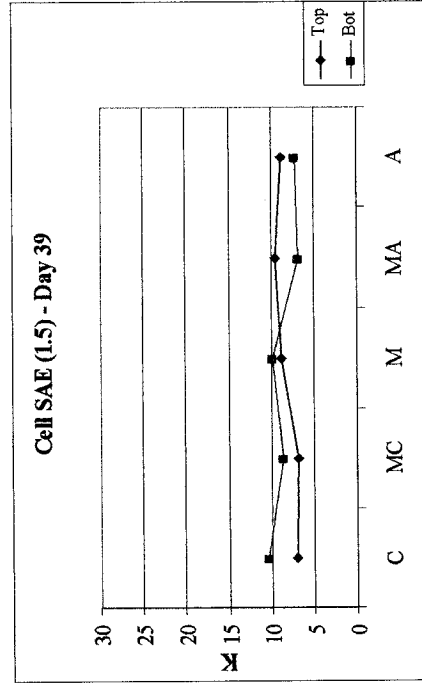
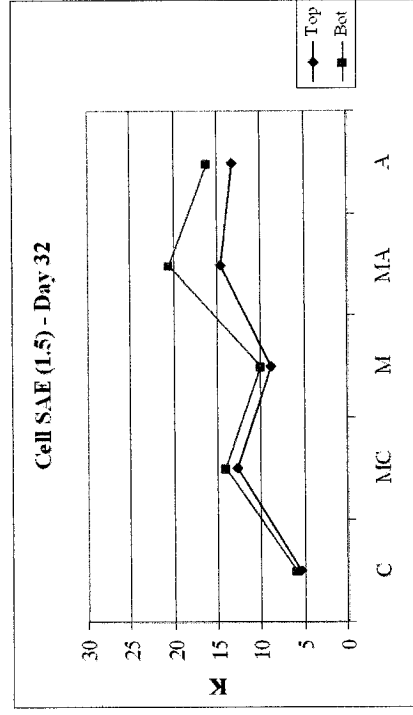
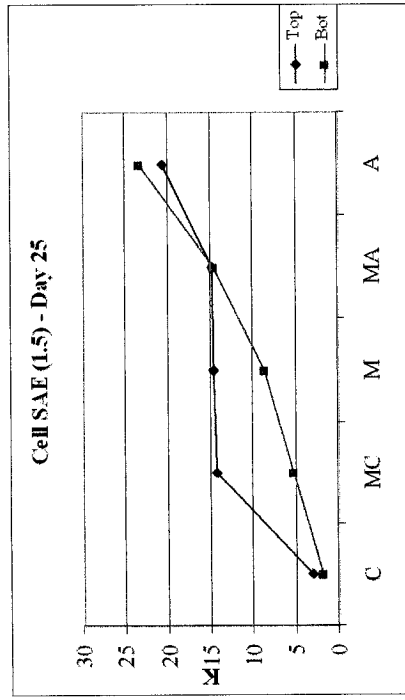


Figure 4-43 UV/VIS spectrometer results for cell SAE (1.5) on different days of sampling

*K = relative aromatic hydrocarbon content

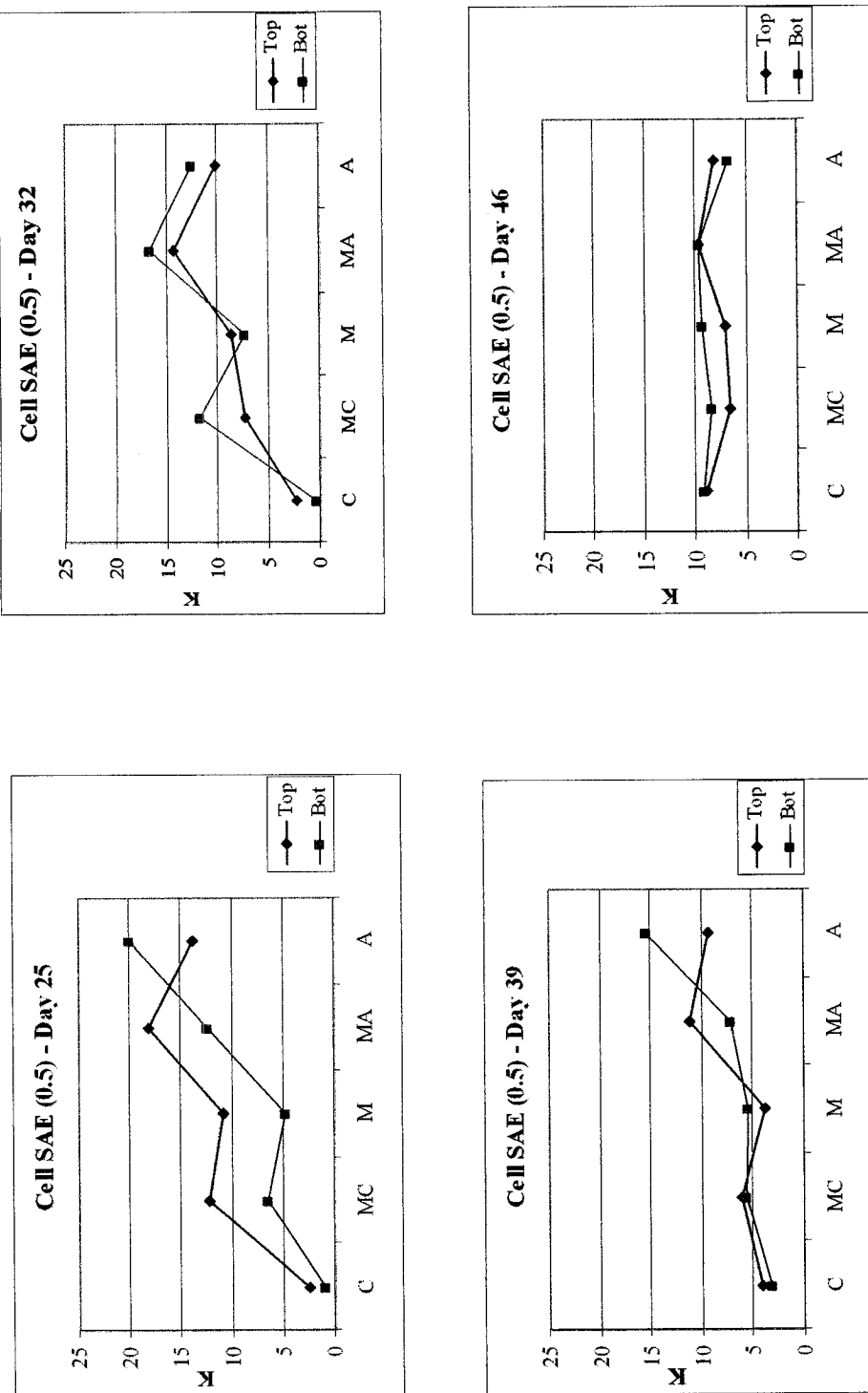


Figure 4-44 UV/VIS spectrometer results for cell SAE (0.5) on different days of sampling

*K = relative aromatic hydrocarbon content

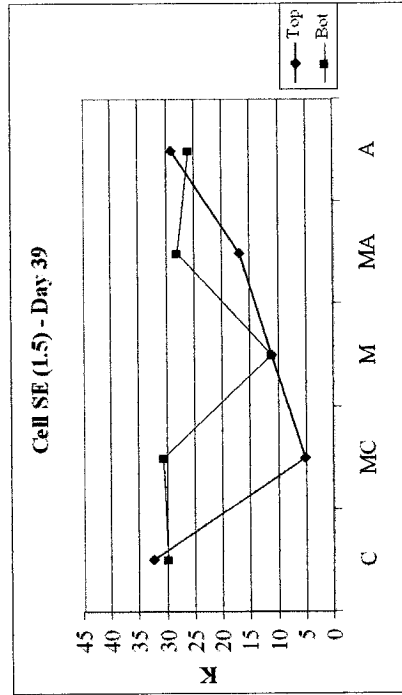
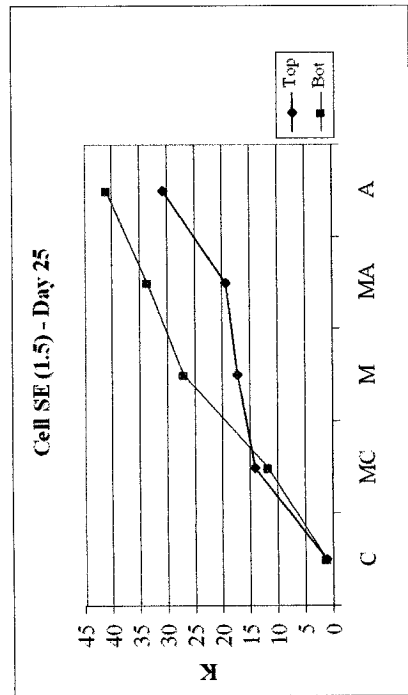
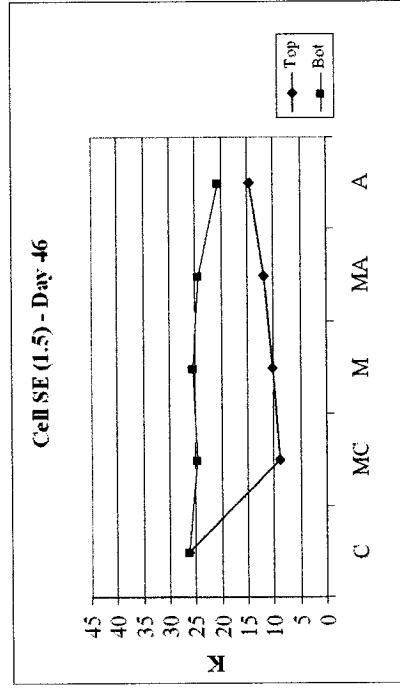
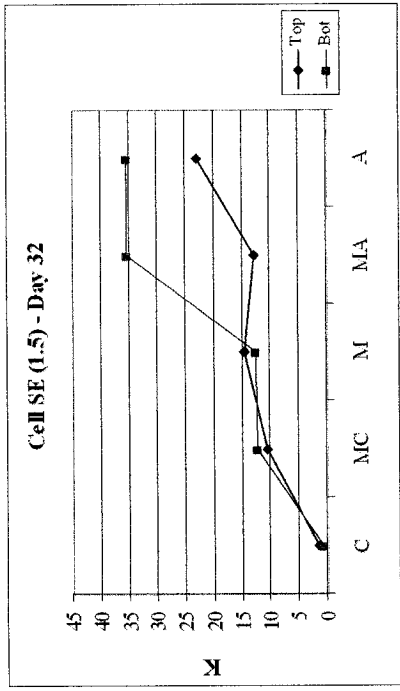


Figure 4-45 UV/VIS spectrometer results for cell SE (1.5) on different days of sampling

*K = relative aromatic hydrocarbon content

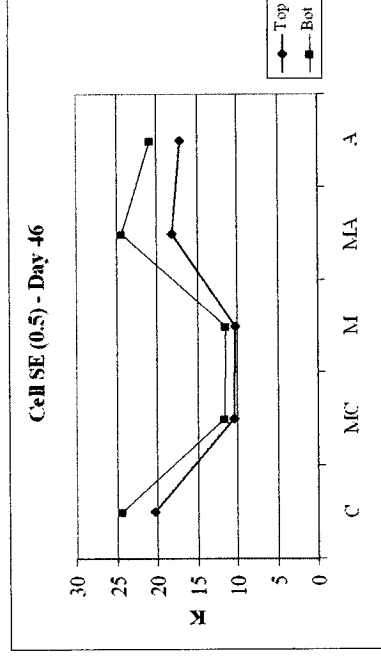
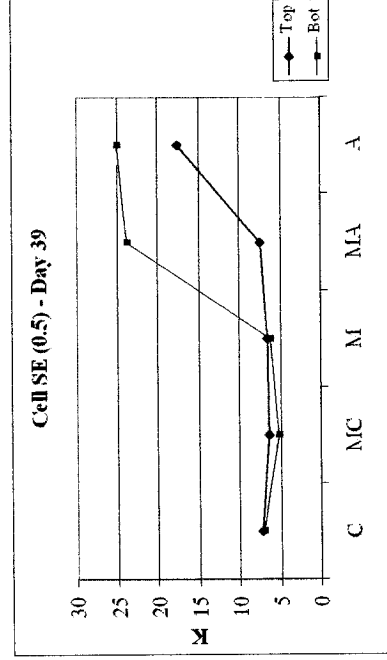
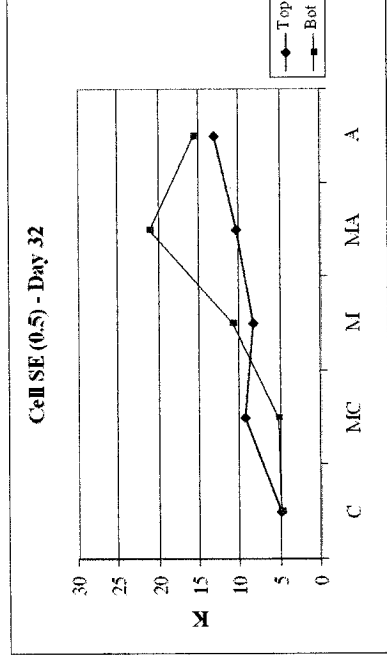
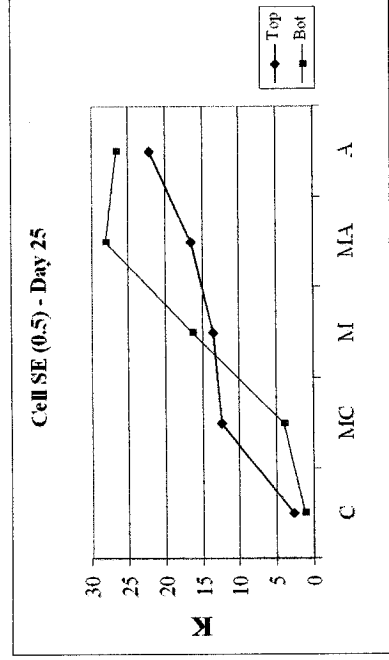


Figure 4-46 UV/VIS spectrometer results for cell SE (0.5) on different days of sampling

*K = relative aromatic hydrocarbon content

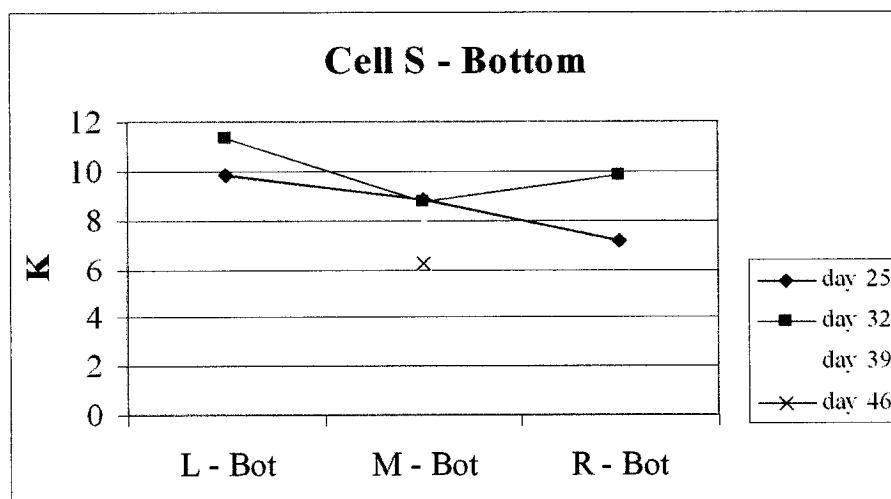
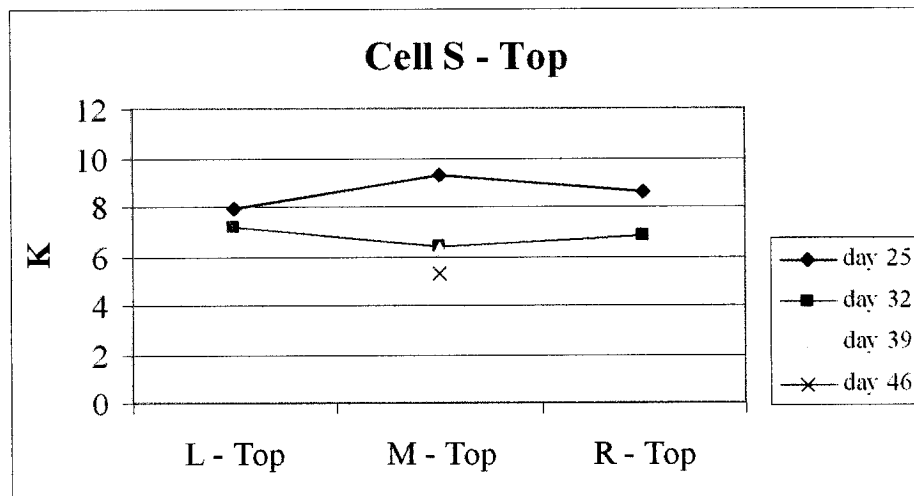


Figure 4-47 UV/VIS spectrometer results for cell S (control cell) on different days of sampling

*K = relative aromatic hydrocarbon content

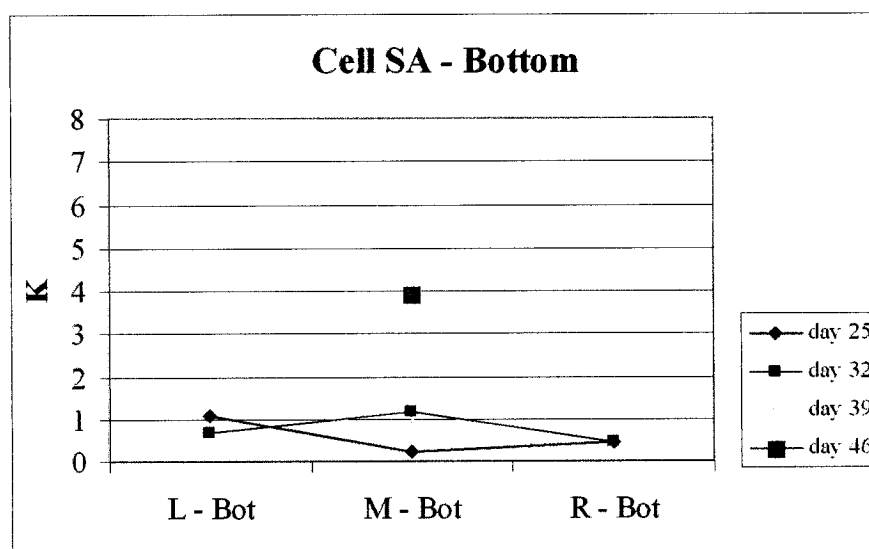
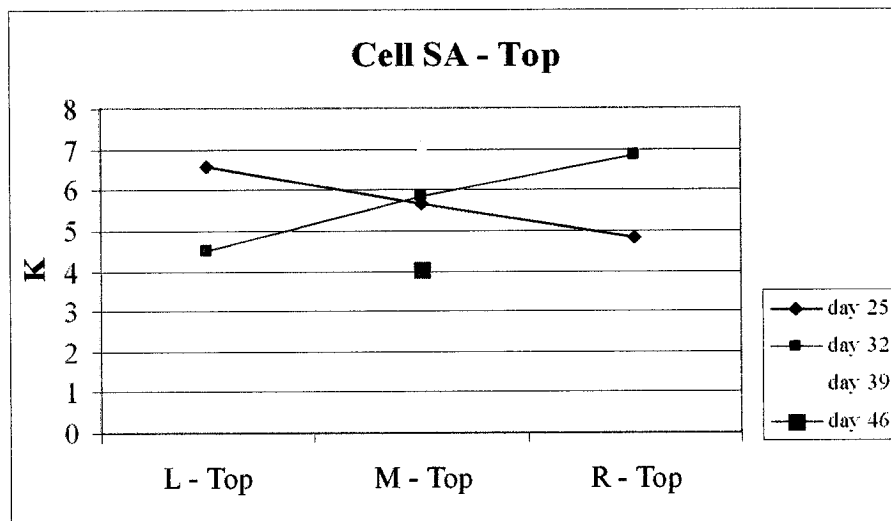


Figure 4-48 UV/VIS spectrometer results for cell SA (control cell) on different days of sampling

*K = relative aromatic hydrocarbon content

4-6) Relative aliphatic hydrocarbon content

This section deals with the results of the FTIR spectrometer test. Figure 4-49 shows the K'_2 value (relative aliphatic hydrocarbon content) for the top and bottom of cell SAE (1.5) on different days of sampling. On day 25, there were some differences between the top and the bottom values in the middle anode area. On day 32, the K'_2 value in the cathode was higher than the anode area, perhaps the result of movements of soils by electrophoretic forces to the anode area. After disconnection, the difference between the top and the bottom values increased.

Figure 4-50 shows the K'_2 value in the top and bottom of cell SAE (0.5). On day 25, the K'_2 value was increasing from the anode to the middle cathode, possibly as a result of horizontal movements (electroosmotic and electrophoretic). The soil was moving toward the anode, so the K'_2 value decreased in that area. The cathode area had mostly water, so the amount of solid was too low to allow performance of the FTIR test. On day 32, the difference between the anode and the cathode values increased, but the top and bottom values were almost equal. After disconnection, the difference between the top and bottom values in all points increased, as had been already observed in cell SAE (1.5). However, this increment was now slow due to the lower voltage, possibly an effect of surfactant on the vertical separation.

Figure 4-51 shows the aliphatic hydrocarbon content for the top and bottom of cell SE (1.5). On day 25, the amount of solid part in the bottom was small, showing that almost all fractions in the cathode area were liquid. On day 32, the difference between the top and bottom values in three points (cathode, middle cathode, and middle areas) decreased, but the difference between the top and bottom values in the anode and the middle anode

increased. This shows that the cathode and middle areas had more liquid in the top and bottom. On day 39 (one week after disconnection), the sample from the top in the cathode area was mostly liquid meaning insufficient solids for a FTIR test. On day 46, again there were some variations in the middle point.

Figure 4-52 shows the K'_2 value in the top and bottom of cell SE (0.5). On day 25, the difference between the top and bottom values in the cathode, middle cathode, and middle areas was high, but the top and the bottom of the anode area showed almost the same K'_2 . On day 32, the difference between the cathode and anode values in both top and bottom increased. The data appear to show that on day 25 there was more vertical separation, and on day 32 more horizontal movements of particles. On day 39 (one week after disconnection), the difference between the anode and cathode values decreased, and on day 46 this difference increased again. The lower amount of K'_2 near the anode area could be as a result of existence of more soil in that area.

Figure 4-53 shows the K'_2 value in the top and the bottom of the control cell S. The results of FTIR for the top and the bottom of all points in cell S were approximately equal. The aliphatic hydrocarbon content in the bottom was a little higher because of sedimentation phenomena; these differences were negligible.

Figure 4-54 shows the aliphatic hydrocarbon content in the top and bottom of control cell SA. On day 25, K'_2 (hydrocarbon/soil) in the top was a little higher than on other days, but the other points showed almost the same values. The difference could be the result of errors during the test. In the bottom, K'_2 was very low because the sample was mostly water. On day 46, the K'_2 value increased because the water was evaporated;

subsequently, the top and the bottom showed nearly the same K'_2 values. The average error calculated for FTIR analysis was 12.6%.

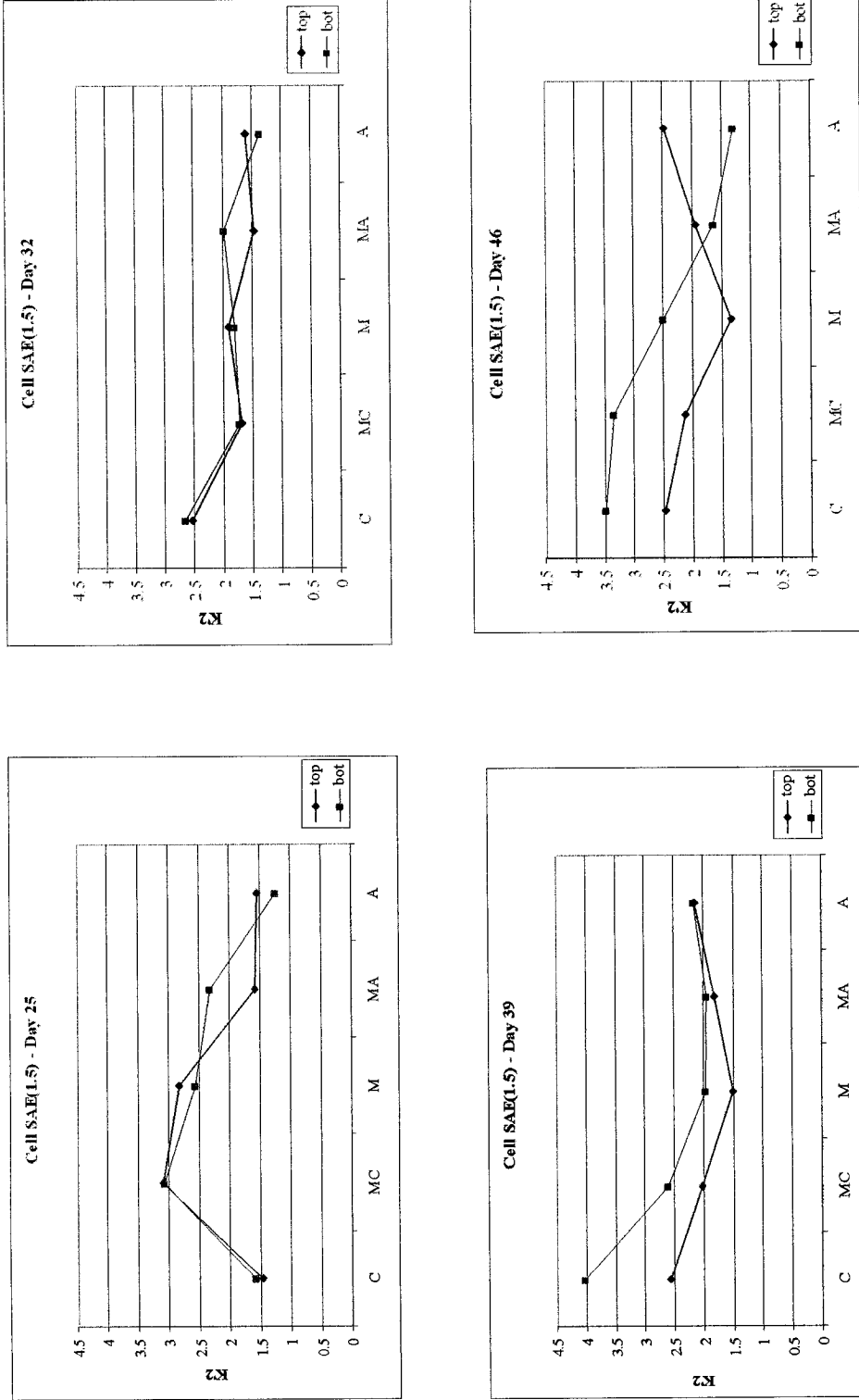


Figure 4-49 FTIR test results for cell SAE (1.5) on different days of sampling

*K₂ = relative aliphatic hydrocarbon content

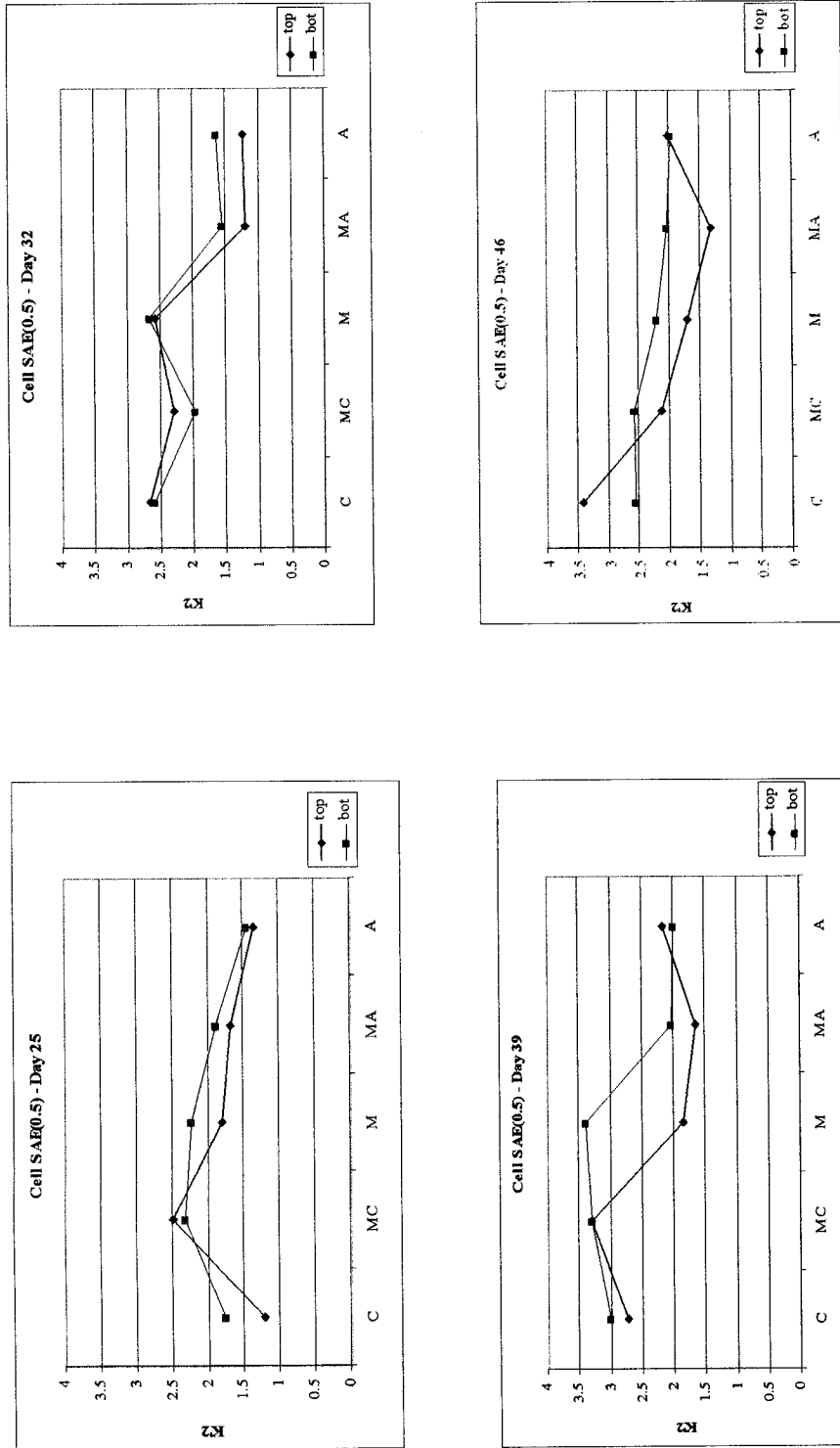


Figure 4-50 FTIR test results for cell SAE (0.5) on different days of sampling

* K_2 = relative aliphatic hydrocarbon content

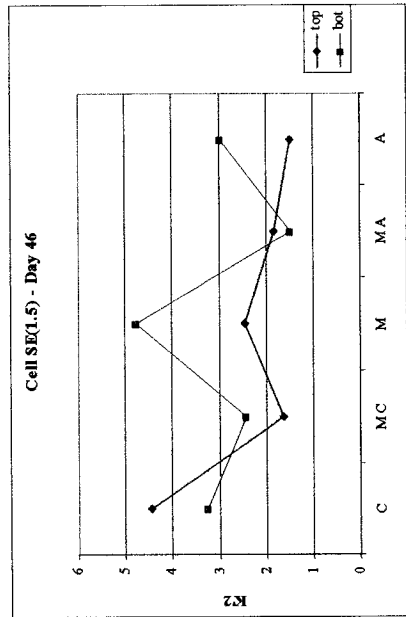
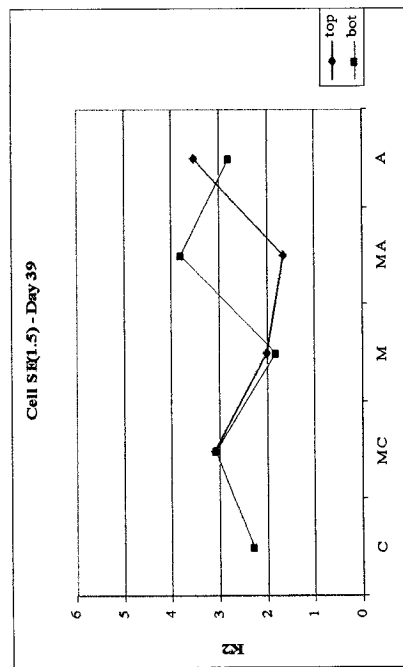
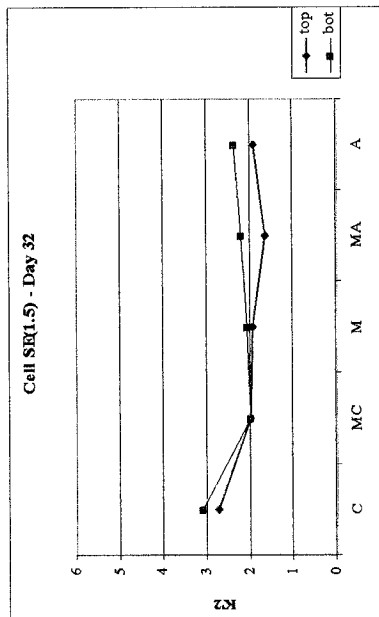
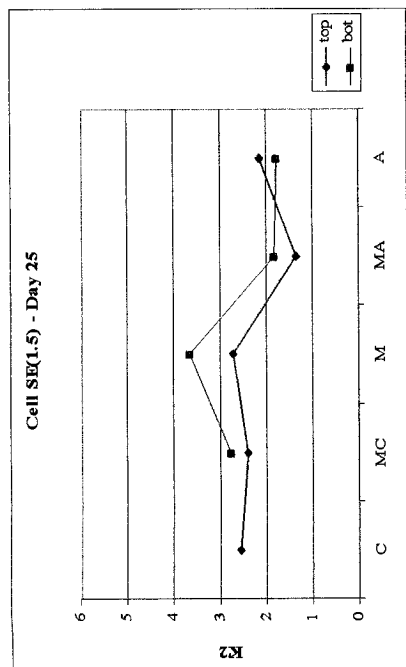


Figure 4-51 FTIR test results for cell SE (1.5) on different days of sampling

*K₂' = relative aliphatic hydrocarbon content

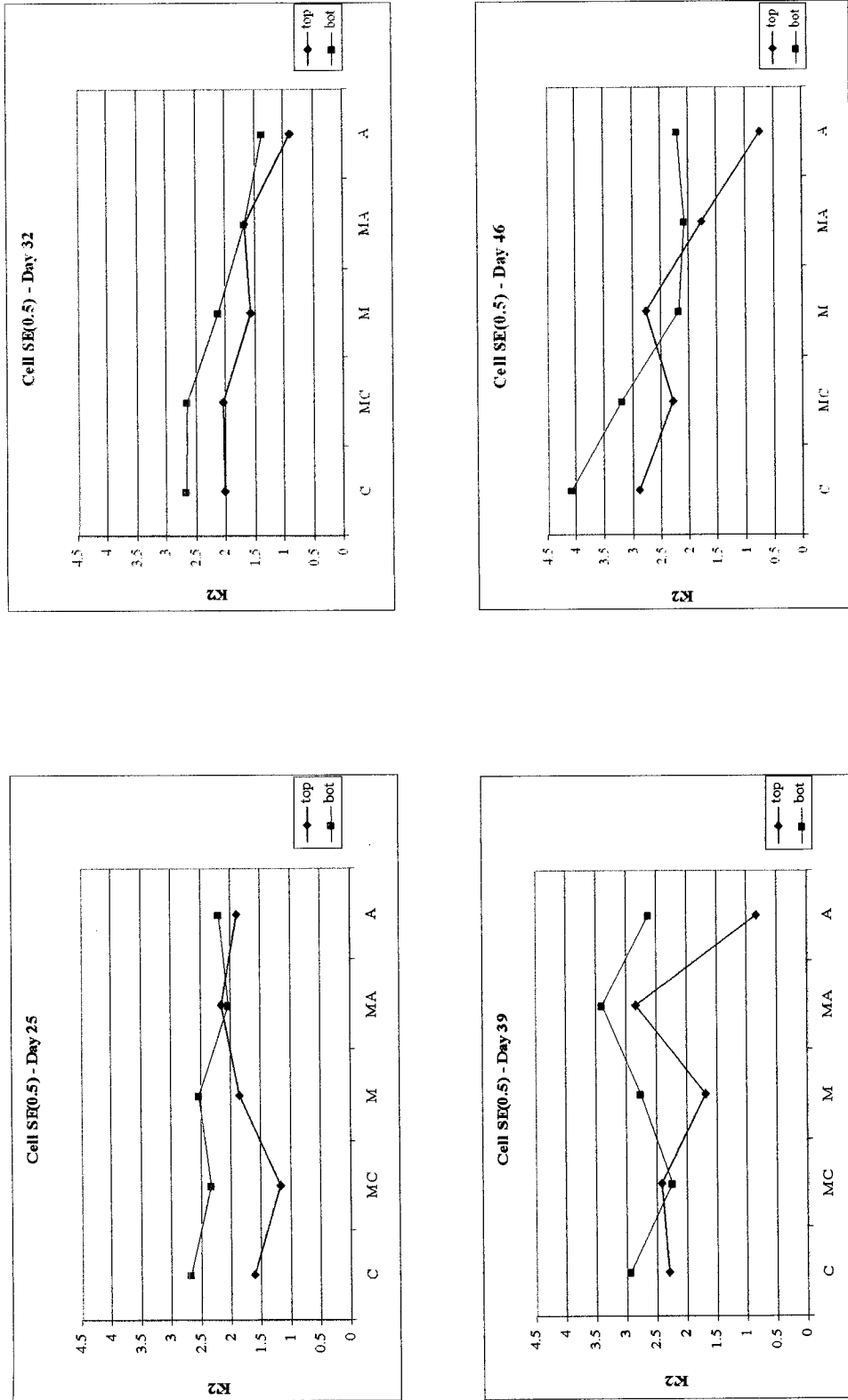


Figure 4-52 FTIR test results for cell SE (0.5) on different days of sampling

*K₂' = relative aliphatic hydrocarbon content

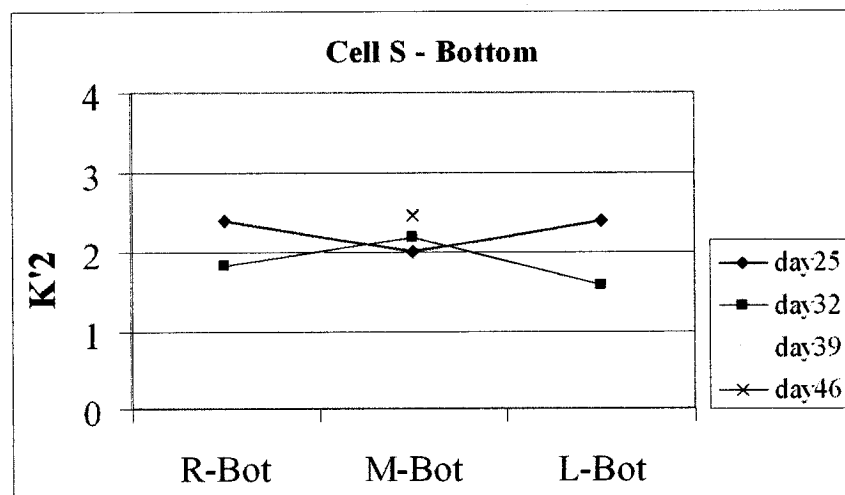
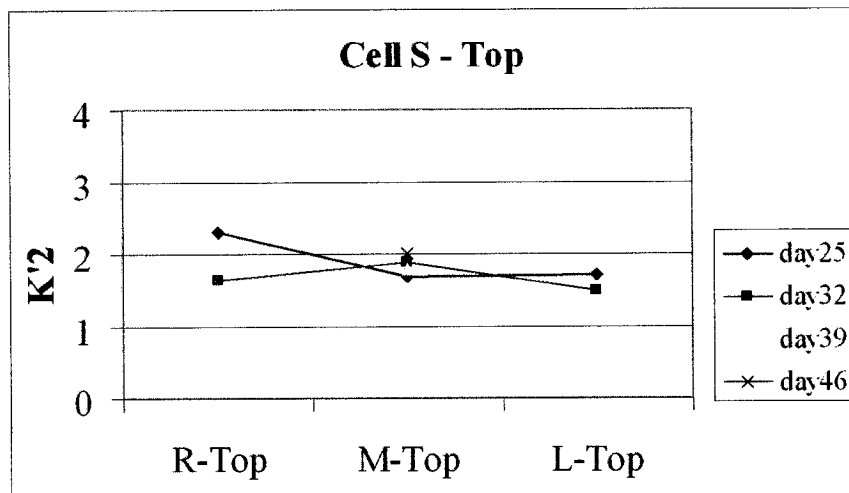


Figure 4-53 FTIR test results for cell S on different days of sampling

*K'₂ = relative aliphatic hydrocarbon content

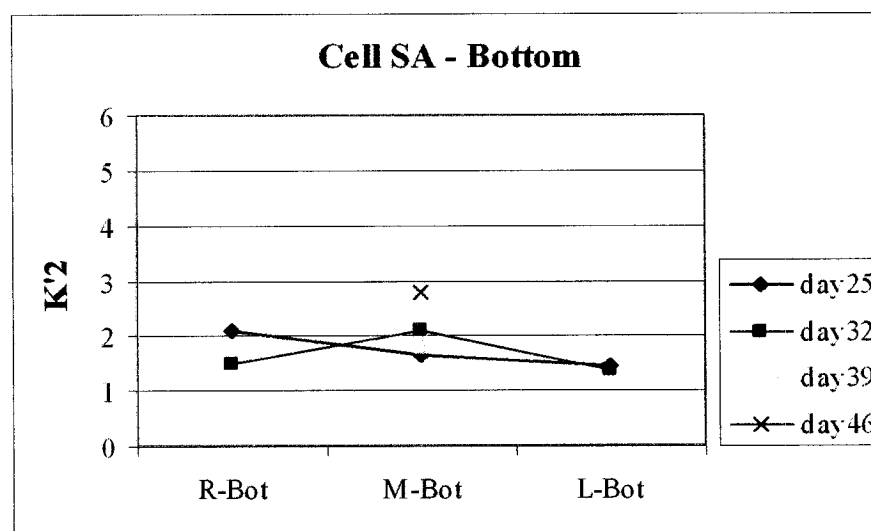
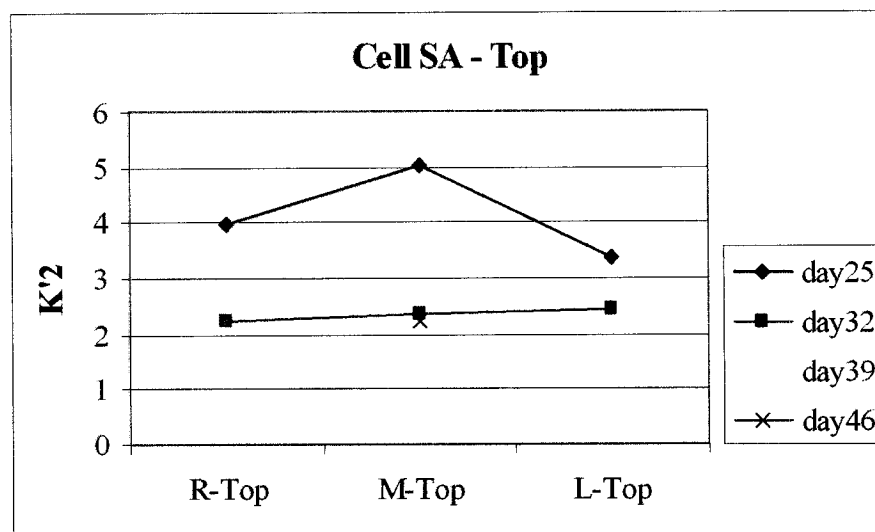


Figure 4-54 FTIR test results for cell SE on different days of sampling

* K'_2 = relative aliphatic hydrocarbon content

4-7) Fractal analysis

Table 4-3 shows the results for fractal analysis of the remaining solid phase in each cell after the experiment.

Table 4-3 Results of fractal analysis

Cell	D_f
SE (1.5)	1.77
SAE (1.5)	1.71
SE (0.5)	1.79
SAE (0.5)	1.75

The fractal dimension for all cells was around 1.7. In this experiment, two-dimensional fractal analysis was applied.

4-8) Power and energy consumption

Figure 4-55 illustrates the power consumption in all cells on different days; cells with higher electrical potential showed much higher power consumption during first 13 days. In all cells, power consumption decreased with time. For the same electrical potential, the cells that contained amphoteric surfactant consumed more power. After 25 days, all cells showed very low power consumption, perhaps as a result of accumulation of solid particles near the anode area and increment of the resistance in the cells.

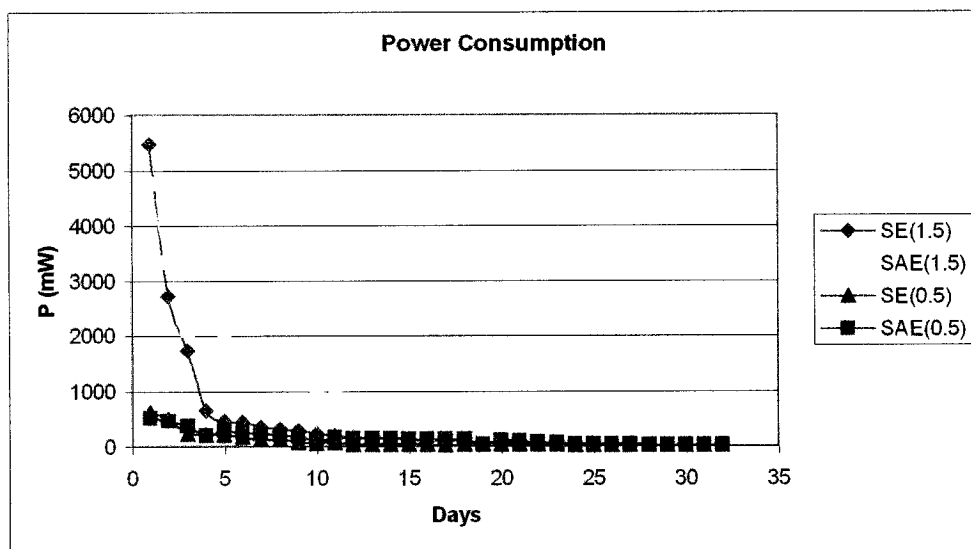


Figure 4-55 Power consumption changes

Figure 4-56 summarizes the energy consumption of each cell. The highest energy consumption occurred for the cell SAE (1.5), which had a higher electrical potential and amphoteric surfactant than other cells. The lowest energy consumption occurred for the cell without amphoteric surfactant and lower electrical potential (SE (0.5)).

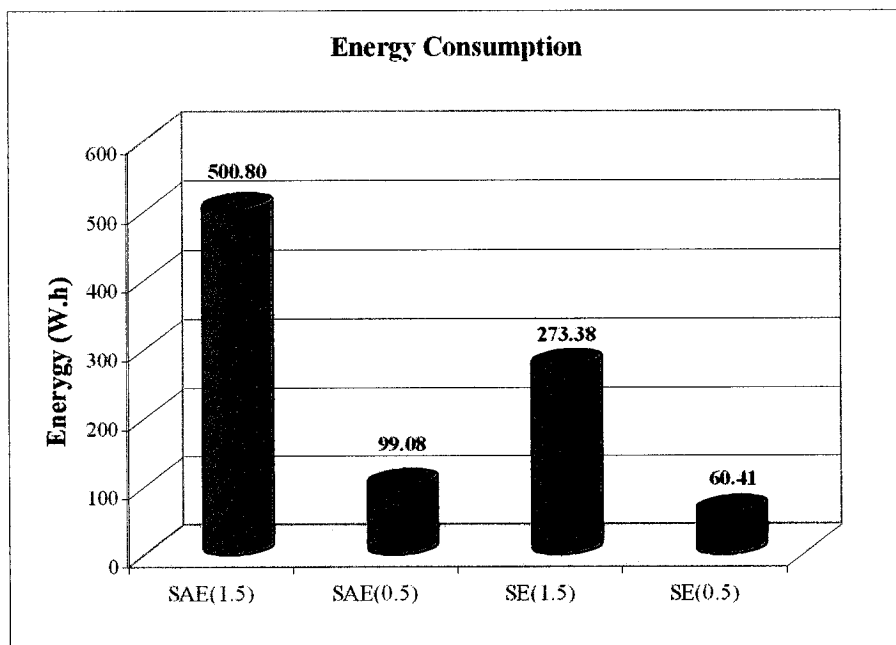


Figure 4-56 Energy consumption in different cells

The results show that most of electrokinetic phase separation took place during the first 21 days. Using \$0.03/kWh as the price of electric power, the cost of power for different cells for 21 and 32 days of the experiment are summarized in Table 4-4.

Table 4-4 Cost of power consumption in each cell

		SAE (1.5)	SAE (0.5)	SE (1.5)	SE (0.5)
21 days experiment	KWh	0.482	0.089	0.265	0.056
	KWh/ m ³ of oily sludge	482	89	177	37
	\$/ m ³ of oily sludge	14.46	2.67	5.31	1.11
32 days experiment	KWh	0.500	0.099	0.273	0.060
	KWh/ m ³ of oily sludge	500	99	182	40
	\$/ m ³ of oily sludge	15	2.97	5.46	1.2

4-9) Repeatability of the experiment

As mentioned in Chapter 3, Concordia research team under supervision of Dr. Elektorowicz has performed an extensive research on the application of electrokinetics to soil and diesel-soil-water-surfactant media (Hatim 1999; Norssair 1995, 1996a, b; Jesien 1995, 1996). Those previous experiments demonstrated a high repeatability of results with a relatively small errors (10-15%). Subsequently, instead to repeat the experiment on identical media, the developed technology was verified on the same system (oily sludge) where the ratio of the components in the suspension varied (Chap. 7). Although different

media was studied; this case study permitted to observe the same processes and confirm validity of developed theories.

Chapter 5

Theory of electro-separation and model development

The results from previous chapters permitted an assessment of the thermodynamics of the proposed process and the introduction of a new model for the colloidal fraction behavior in oily sludge under different electrical potentials. In addition, i) the effect of amphoteric surfactant on the system was explained, ii) value-added products was defined in relation to revitalization of oily sludge.

As mentioned in Chapter 4, following the electro-demulsification, the electro-coagulation of the separated solid phase started near the anode area. The separated water and liquid hydrocarbon produced secondary oil-in-water emulsions. They were not very stable and could move toward the cathode area (Figure 5-1). These secondary oil-in-water emulsions gradually electro-coalesced along the cell, mostly near the cathode area, and two separated phases of water and hydrocarbon formed. Visual observations confirmed this statement.

Gradually, the concentration of separated solid phase in the anode area increased (difficulties during sampling confirmed this idea), and collision between suspended solids increased, so the rate of sedimentation near anode and, consequently, the resistance in that area also increased. The rate of aggregation depends strongly on the electrical potential, a phenomenon that can be explained by the coagulation theory of colloids. As mentioned in the literature review, there are two kinds of coagulation: fast coagulation that produces looser particles and slow coagulation that produces compact particles (Figure 5-2). In this experiment, higher electrical potential produced faster coagulation, but the remaining solid particles were loose. However, while lower electrical potential

Cells without Surfactant

Cells with Surfactant

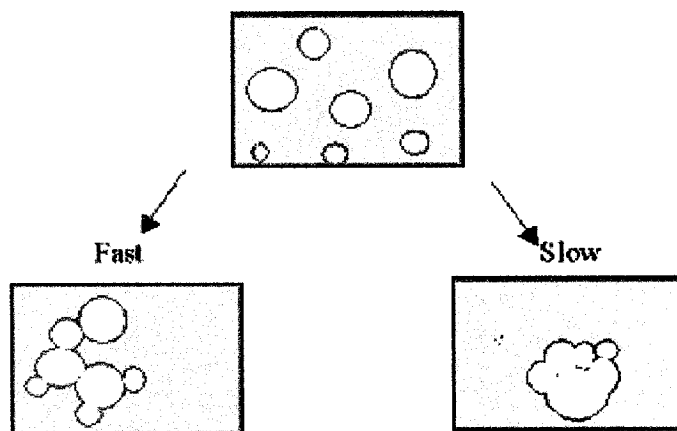
Higher
Voltage

Lower
Voltage



Figure 5-1 Behavior of colloidal particles

was applied, the remaining solids showed a more compact structure. The formation of the remained solids was slower in the cell with the lower voltage, but it was higher than in the cell with higher voltage. It can be concluded that lower electrical potential separated



solid phases more efficiently.

Figure 5-2 Fast and slow coagulation

As noted in the literature review, the oily sludge is water slurry that contains a high level of oil and grease, corrosion products, sulfur, water, minerals, metals and petroleum solid particles in various proportions depending on its origin. Asphaltenes are identified as the stabilizing agent for water-in-crude oil emulsions. They can exist in a hydrocarbon mixture as colloidal particles, particulate, or molecular surfactant (Gafonova and Yarranton, 2000). It is believed that solids precipitate with the asphaltenes.

5-1) New developed model

Several forces influence the movements of colloidal particles in this experiment. The sketch in Figure 5-3 shows different forces in the x-axis and y-axis, and also the total driving force resulting from the momentum balance between these forces.

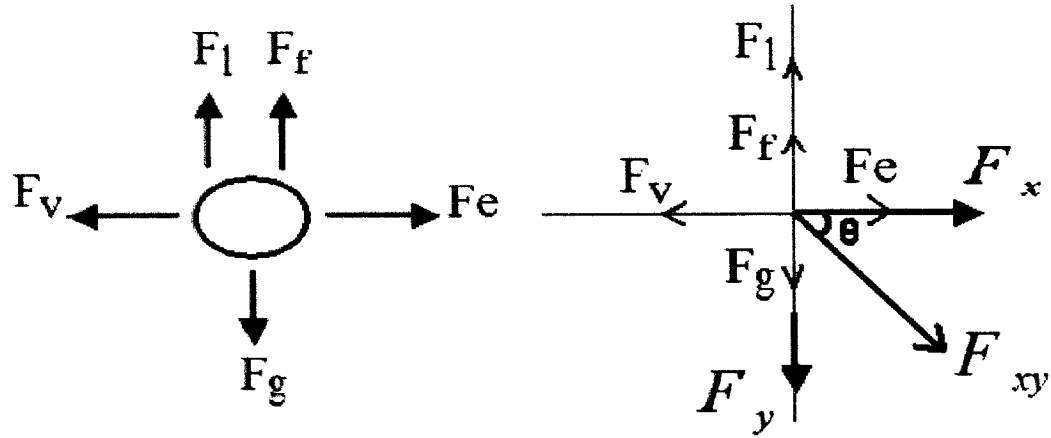


Figure 5-3 (a) Forces acting on a colloid particle,
(b) The total driving force (F_{xy}) and its direction

5-1-1) Momentum balance between forces in x- axis (F_x)

The driving force of a colloid, F_e , (electrophoretic) in an electrical field is equal to the electrical field strength, E (Volt/cm), times the charge of the colloid, Q (Coulomb).

$$F_e = EQ \quad (5.1)$$

The rate of migration of a colloid particle can be altered by changing the distance between electrodes as well as by changing the electrical potential. By assuming the colloidal particles are spheres, and recalling that the zeta potential, ζ , on a charged sphere is related to the charge by the following equation

$$\zeta = \frac{Q}{4\pi\epsilon a} \quad (5.2)$$

where ϵ is dielectric constant of the liquid phase and a is the radius of the colloid particle, so the electrical force will be

$$F_e = f(ka)E\zeta\pi\epsilon a \quad (5.3)$$

where “ $1/k$ ” is the thickness of the double layer and $f(ka)$ is a function introduced by Henry in the 1930s, which varies from 1 to 1.5 as ka varies from 0 to ∞ . In this situation, the double layer around the particle is very thin compared with its radius ($ka \gg 1$), so based on Smoluchowski's solution, $f(ka)$ equals 1.

The resisting force in the x-axis direction (F_v) is given by the Stokes equation, which is proportional to the frictional coefficient (f) and the velocity of the colloidal particle (v_x).

$$F_v = f v_x \quad (5.4)$$

The friction factor f , which measures how strongly the surrounding fluid resists the motion of the particle, is a function of the size and shape of the particle and the viscosity of the fluid. In this case, it is assumed that the colloid particle is spherical with radius a , immersed in an emulsion of water and liquid hydrocarbon with dynamic viscosity of η , so using Stokes relation

$$f = 6\pi\eta a \quad (5.5)$$

the resisting force will be

$$F_v = 6\pi\eta a v_x \quad (5.6)$$

By applying Newton's second law, the total driving force in x-axis direction (F_x) can be measured.

$$F_x = F_e - F_v \quad (5.7)$$

$$F_x = 4E\zeta\pi\epsilon a - 6\pi\eta a v_x \quad (5.8)$$

$$F_x = 2\pi a(2E\zeta\epsilon - 3\eta v_x) \quad (5.9)$$

5-1-2) Momentum balance between forces in y- axis (F_y)

As shown in Figure 5-2, in y-axis, a colloidal particle is subject to forces, such as gravity force (F_g), lifting force (F_l), and frictional drag force (F_f).

The gravity force is given by

$$F_g = \rho_p V_p g \quad (5.10)$$

where

ρ_p is the density of the colloid particle

V_p is the volume of the colloid particle

g is gravitational acceleration

The lifting force (F_l) is given by

$$F_l = \rho_l V_p g \quad (5.11)$$

where ρ_l is the density of the liquid phase.

The frictional drag force in y-axis (F_f) depends on the particle velocity, density of liquid phase, projected area, and a drag coefficient, which is given by

$$F_f = \frac{C_d A_p \rho_l v_y^2}{2} \quad (5.12)$$

where

C_d is the drag coefficient

A_p is the projected area of the particle perpendicular to the velocity

v_y is the velocity

To find the total driving force in y-axis (F_y) Newton's second law gives us

$$F_y = F_g - F_l - F_f \quad (5.13)$$

Inserting F_g , F_l and F_f in (5.13) yields

$$F_y = g(\rho_p - \rho_l)V_p - \frac{C_d A_p \rho_l v_y^2}{2} \quad (5.14)$$

By assuming that the colloid particle is a sphere with a radius of a , the V_p and A_p can be calculated by

$$V_p = \frac{4}{3}\pi a^3 \quad (5.15)$$

and

$$A_p = \pi a^2 \quad (5.16)$$

In this system, the flow is assumed to be laminar, so C_d can be calculated by

$$C_d = \frac{24}{R_n} \quad (5.17)$$

where R_n is the Reynolds number and is given by

$$R_n = \frac{2v_y a \rho_l}{\eta} \quad (5.18)$$

By inserting V_p , A_p , C_d , and $\rho = (\rho_p - \rho_l)$ in equation (5.14), it can be simplified as

$$F_y = \frac{4}{3}\pi g a^3 \rho - 6\pi\eta a v_y \quad (5.19)$$

5-1-3) Momentum balance (F_{xy})

The total driving force (F_{xy}) on the colloid particle in the electrical field in this experiment can be calculated by the momentum balance between F_x and F_y .

$$F_{xy} = m_t \frac{d\bar{v}}{dt} = \sqrt{F_x^2 + F_y^2} \quad (5.20)$$

where \bar{v} is the velocity of particle in F_{xy} direction and m_t is the total mass of colloidal particle, which is a function of time and distance from cathode and can be calculated by

$$m_t = m_w + m_{lh} + m_s \quad (5.21)$$

where

m_w is mass of water phase

m_{lh} is mass of liquid hydrocarbon phase

m_s is mass of solid phase

As the colloid particle moves because of horizontal and vertical forces, electro-demulsification takes place and these phases move in different directions. The separated water and liquid hydrocarbon move toward the cathode as a result of electroosmosis. The remaining particles move in the direction of F_{xy} and they eventually loose their liquid parts and settle in the anode area.

By inserting F_x and F_y in equation (5.20), F_{xy} can be calculated as follows:

$$F_{xy} = m_t \frac{d\bar{v}}{dt} = \sqrt{[2\pi a(2E\zeta\varepsilon - 3\eta v_x)]^2 + \left(\frac{4}{3}\pi g a^3 \rho - 6\pi\eta a v_y\right)^2} \quad (5.22)$$

which can be simplified to

$$F_{xy} = m_t \frac{d\bar{v}}{dt} = \sqrt{F_v^2 \left[\left(\frac{v_x}{v_y} \right)^2 + 1 \right] + 2F_f F_e + F_e^2 + 16\pi^2 g a^4 \left(\frac{g a^2 \rho}{9} - \rho \eta v_y \right)} \quad (5.23)$$

By considering $K_f = 16\pi^2 g a^4$ as a constant, equation (5.23) can be simplified as

$$F_{xy} = m_t \frac{d\bar{v}}{dt} = \sqrt{F_e^2 + 2F_f F_e + F_v^2 \left[\left(\frac{v_x}{v_y} \right)^2 + 1 \right] + k_f \rho \left(\frac{g a^2 \rho}{9} - \eta v_y \right)} \quad (5.24)$$

As the colloid particle moves, its total mass decreases and the difference between the density of the liquid and solid increases because more liquid is being separated, so the density of solid increases.

Equation (5.24) is the simplified version of the total driving force on a colloidal particle in a system that contains oily sludge under the influence of the electrical field. The direction of this force can be measured by

$$\tan \theta = \frac{F_y}{F_x} \quad (5.25)$$

5-2) Rate of electro-demulsification of aromatic hydrocarbons

As mentioned in Chapter 4, the relative aromatic hydrocarbon content of each cell was measured by UV/VIS spectra on different days. Figure 5-4 shows the changes in relative aromatic hydrocarbon content due to the electro-demulsification at different distances from the cathode in the top layer of the cells.

As illustrated in Figure 5-4, the relative aromatic hydrocarbon decreases as the distance from the cathode rises. Kinetic explanation for the electro-demulsification process has been attempted. The figure represents the changes in the relative aromatic hydrocarbon for all cells during 25 to 32 days of the experiment. The demulsification rate constant for each point can be estimated from the slope of the line that shows the changes of that point versus time. The rate constant as a function of distance from the cathode for each cell can be expressed as follows:

$$\text{Cell SE (1.5):} \quad K_a = -5.7678 \ln(x) + 0.103 \quad (5.26)$$

$$\text{Cell SE (0.5):} \quad K_a = -6.2201 \ln(x) + 1.8525 \quad (5.27)$$

$$\text{Cell SAE (1.5):} \quad K_a = -7.3592 \ln(x) + 2.7414 \quad (5.28)$$

$$\text{Cell SAE (0.5):} \quad K_a = -2.638 \ln(x) - 0.4273 \quad (5.29)$$

Where K_a is rate of electro-demulsification and x is the distance from the cathode. The r^2 (coefficient of determination) is approximately 0.9 for all equations. The general form for the rate of electro-demulsification of aromatic hydrocarbon from colloidal particles can be expressed by:

$$K_a \propto -n(V, C_s) \ln(x) \quad (5.30)$$

The rate of electro-demulsification (K_a) is proportional to $\ln(x)$. K_a is related to distance by n , which is a function of electrical potential (V) and concentration of surfactant (C_s). The negative sign demonstrates that the rate of separation of liquid hydrocarbon is higher near the cathode and, by moving toward the anode area, this rate decreases. This phenomenon can be explained by the amount of solid particles in these two areas. Yan et al. (1997) found that as the amount of solid particles increases as the rate of demulsification decreases. Because of horizontal movement, the particles move toward the anode area (electrophoresis) and the liquid part moves toward the cathode area (electro-osmosis); therefore, the amount of solid particles decreases in the cathode area and the rate of aromatic hydrocarbon separation increases. As described in the literature review, higher pH value in the cathode area is another factor that may enhance the separation of solid particles and, therefore, increase the demulsification rate in that area.

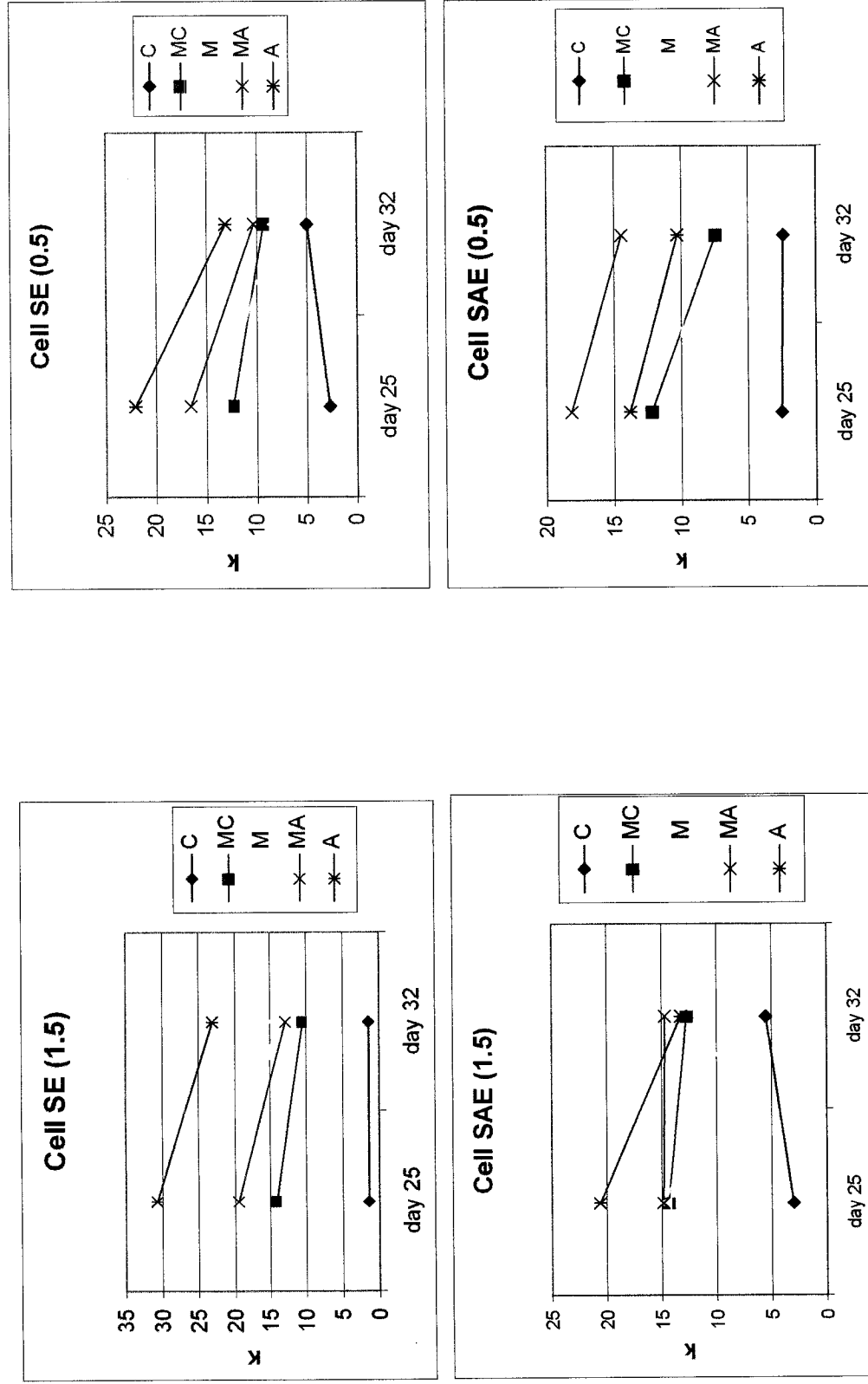


Figure 5-4 Relative aromatic hydrocarbon content at different distances from the cathode

5-3) Demulsification rate

Demulsification of a stabilized water-in-oil emulsion during a batch operation proceeds as (Hartland and Vohra, 1980; Yan and Masliyah, 1995b)

$$\frac{H}{H_0} = \exp(-k_d t) \quad (5.31)$$

where H_0 and H represent the height of the emulsion before and after the experiment, respectively. k_d is the overall demulsification rate constant, and t is the duration of the experiment.

The demulsification rate constant for each cell during 32 days of the experiment (during the period when the electrical current was connected to the system) is summarized in Table 5-1.

Table 5-1 Demulsification rate in electrokinetic cells

Cell	H_0	H	k_d (1/day)
S	4.5	3.5	0.007
SA	5	4.2	0.005
SAE (1.5)	5.3	3.1	0.0167
SAE (0.5)	5	2.8	0.0181
SE (1.5)	5	3	0.0159
SE (0.5)	5	2.5	0.021

By comparing cell SE (0.5), which is the cell without surfactant and with lower electrical potential to cell S, which is the control cell with sludge and without electrical connection, it can be concluded that this amount of electrical potential has increased the demulsification rate by 200 %. As shown in Table 5-1, electrokinetics increased the

demulsification rate by high percentages. The lower the applied electrical potential, the higher the demulsification rate. The best demulsification result was obtained for the cell with lower electrical potential and without surfactant; it was almost 16 % higher than in the cell with the same electrical potential and with amphoteric surfactant.

5-4) Effect of resistance distribution on the dynamics of the process

In this section, the resistance distribution in each cell during the experiment and its effect on the thermodynamics of the process is defined. By drawing comparisons between cells, it was found that the cells, which contained sludge and surfactant, (SAE (1.5) and SAE (0.5)), showed high resistance. Two separated areas could be distinguished in these cells. The rate of vertical separation (electro-demulsification) of phases in the first days of the experiment was higher than electroosmotic and electrophoretic movements (horizontal movements). After a time, because of accumulation of solid particles near the anode, the electroosmotic and electrophoretic movements showed higher rates, so the resistance near the anode increased. Solid phase formation in cell SAE (1.5) started faster than in cell SAE (0.5).

The highest resistance value reported in all cells was in the anode area of cell SAE (1.5), which was almost 3100 Ω . During the first days of the experiment, when the rate of vertical separation was higher, the resistance in cell SAE (0.5) was a little higher than in cell SAE (1.5). This could be as a result of formation of cylindrical micelles in cell SAE (0.5). Petit et al. (2001) in an experiment without using electrokinetics demonstrated that at low water content, spherical reverse micelles are formed in sludge. It was found that with some surfactants, or due to increasing the water content, spherical water-in-oil

droplets change to cylindrical. As stated in the literature review, the reduction in repulsive forces between hydrophiles in amphoteric surfactants, increases the number of molecules in the micelle. This can cause closer packing of molecules within a spherical micelle that may be followed by a sphere-to-rod transition. One method for reducing the hydrophilic repulsion is reducing the pH; as the pH decreases, the hydrophilic repulsion decreases. In present electrokinetic experiment, the lower pH in cell SAE (0.5) during the first days of the experiment followed this theory.

As stated in Chapter 4, the behavior of the resistance in cells SAE (1.5) and SAE (0.5) can be best described by equation (5.32)

$$R = b' \exp (c' t) \quad (5.32)$$

where b' and c' are function of sludge characteristics, surfactant characteristics, electrical potential and the distance from the cathode. R is the resistance and t is the duration time.

Different zones were observed in two cells without surfactant (SE (1.5) and SE (0.5)). These zones differ with changes in electrical potential. Solid phase formation in cell SE (1.5) started sooner than in cell SE (0.5). Electroosmotic and electrophoretic movements in cell SE (1.5) started on day 1 of the experiment, but in cell SE (0.5) they started one day later. During days 4 to 9, both cells had faster vertical separation than horizontal movements. After day 19, they started to act differently. Because of higher voltage, the horizontal movements in cell SE (1.5) were faster than in cell SE (0.5). Therefore, the resistance in the anode area in cell SE (1.5) was increasing very fast until day 18.

In cell SE (0.5), these horizontal movements were slower; consequently, the vertical movement (electro-demulsification) had a greater chance to act at the same time. After day 15, the amount of liquid in the anode area was again increased, so the resistance

decreased. In cell SE (1.5) very fast movements of solid particles toward the anode area did not permit a substantial vertical separation. Therefore, the effect of vertical separation was much lower than in cell SE (0.5). The increment in rate of resistance in the cell with higher voltage was faster than in the cell with lower voltage as a result of faster accumulation of solid particles in the anode area. In the cell with lower voltage, cell SE (0.5), the increment of resistance was slower, so enough time was available for vertical and horizontal movements. Thus, more efficient separation of phases occurred in this cell. As mentioned already, the vertical and horizontal movements in the cell SE (0.5) allowed more liquid separation from the colloids. This was the reason for the lowest resistance in this cell compared to the other three cells.

As noted in Chapter 4, the behavior of the resistance in the cells SE (1.5) and SE (0.5) can be best described by equation (5.33)

$$R = b t^c \quad (5.33)$$

where b and c are function of sludge characteristics, electrical potential and the distance from the cathode. R is the resistance and t is the duration.

By comparing equation (5.32) with equation (5.33), it can be concluded that the addition of surfactant increased the resistance exponentially, so the power consumption increased more in these cells. Also, the amount of solid in emulsions that remained at the end of the experiment was higher in cells with surfactant, which means a lower efficiency in the electro-demulsification of phases. Power consumption comparison between the cells will be discussed in section 5-14.

5-5) Amphoteric surfactant behavior under the electrical field

In this section the behaviour of an amphoteric surfactant (C12-C14-Alkyl-Dimethyl-Betain) within the electrical field is investigated. Comparison between the resistance distributions of two cells that contained surfactant solution under different electrical field showed that, in cell AE (0.5), the resistance was a little higher than in cell AE (1.5). This could be as a result of formation of different kinds of micelles. These two cells had different gradients of pH, mostly during the first 10 days. During these 10 days, the pH value in the cathode area of the cell with lower voltage (AE (0.5)) was lower than in the cell with higher voltage (AE (1.5)). As stated in the literature review, in a low pH environment, hydrophilic repulsion in micelles is reduced and the molecules aggregate more easily. This causes closer packing of molecules within a spherical micelle that may be followed by a sphere-to-rod transition. Consequently, they may show different rate of mobility under the electrical field in the solution.

In the first 10 days of the experiment, there were some differences between pH values of the cell with higher voltage (AE (1.5)) and that with lower voltage (AE (0.5)) in the anode area. This higher voltage could cause faster oxidation of the anode in that area leading to the presence of ion species (for example $\text{Fe}(\text{OH})_3$)

In the second day of the experiment, some orange precipitation was seen at the bottom, near the cathode area of cell AE (0.5). This could be attributed to precipitation of micelles, which were larger. As it has been pointed out already, the pH in cell AE (0.5) was lower than in cell AE (1.5). At the lower pH value, the hydrophilic repulsion decreased so it seems that the cylindrical micelles were formed. The sphere-to-rod

(cylindrical micelles) transitions can cause a considerable increase in viscosity, so the resistance in cell AE (0.5) increased.

5-6) Effect of electrical potential on the polarity of the hydrocarbon

The hydrophobic fraction of the crude oil consists of aromatic and aliphatic hydrocarbons. The polarity of the hydrocarbon of the crude oil is mostly related to the aromatic fraction. It has been shown (Lin and Osseo-Asare, 1984) that the organic-aqueous interface is generally negatively charged at high pH values due to adsorption of hydroxyl ions. The aromatic fraction has higher negative charge than the aliphatic fraction, and the polarity of the hydrocarbon can be measured as follows:

$$P = \frac{C_{Ar}}{C_{Al}} \quad (5.34)$$

where P is the polarity of hydrocarbon, C_{Ar} and C_{Al} are the concentrations of aromatic and aliphatic hydrocarbons, respectively. In this experiment, C_{Ar} is the relative aromatic hydrocarbon content, which was measured by UV/VIS spectra, and C_{Al} is the relative aliphatic hydrocarbon content, which was measured by FTIR spectra. The rate of phase separation depends on the polarity of the hydrocarbon mixture. Figures 5-5 and 5-6 show, for the different sampling day, the polarity of hydrocarbons in the top and bottom of the cells without and with surfactant. As illustrated, in all cells there is a great difference between the polarity of cathode and anode in sampling days 25 and 32. In these two days, all four cells were connected to the electrical power. All cells did not show the same behavior on days 39 and 46 of the experiment (after the disconnection of the electrical power).

As stated in the literature review, asphaltenes are large polyaromatic and polycyclic condensed ring compounds that contain heteroatoms such as N, S, and O to form polar groups (Andersen, 1994). Asphaltenes are responsible for the hydrophobicity of the minerals and the stability of the emulsions; decreasing the asphaltene adsorption can decrease this hydrophobicity. Changing the fluid-particle and particle-particle interactions decreases the stability of the emulsions (Yan and Masliyah, 1996).

Electrokinetic phenomena can change the interactions between the particles and also between particles and fluid. In this experiment, colloidal particles in the oily sludge contained asphaltene and minerals, as well as trapped water and lower molecular weight hydrocarbons. The vertical separation (electro-demulsification) and horizontal movements (electro-osmosis and electrophoresis) were responsible for changing the particle interactions in the electrokinetic cells.

The total driving force described in section 5-1 was responsible for the demulsification of the colloidal particles and separation of the solid phase, which mostly contained minerals and asphaltenes. This separated solid phase moved toward the anode area due to electrophoretic phenomena. These solid particles increased the polarity of the anode area compared with in the cathode area (Figure 5-5 and 5-6). Separated liquid, which was a secondary emulsion of water and liquid hydrocarbons, moved toward the cathode area as a result of electro-osmosis. This secondary emulsion contained less aromatic hydrocarbon so the hydrophobic polarity was less than in the anode area. After disconnection, the systems tended to reach a stable condition.

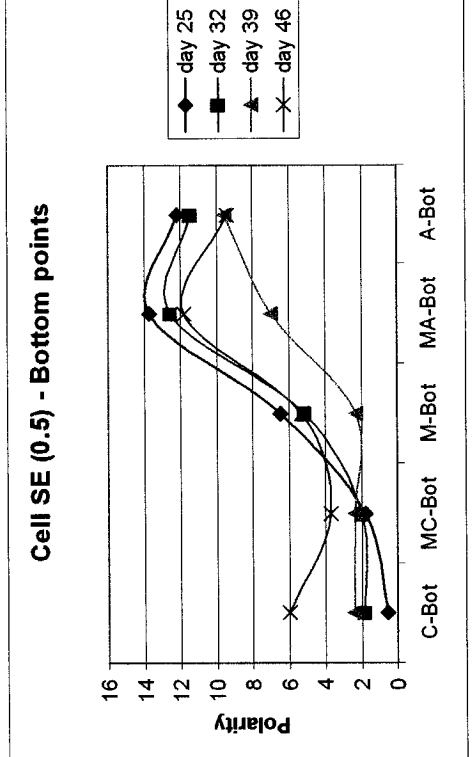
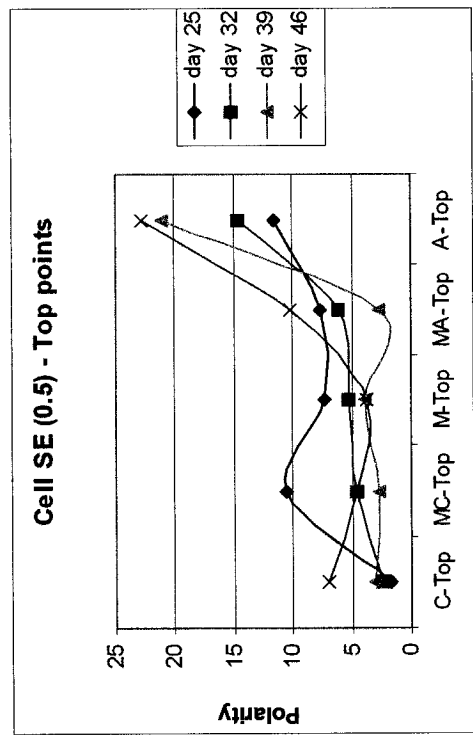
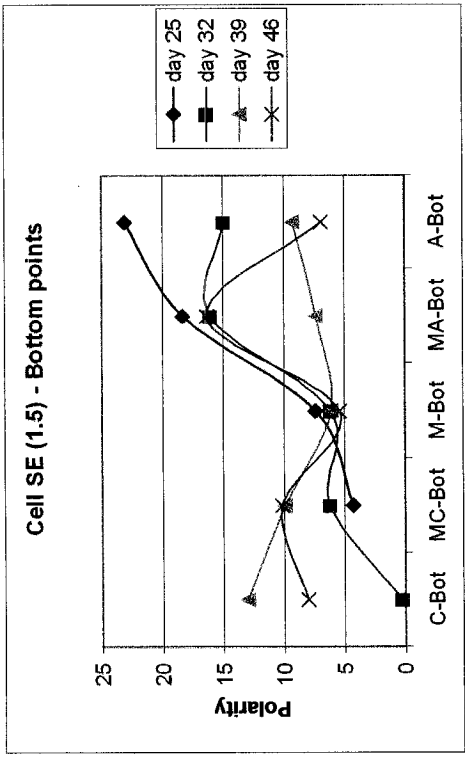
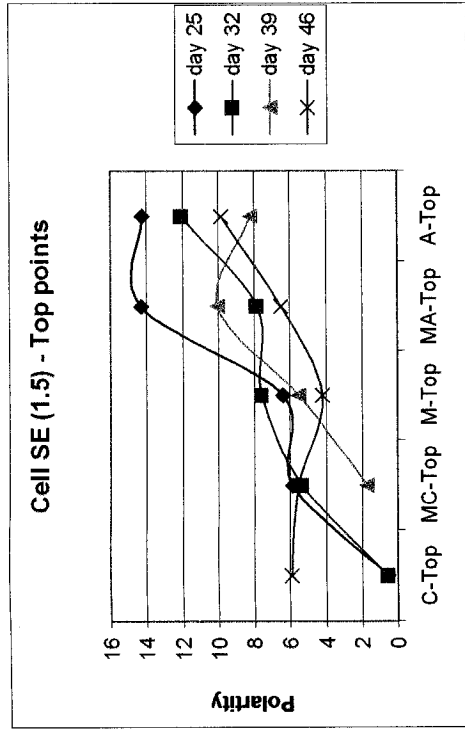


Figure 5-5 Polarity of hydrocarbon in the cells without surfactant

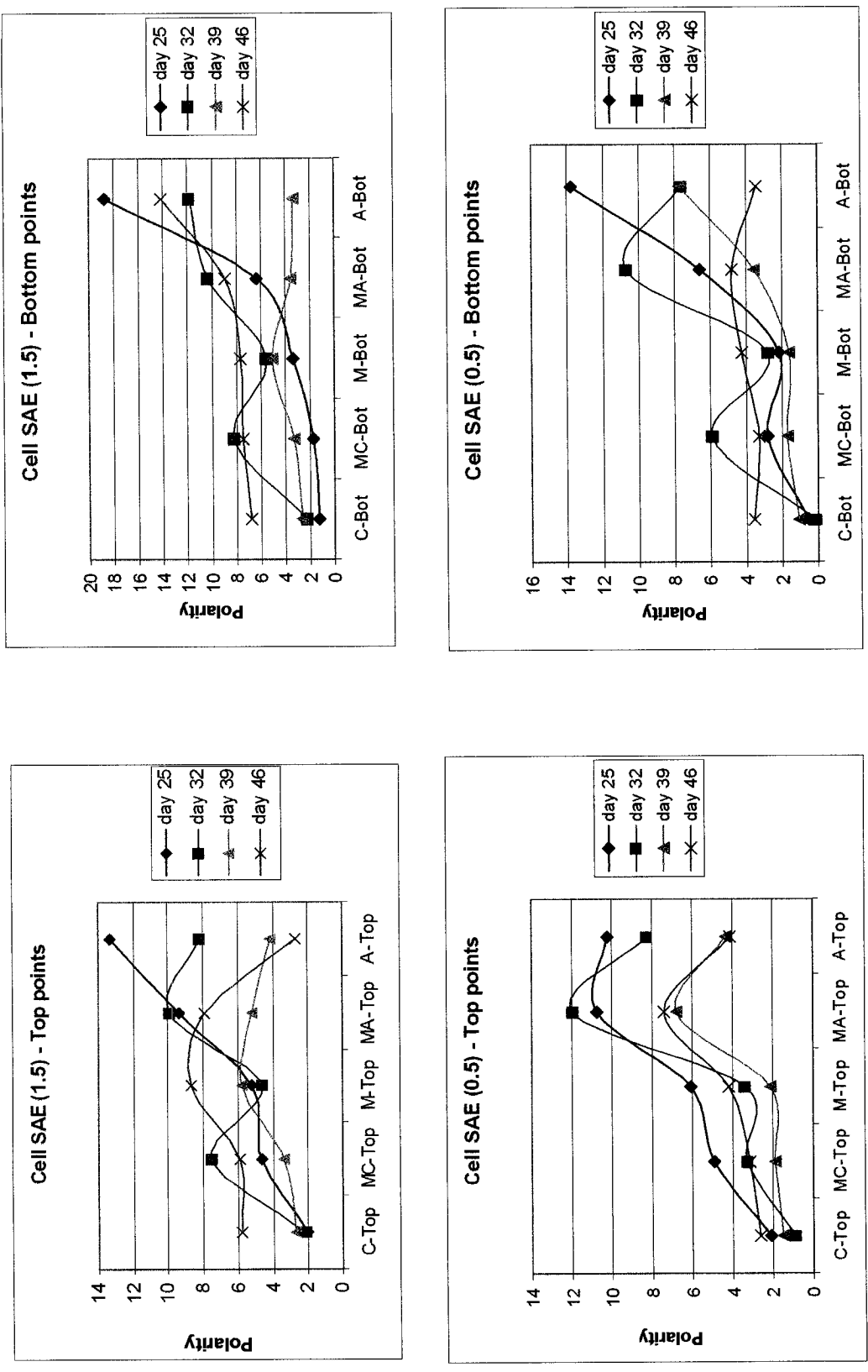


Figure 5-6 Polarity of hydrocarbon in the cells with surfactant

In cells with higher electrical potential, because of fast coagulation, the separated solid particles in the anode area were looser, so after the disconnection system lost its previous condition quickly and polarity distribution had a tendency to be the same in different parts of the cell. In cells with lower electrical potential, as a result of slow coagulation, the separated solid phase in the anode area was more compacted. Therefore, after the disconnection, the polarity distribution was more stable in these cells. This phenomenon is more obvious in cell SE (0.5), which had lower electrical potential without addition of surfactants. In this cell, even after the disconnection, the system kept its previous distribution of polarity.

5-7) Effect of pH distribution on the dynamics of the process

In this section, the pH distribution in each cell during the experiment and its effect on the thermodynamics of the process is defined. As outlined in the literature review, finely divided solids in contact with oil and water form solid-stabilized emulsions. These fine particles are adsorbed at the droplet surface and act as a barrier preventing droplet coalescence and decreasing the demulsification rate constant (Yan et al., 1997). The ability of finely divided solids to stabilize these emulsions is due to the adsorption of asphaltenes and other heavy ends from the oil on the mineral surface, which imparts to the solid hydrophobic nature (Menon and Wasan, 1986). The desorption of solid particles from the oil-water interface can be done by changing the pH value or asphaltene content. Changes in the pH affect the adsorption behavior of solid particles at the oil-water interface. At higher pH values, the solid particles become more hydrophilic, so they are

desorbed from the oil-water interface. Consequently, demulsification can be performed at higher pH environment.

The interfacial tension at the oil-water interface reaches its maximum value at about neutral pH (Menon and Wasan, 1986). It is assumed that the dissociation of the surface asphaltic species contributes significantly to the modification of the electric double layer interaction between the particles. The variation in pH results in dramatic changes in the particle interaction energy; therefore, by changing the pH, the zeta potential of the system can be changed (Yan and Masliyah, 1995).

In this experiment, the electrokinetic phenomena were responsible for the changes of the pH in the system. As mentioned in Chapter 4, the pH value of the initial sludge was around neutral and, during the experiment, a pH gradient was created along the cells. Higher pH values in the cathode area caused more desorption of solid particles from the interface of stable water-in-oil emulsions, so this higher pH value increased the vertical demulsification rate of the colloidal particles.

By comparing values in cells, it is found that at different voltages, the cathode area showed almost the same variations in pH, but the anode area demonstrated very different pH variations. This could be as a result of different degrees of phase separation and movements in these areas. Cell SE (0.5) exhibited the highest difference in pH values between cathode and anode. The rate of the horizontal movements in this cell were slower, but were continuous and more effective. This slow rate permitted more desorption of the solid particles from the interface and, consequently, more liquid separation from the stable water-in-oil emulsions. As it is demonstrated in section 5-3, this cell had the highest demulsification rate among all cells.

5-8) Effect of temperature on the dynamics of the process

During the experiment, the temperature was around 24°C. Forty-three days after disconnecting the system, the separated phases (liquid and solid) from cells were transferred to different containers. All containers were kept at room temperature for two months. To determine the effect of temperature on the separated colloidal solids, they were stored in a refrigerator at 4° C for an additional month. No further separation was observed in the remained colloidal solids of the cells having amphoteric surfactant. The situation in the cells without surfactant was different: lower temperature caused more demulsification of colloidal particles, so more liquid phase was separated. The solid phase settled in the bottom of the container. It might be assumed that amphoteric surfactant stabilizes the remaining solid phase and do not permit further demulsification.

As mentioned already, the cell without surfactant and with lower electrical potential showed better phase separation and higher demulsification rate than did other cells. A combination of electrokinetic with lower electrical potential and cool weather could be a condition very favorable for demulsification of the stable water-in-oil emulsions. For Canada this new technology promises to be a successful and cost-effective method for treatment of oily sludge, spatially in Northern territory.

5-9) Fractal analysis

As discussed in Chapter 4 (section 4-7), the fractal analysis results for all cells were fairly similar. The cells that did not contain the amphoteric surfactant had slightly higher fractal dimensions. As stated in the literature review (Hunter, 1993), the lower the fractal dimension, the more open the aggregate structure, therefore, it can be concluded that

amphoteric surfactant makes the remaining solid phase more loose in structure. A comparison of results suggests that the electrical potential also affects the structure of the flocs; lower electrical potential produces more compact structure and higher fractal dimension.

5-10) New theory of colloids behavior in electrokinetic cell

Oily sludge with different colloidal particles contains oil as a continuous phase, water as dispersed phase, and solid particles that play an important role in the stabilization of this water-in-oil emulsion. In this experiment, by using electrokinetic, the demulsification of these stable water-in-oil emulsions was enhanced. Figure 5-6 illustrates the movement of these colloidal particles in the system, where four colloid particles were considered to explain the effect of different forces.

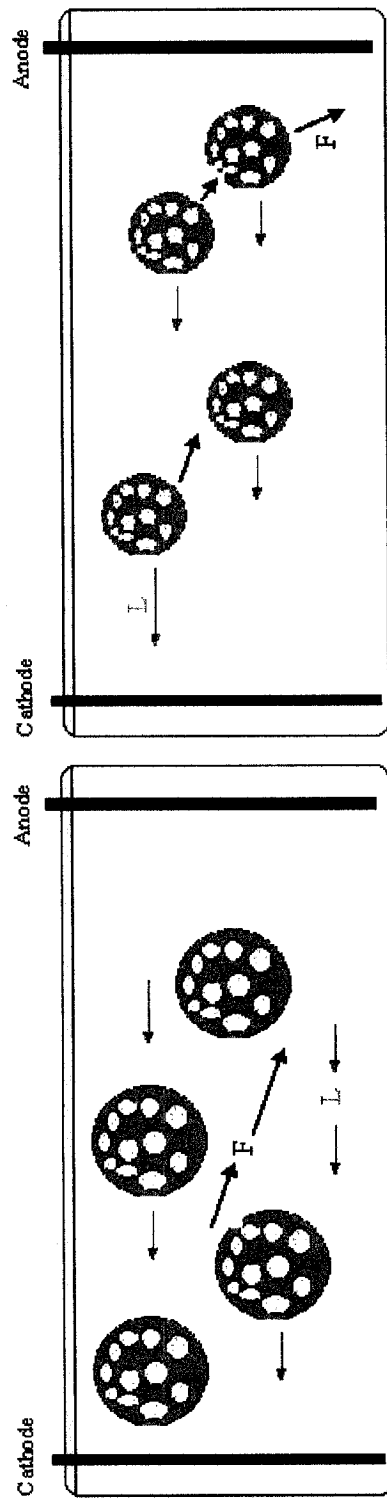
As mentioned in section 5-1, the result of momentum balance between different forces that can influence the movement of a particle is F_{xy} , which is in the direction that settles the particle in the bottom of the cell near the anode area (Figure 5-7). The electrical field forces each colloid particle to move in the F_{xy} direction. As a result of vertical forces and pH variations, some of these stable water-in-oil emulsions will be demulsified, so a separated liquid fraction (water and hydrocarbon) will be produced and will move toward the cathode area because of electro-osmotic forces (Figure 5-7 a). The cathode area had a higher pH value and, as noted in the literature review, changes in pH affect the adsorption behavior of solid particles at the oil-water interface. At higher pH, the solid particles become more hydrophilic, so they are desorbed from the oil-water interface.

Consequently, demulsification can be performed in a high-pH environment, which is in agreement with Yan and Masliyah (1996).

After demulsification, the volume and mass of the particle decrease and the solid fraction of the particle increases so the density will increase too. As the colloid particles are moving toward the anode area, the van der Waals forces between these particles increase, so they tend to attract each other (Figure 5-7 b). By getting closer to the anode area, the solid fraction that contains a high amount of asphaltene increases. After some period of time, this asphaltene content will be very high, promoting the demulsification of these stable water-in-oil emulsions.

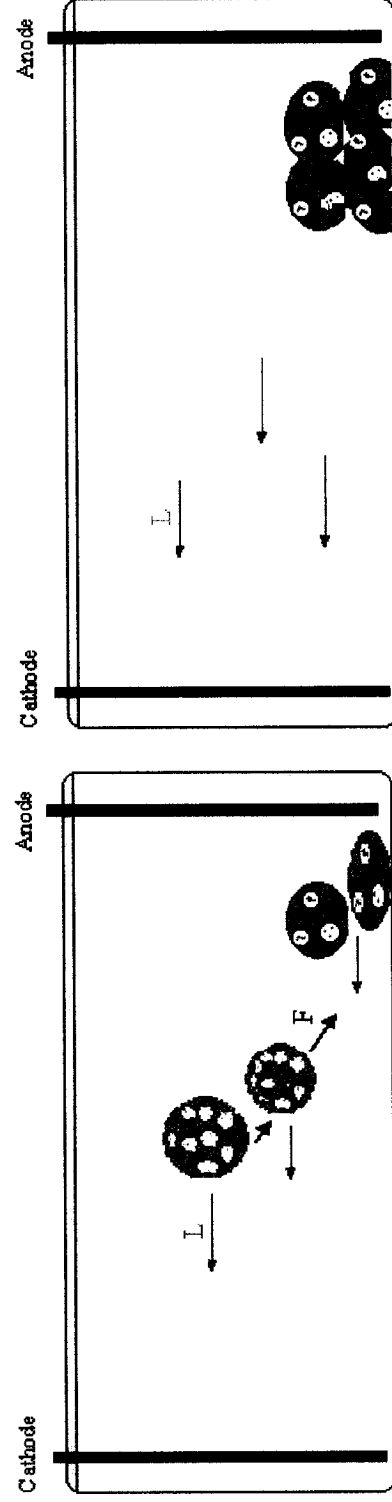
As mentioned in the literature review (Gafonova and Yarranton, 2001), at very high asphaltene concentrations, the reduction in stability of emulsions could be related to the reduction in asphaltene adsorption on the emulsion interface. The solvated molecules are more loosely packed on the interface, thus decreasing the effective surface coverage.

As illustrated in Figure 5-7 c, the dense and smaller volume colloidal particles settle to the bottom of the cell near the anode area. As time passes, more particles join them (Figure 5-7 d), so the resistance in that area increases dramatically. In a lower electrical potential, the velocity of the settling is lower, so the remaining solid produces a more compact residue as a result of slow coagulation between the particles, but in a higher electrical potential, rapid coagulation produces a looser residue.



(a)

(b)



(c)

(d)

Figure 5-7 Behavior of colloidal particles in electrokinetic cell (L=liquid and F= total force)

Chapter 6

Impact of the new technology on environment and sustainable development

6-1) Average volume reduction rate

As was demonstrated in section 4-2, the rate of volume reduction in control cells is much lower than in electrokinetic cells. The reduced volume in these cells could be related to the evaporation of water and volatile hydrocarbons at the surface of the cells. In electrokinetic cells, not only evaporation but also volume reduction can occur as a result of phase separation and movements of liquid, colloid, and solid particles under the influence of an electrical field. Cell SAE (1.5) showed the highest average volume reduction rate among the cells, based on 75 days of the experiment. It is noted that after 32 days of the experiment the electrical power was disconnected.

6-2) Emission mitigation

Gradually, release of volatile hydrocarbons, which are trapped in the colloidal particles, causes an increase in the amount of greenhouse gases (GHG) worldwide. Light hydrocarbons are very important in the GHG concept, for example, methane has 21 times higher heat-trapping effect than carbon dioxide. Therefore, release of these gases to the atmosphere could have an impact on global warming. It has been shown (section 4-1) that the amount of light hydrocarbons was reduced after the electrokinetic application by 43 %, and after addition of amphoteric surfactant by 50 %, meaning that the process

accelerates the release of light hydrocarbon by breaking down the colloidal particles. This separated gas phase can be collected and treated, or reused as fuel in other units.

The developed electrokinetic phase separation is a new cost-effective technology, which in turn will permit revitalization of petroleum sludge. This method can significantly reduce the amount of wasted sludge and recover hydrocarbon components free of metals and water. Only recovery of 30% of sludge components per refinery will lead to generation of 10 000 tonnes of fuel per year per refinery. At the same time, an important decrease of the emission of VOCs and sulphur derivatives will have impact on better air quality. The Life Cycle Analysis of the recovered fuel shows that new technology will reduce emission of major greenhouse gases such as CO₂, CH₄ and N₂O by 40 026 000 kg, 1057 kg, 566 kg respectively per refinery per year (Habibi and Elektorowicz, 2003).

6-3) Value-added products

Waste reduction provides an opportunity to save money. Reducing the waste reduces the costs of treatment and disposal, as well as the resources needed to permit and track the waste. Refinery wastewater treatment experience indicates that, for every kg of solid introduced into an oily water sewer, ten kg of oily sludge requiring disposal is generated (Moores, 2001). If the refinery's oily sludge disposal could be reduced, the facility could save a great deal of money every year. By revitalization of oily sludge (Figure 6-1) with the new method, an important preservation of natural resources takes place, the sustainable reuse of separated fractions permits the energy recovery, decrease the generation of hazardous waste and increase a number of new values added products.



Figure 6-1 Initial oily sludge

6-3-1) Separated solid fraction

As discussed in Chapter 4 (section 4-1), in the proposed technology the water content and light hydrocarbon content of the sludge can be reduced by almost 63% and 50% respectively, a considerable waste volume reduction. The non-volatile part of the remaining solid is almost 48% higher than that of the initial sludge. This higher amount of non-volatile hydrocarbons and lower amount of water increases the heating value of the remaining solid (Figure 6-2), and making it more useful as fuel. A large part of these non-volatile hydrocarbons is related to asphaltene, so the remaining solid can also be sent to the asphaltene unit for additional treatment to be used as a value-added road material.

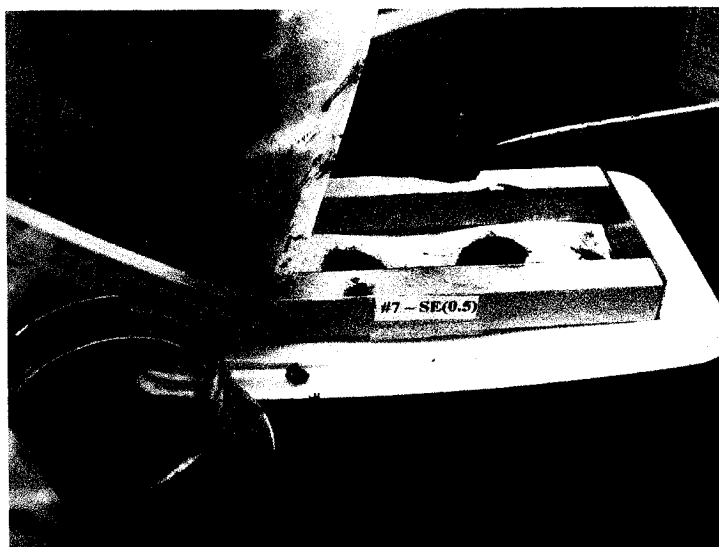


Figure 6-2 Remained solid Phase after the elektrokinetic test

6-3-2) Separated liquid fraction

The separated liquid fraction (Figure 6-3) contained water and liquid hydrocarbon. As was mentioned already, water could be separated near the cathode area. Visual observation confirmed results from previous research (Norssair, 1996b) and showed that the hydrocarbon content of the separated water was low so it could be sent to a wastewater treatment plant. The remaining liquid phase is a good quality fuel with negligible amount of water. The amount of metals after electrokinetic test in liquid fraction was also very low, for example vanadium reduction was almost 75% in the separated liquid phase (Badowieh, 2004). This high quality makes it possible to use the separated liquid fraction as a fuel or can be sent to the refinery for further treatment.



Figure 6-3 Recovered liquid phase after the elektrokinetic test

6-3-3) Separated volatile fraction

The separated volatile hydrocarbon phase can be captured and used as fuel in different units of the refinery. This value-added product can be used as a fuel in other industrial units including incinerators. One suggested method is blending of this recovered lighter hydrocarbons with other appropriate streams of petroleum refineries to produce a high quality fuel.

6-4) Energy consumption analysis

As mentioned in Chapter 4 (section 4-8), the energy consumption changed dramatically with the value of the applied electrical potential and the presence of amphoteric surfactant. By comparing cell SAE (1.5) with cell SE (1.5), which had the same electrical potential, it can be found that cell SE (1.5) that did not contain amphoteric surfactant consumed 45 % less energy. By comparing cells with lower electrical

potentials (SAE (0.5) and SE (0.5)), it can be concluded that cell SE (0.5) consumed 39% less energy than cell SAE (0.5). It was found that amphoteric surfactant increases the energy consumption almost by 40 %.

To determine the effect of different electrical potentials, the energy consumptions of cells SAE (1.5), SAE (0.5), SE (1.5), and SE (0.5) were compared. The energy consumption of cell SAE (1.5) was 80 % higher than in cell SAE (0.5), and the energy consumption of cell SE (1.5) was 80 % more than in cell SE (0.5). It can be concluded that cells with higher electrical potential consumed almost 80% more energy during the experiment.

As stated in section 4-8, most of the electrokinetic phase separation took place in the first 21 days of the experiment. Continuing the application of an electrical field produces a higher quality of remaining solid phase. The efficiency of the system could increase by parallel extraction of the separated liquid phase from the cathode area. As illustrated in Table 4-4, the difference between power consumption for 21 days and 32 days was not remarkable, and the disconnection date could be changed depending on the desirable quality of the remaining solid phase. By considering the cost of electrical power consumption of the cells (Table 4-4), it can be concluded that the cell with lower electrical potential, and without an additive, had the lowest cost by almost \$1.1/ m³ of oily sludge.

Chapter 7

Case Study – Validation of the new theories

In order to verify the defined theories and validate the model of electro-revitalization processes that was developed, a case study was performed (Banowicz, 2003). Four identical cells as described in Chapter 3 were used. Cationic surfactant (Hexadecylmethyl ammonium bromide ($C_{19}H_{42}NBr$), $CMC = 0.92-1.32 \times 10^{-3} \text{ M}$) with concentration of 0.08 M was applied to two of the cells. The change of surfactant permitted a determination of the effect of cationic surfactant on the elektorokinetic phase separation, and assessment of its effectiveness compared with amphoteric surfactant. Two rows of electro-probes to study the resistance changes were also considered. Oily sludge from Shell Canada's bottom of crude oil tank was used, having the same components as the sludge described in Chapter 4, but with different ratio. The amount of liquid hydrocarbon in this sludge was much higher. Two different electrical potentials of 0.5 Volt/cm and 1.5 Volt/cm were applied. Table 7-1 provides a summary of each cell in this case study.

Table 7-1 Summary of cells in the case study experiment

Cell No.	Symbol	Voltage / cm	Cell Content
1	SE' (1.5)	1.5	Sludge
2	SE' (0.5)	0.5	Sludge
3	SCE' (1.5)	1.5	Sludge + Cationic Surfactant
4	SCE' (0.5)	0.5	Sludge + Cationic Surfactant

As outlined in Chapter 5 (section 5-4), the resistance changes reflect the processes that take place in the electrokinetic cell in 2D-dimension. Subsequently, change of resistance versus time is the most important factor that reflects the effectiveness of electro-separation of phases. The results of the resistance changes during the case study experiment are presented in Figures 7-1 to 7-4. Figure 6-1 shows that in the cell with higher voltage, SE' (1.5), after 5 days the resistance near the anode area increased rapidly, possibly as a result of fast electro-coagulation and accumulation of solid particles. The resistance changes in the anode area can be best described by equation (6.1)

$$R = 224.6 t^{1.1817} \quad \text{with } r^2 = 0.87 \quad (6.1)$$

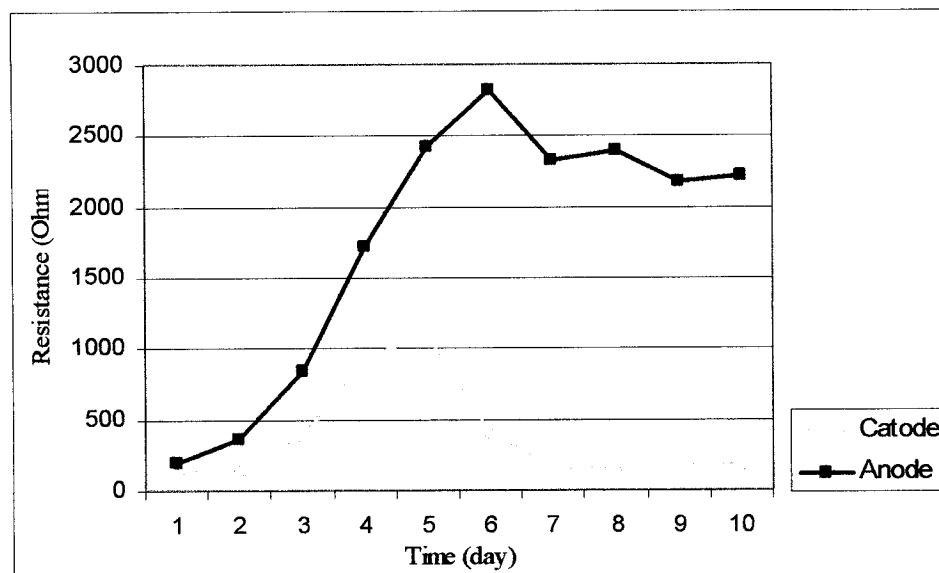


Figure 7-1 Resistance changes in the cell SE' (1.5)

The resistance changes in the cell with lower voltage, SE' (0.5), are illustrated in Figure 7-2. As for the last experiment (Chapter 4), this cell showed lower resistance than

did the cell with higher voltage, SE' (1.5) in the anode area. After day 5, the resistance in the anode area started to increase but it moved slower than in the cell with the higher voltage. It can be concluded that the electro-coagulation was slower in cell SE' (0.5). The resistance was increasing near the cathode area as a result of a high amount of liquid hydrocarbon in the cell. The resistance changes in the anode area of this cell can be best described by equation (7.2)

$$R = 118.9 t^{0.8396} \quad \text{with } r^2 = 0.96 \quad (6.2)$$

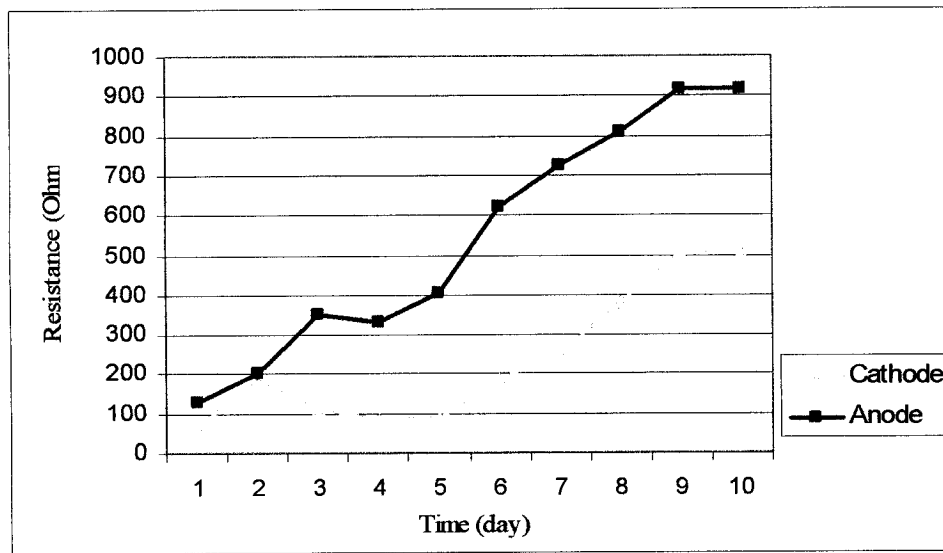


Figure 7-2 Resistance changes in the cell SE' (0.5)

These results show a behavior similar to those described by $R = b t^c$ (equation (5.34)) where b and c are functions of sludge characteristics, electrical potential and distance from the cathode. Comparing the electro-separation in two experiments (equation 4.5 and 7.1), it is clear that the coefficient b in equation 7.1 is much higher than in equation 4.5, perhaps due to the presence of higher amount of the liquid phase. Based on the developed theory (Chapter 5) it might be stated that the transportation forces in horizontal direction

(F_Y) were much higher in the cell with higher liquid content, SE' (1.5), comparing to the vertical electro-separation (F_X). This situation permitted a fast accumulation of solid phase observed in the first day of the experiment.

In the case of the lower electrical potential, by comparing equation 4.7 with 7.2 it can be seen that there is not a significant difference between the b coefficients. It seems that, in lower electrical gradient, the slow horizontal transportation and vertical separation processes have not been strongly affected by the high liquid content, meaning a more effective separation within the sludge. These results confirm the validity of theories describing the electro-separation processes and the applicability of the electro-revitalization method to different characteristics of oily sludges.

Figures 7-3 and 7-4 show the resistance changes in the cells containing sludge and cationic surfactant. The resistance changes of cell SCE' (1.5) and SCE' (0.5) can be fitted best with equations (7.3) and (7.4), respectively.

$$R = 199.9 \exp (0.1923 t) \quad \text{with } r^2 = 0.73 \quad (7.3)$$

$$R = 148.8 \exp (0.1534 t) \quad \text{with } r^2 = 0.80 \quad (7.4)$$

The above-mentioned formulas follow equation (5.35), $R = b' \exp (c' t)$, that was defined for previously tested oily sludge. As explained in section 5-4, b' and c' are functions of sludge characteristics, surfactant characteristics, electrical potential, and the distance from the cathode. These results follow an agreement between both electro-revitalization experiments. As illustrated, the difference between the resistance of the cathode and anode is very low. This observation shows that these kinds of additive did not have a beneficial effect on the system, and even acted as a barrier on the electrokinetic movements of the colloidal particles. These results confirmed the correct

choice of amphoteric surfactant that was applied for the phase separation system in the new method (Chapter 3).

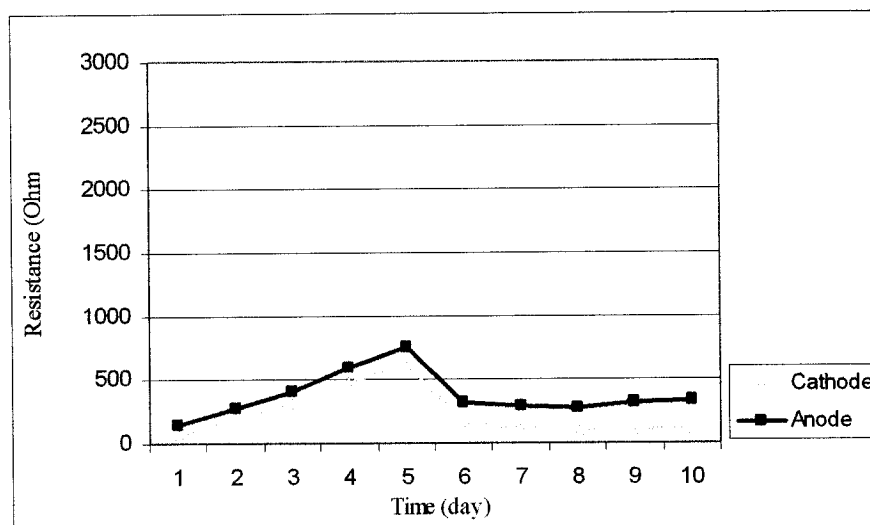


Figure 7-3 Resistance changes in the cell SCE' (1.5)

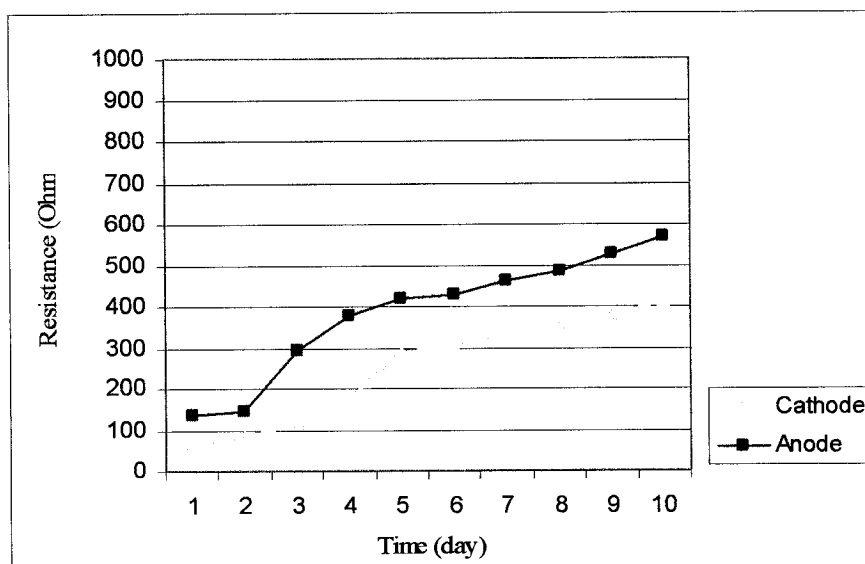


Figure 7-4 Resistance changes in the cell SCE' (0.5)

By comparing the results, it can be concluded that a lower electrical potential has a higher efficiency in the electro-separation of phases. In this system, application of the cationic surfactant does not improve the efficiency of phase separation.

To establish the effect of high liquid hydrocarbon content, the weight percent of different fractions of the separated solid phase from the cell with lower electrical potential and without additive (the best cell with the highest efficiency) was measured using the procedure explained in section 3-1 and presented in Figure 7-5.

By comparing data in Figures 7-5 and 7-2, it can be concluded that, even with higher liquid hydrocarbon content, there occurred a 28 % reduction in water content and a doubling of the solid content in the remaining residue.

The data indicate that electrokinetic revitalization can also be efficiently used for low-density oily sludges. As the density of the sludge increases, the total polar fraction of hydrocarbons, which is mostly related to asphaltenes, and the total amount of trapped water increases also. Therefore, the polarity of the system not only increases, but also affects the movements of the colloidal particles and phase separation under the influence of an electrical field.

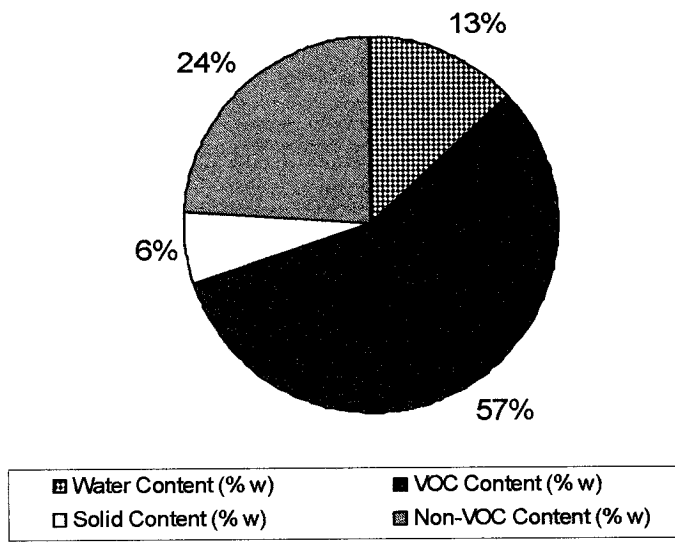


Figure 7-5 Electrokinetic separated solid phase of the cell SE' (0.5)

The results of the case study have shown that the developed model of solid phase separation (Figure 5-6) and the theory of the total driving force to colloidal particles (section 5-10) and their movements under the influence of the electrical field can be confirmed for different types of sludge. In this case, because of higher liquid content, the movement of the colloids grew faster, but the structure of the remaining phase near the cathode became looser. It seems that vertical separation (F_Y) is slower than horizontal movements (F_X), so the angle of total driving force (θ) (equation 5.26) in this case is smaller.

The case study shows with higher confidence, that the introduced colloidal behavior theory can be applied to various oily sludges under the influence of the electrokinetic phenomena.

Chapter 8

Conclusion

This research has led to development of a method for the sustainable management of oily sludge. The first time applied elektrokinetic phenomena to oily sludge permitted its revitalization in order to reuse sludge fractions as value-added products.

The results of this study have demonstrated a new and effective process for the separation of sludge phases, the phases being water, hydrocarbons, and solids. The theory defined here governs that the separation of sludge components has advanced the frontier of academic knowledge in the electro-separation to a new horizon.

This new method offers several advantages over conventional methods. First, it increases the total recovery of hydrocarbon residue from oily sludge; second, it allows the recycling of hydrocarbon residue from a waste stream product to a usable refinery product by a 63% reduction in water content, eliminating potential liability for environmental contamination that might result from the disposal of the hazardous waste stream product; third, it decreases the overall cost and time burdens for recovery and disposal of hydrocarbon residue; and fourth, it demonstrates a process capable of reducing capital cost, investing yields, and improving the quality of petroleum sludge.

In these research experiments, the effects of different electrical potential gradients and amphoteric surfactant on the effectiveness of phase separation were investigated. It is concluded that lower electrical potential can produce a higher demulsification rate. The solid phase remaining after the experiment was of a more compact and stable consistency. Cell SE (0.5), which had lower electrical potential and did not contain an additive, represented the optimum.

The role of oil constituents in stabilizing water-in-oil emulsions, and their effect on the thermodynamics of the process, were considered in every step of the experiment. Different colloidal movements in the system under the influence of an electrical field were defined. Analyzing the pH variations and resistance distribution has led to a better understanding of both the thermodynamics of the process and the solid phase separation model. To introduce the optimum conditions, different factors were considered, such as energy consumption, quality of the remaining solid, and amount of phase separation. It can be concluded that application of the amphoteric surfactant dose not improve the total efficiency of the process.

The processes governing electro-revitalization of oily sludge were defined and verified in this research. Results from a case study showed excellent agreement with developed theories and demonstrated that the new method is applicable to a diverse range of oily sludges.

The recovered solid phase exhibited high hydrocarbon content; therefore, it can be reused. The separated liquid hydrocarbon can be reused in other processes. Some volatile hydrocarbons were released during the process. Advantageously, these gaseous hydrocarbons can be captured and burned as fuel. The results show that the separated water had a low concentration of hydrocarbons, making it suitable for being sent to the wastewater treatment plant.

As discussed in section 5-8, a cold climate can increase the efficiency of the proposed method; however, further research is required to develop a full understanding of the effects of temperature on the system.

The results of this research permit the introduction of a new technology, one that can recycle petroleum hazardous waste, render the operation process safer, decrease energy use, and place Canada in the avant-garde of countries actively pursuing sustainable development principles. This technology has the potential to change the management of petroleum wastes and permit rapid dewatering, revitalization and reuse of separated components, and solve the waste disposal problems created by land bans. The process provides the ability to decrease the emission of VOC's, by 43%, yielding better air quality in compliance with the Kyoto resolution and reducing the global inventory of "greenhouse gases". The exposure of the environment to petroleum waste will be curtailed through this technological breakthrough, decreasing the impact on climate changes. Waste volume and operational costs will be reduced, and workers and the public will be given increased protection. Due to lower costs, this treatment may be widely applied by industries across Canada.

As discussed in Chapter 3, the use of existing storage pools of oily sludge in refineries can realize significant cost savings through the new technology; the pools should be equipped with a suitable system for collecting the separated volatile hydrocarbons. The results of the case study shows that parallel extraction of the separated liquid phase from cathode area can increase the efficiency of the system. The capital cost of the system can be compensated for by profit from the recovered fuel. The anticipated cost of electrical consumption is as low as \$1.2 CDN / m³ of sludge. The cost of this process is much lower than that of conventional remediation techniques, which may reach \$800 USD /ton of sludge.

Chapter 9

Future work

This section presents suggestions for future work in areas related to this study. There are several lines of research arising from this work, which should be pursued. Ideas for future work include:

- Bio-electrokinetic neutralization of remained solid phase
- Polishing the separated solid phase from metallic components
- Effect of temperature (cold climate) on the process
- Optimizing the design of electrodes and the system
- More investigation on the behavior of the amphoteric surfactant under electrical field

References

- Abrishmian R., Kabrick R. and Swett G., 1992, "*Two On Site Treatment Methods Reduce Sludge Waste Quantities*", Oil and Gas Journal.
- Abdulwahed F. A., 1998, "*Oily Sludge Treatment at the Terminal Department*" 2nd Middle East Refining and Petrochemicals Conference and Exhibition, Bahrain.
- Anigbogu V. C., Woldeab H., Garrison A. W., and Avants J., 2003, "*Enantioseparation of Malathion, Cruformate, and Fensulfothion Organophosphorus Pesticides by Mixed-mode Electrokinetic Capillary Chromatography*", International Journal of Environmental Analytical Chemistry, v 83, n 2, Feb 1, p 89-100.
- Ali M.F. and Alqam M.H., 2000, "*The Role of Asphaltenes, Resins and Other Solids in the Stabilization of Water in Oil Emulsions and its Effects on Oil Production in Saudi Oil Fields*", Fuel 79, pp 1309–1316.
- Badowieh S., 2004, "*Measurement of Redox and pH Changes within Surfactant Modified Oily Sludge*", M.Eng project, Concordia University.
- Barnsley M. F., Devaney L. R, Mandelbrot B. B., Peitgen H. O., Saupe D., and Voss R. F., 1988, "*The Science of Fractal Images*", Springer-Verlag New York Inc.
- Bhardwaj A. and Hartland S., 1994, "*Kinetics of Coalescence of Water Droplets in Water-in-Crude Oil Emulsions*", Journal of Dispersion Science and Technology, 15 (2), pp 133-146.
- Bishop J., 1995, Environment Solutions. pp. 39-43. In Silva, L. J., Sealock, L. J., Elliott, D. C. and Baker, E. G., 1998. "*Petroleum Sludge Treatment*". Wiley Encyclopedia Series in Environmental Science, Environmental Analysis and Remediation. Vol. 6, pp. 3686-3695.
- Brett C. M. A. and Brett A. M O., 1993. "*Electrochemistry Principles, Methods, and Applications*". Oxford Science Publications.
- Burbridge C. S., Johnson G. W., Nakamura J. P. and Tietavainen G., 2001, "*Method for Recovery and Recycling of Hydrocarbon Residue*" United States Patent, 6,168,708.
- Brundtland G. H., 1987, "*World Commission on Environment and Development*". Prime Minister of Norway (www.learning-network.org/global/issues/s/sustain).
- Bhattacharya S. K., Foster D. H., Reddy J. M., 1996, "*Surfactant Enhanced Electrokinetic Remediation of Gasoline Contaminated Soils*". ASCE Specialty

Conference, Proceedings, Non-Aqueous Phase Liquids (NAPLs) in Subsurface Environment: Assessment and Remediation, p 311-322.

Buehler M. F., Suma J. F., Virden J. W., 1994, "*Transport of Radioactive Ions in Soil by Electrokinetics*". Proc Symp Metals Mater Waste Reduct Recovery Rem, 1994, p 111.

Burya Y.G., Yudin I.K., Dechabo V.A., and Anisimov M.A., 2001, "*Colloidal Properties of Crude Oil Studied by Dynamic Light-Scattering*", International Journal of Thermophysics, 22(5): p. 1397-1410.

Bushell G. C., Yan Y. D., Woodfield D., Raper J. and Amel R., 2002, "*On Techniques for the Measurement of the Mass Fractal Dimension of Aggregations*", Advances in Colloid and Interface Science, 95, pp 1-50.

Cain R. B., 1994. "*Bioremediation of Detergents*". Current Opinion in Biology, Vol. 5, pp. 226-247.

Carberry J. B. and Englande A. J., 1983. "*Sludge Characteristics and Behavior*". Martinus Nijhof Publishers.

Choudhury A., 1998, "*Removal of Nickel and Lead from Natural Clay Soil through the Introduction of EDTA and Coupling Ion Exchange processes with Electrokinetic Methodology*". M.Sc. thesis. Concordia University.

Chew C. F. and Zhang T. C., 1998, "*In-Situ Remediation of Nitrate-Contaminated Groundwater by Electrokinetics/Iron Wall Processes*". Water Science and Technology, v 38, n 7 pt 6, Water Quality: Environmental Contamination and Restoration, p 135-142.

Chifrina R. and Elektorowicz M., 1998, "*Electrokinetic Removal of HOC from Sludge and Sediments*". Proceedings, 5th Environmental CSCE Conference, Halifax, p 183-192

CHMR, 1996. "*Pollution Prevention: Strategies for Petroleum Refining*". Center for Hazardous Materials Research, Environmental Science.

Conaway L. M., 1999, "*Method for Processing Oil Refining Waste*" United States Patent 5,928,522.

Cookson J.T., 1995, "*Bioremediation Engineering Design and Application*". McGraw-Hill, Inc., New York, NY.

Castaldi F. J. and Ford D. L., 1992, "*Slurry Bioremediation of Petrochemical Waste Sludges*". Wat. Sci. Tech. Vol. 25, No. 3, pp. 207-212.

Dold P. L., 1989. "Current Practice for Treatment of Petroleum Refinery Wastewater and Tonics Removal". Water Poll. Res. J. Canada, Vol. 24, No. 3, 363-390.

Derjaguin B.V. and Landau L.D., 1941, "Theory of the Stability of strongly charged lyophobic sols and of the adhesion of strongly charged particles in solutions of electrolytes", Acta Physicochim. U.S.S.R. 14: 633.

Einar S., 2002, "The World Summit on Sustainable Development - The Petroleum Industry, Perspective and Response". Minister of Petroleum and Energy at the 17th World Petroleum Congress.

Elektorowicz M., Hakimpour M., 2003, "Practical Consideration for Remediation of Mix Contaminated Soil", Proceedings, 8th CSCE Conference on Environmental and Sustainable Engineering, Moncton June 2003.

Elektorowicz M., Hatim J., 2000, "Application of Surfactant Enhanced Elektrokinetics for Hydrocarbon Contaminated Soils", Proceedings, 53rd Canadian Geotechnical Conference, Montreal, vol 1, 617-624

Elektorowicz M. and Chifrina R., Konyukhov B., 1995, "Enhanced Removal of Diesel Fuel From Soil by Electrokinetic Method". 30th Annual Central Canadian Symposium on Water Pollution Research, 1995, Burlington, ON.

Elektorowicz M., Jahanbakhshi P., Chifrina R., Hatim G., and Lombardi G., 1996. "Phenol Removal from Groundwater Using Elektrokinetics". Proceedings, 2nd Int. Conf. on Water Supply and Quality, June, Poznan, Poland, Vol. 2, 105-116.

Elektorowicz M. and Hatem G., 1999. "Design of the Electrokinetic System to Supply Surfactant in Pilot Scale Condition". Proceedings, 2nd Symposium on Heavy Metals in the Environmental and Electromigration Applied to Soil Remediation. Lyngby, Denmark, July 1999.

Elektorowicz M. and Hatim J., 1997, "Improvement of Electrokinetic Technology for Increase in Diesel Fuel Mobility in Subsoil". 32nd Central Canadian Symposium on Water Pollution Research, February, Burlington ON.

Eow J. S., Ghadiri M., Sharif A. O. and Williams T. J., 2001, "Electrostatic Enhancement of Coalescence of Water Droplets in Oil: a Review of the Current Understanding", Chemical Engineering Journal, 84, pp 173-192

EPA, 1996, "Bioremediation of Hazardous Waste Sites: Practical Approaches to Implementation," Land Treatment Seminar.

EPA, 1991, "Safe, Environmentally Acceptable Resources Recovery from Oil Refinery Sludge". 68D10034.

ETPI (Environmental Technology Program for Industry), 2000, "*Petrochemical Sector Report*" Pakistan

Evans D. F. and Wennertrom H., 1994, "*The Colloidal Domain, Where Physics, Chemistry, Biology, and Technology Meet*". VCH Publishers, Inc.

Eykholt G. R. and Daniel D. E., 1994, "*Impact of System Chemistry on Electroosmosis in Contaminated Soil*". Journal of Geotechnical Engineering. Vol. 120, No. 5, pp. 797-815.

Fang C. S. and Lai P. M. C., 1995. "*Microwave Heating and Separation of Water-in-Oil Emulsions*". Journal of Microwave Power and Electromagnetic Energy. Vol. 30, No. 1, pp. 46-57.

Filippi R. and Markiewicz J., Sept. 9, 1991. Oil and Gas Journal, pp. 52-54.

Galil N. and Rebhun M., 1992, "*Waste Management Solutions at an Integrated Oil Refinery Based on Recycling of Water, Oil, and Sludge*". Wat. Sci. Tech. Vol. 25, No. 3, pp. 101-106.

Gafonova O. V. and Yarranton H. W., 2001, "*The Stabilization of Water-in-Hydrocarbon Emulsions by Asphaltenes and Resins*", Journal of Colloid and Interface Science 241, pp 469–478.

Gregory J., 1993, "*Role of colloid interactions in solid-liquid separation*", Water Science and Technology, v 27, n 10, pp 1-17.

Habibi S. and Elektorowicz M., 2003, "A New Sustainable Technology for Recovery of Fuel from Petroleum Wasted Sludge", CJCE Special Issue on Sustainable Engineering (Submitted).

Habibi S., Elektorowicz M., Chifrina R. and Esmaeily A.(2003) "*Development of a Sustainable Technology for Revitalization of Petroleum Wastes*". Proceedings, 31st Annual Conference of the Canadian Society for Civil Engineering (CSCE), Moncton, NB.

Hakimpour, M, 2001, "*Development of a Hybrid electrokinetic System for the Simultaneous Removal of Heavy Metals and PAHs from Clayey Soil*". M.Sc. thesis. Concordia University.

Hano T., Ohtake T. and Takagi K., 1988, "*Demulsification Kinetics of W/O Emulsion in an A.C. Electric Field*", Journal of Chemical Engineering, Japan, 21 (4), pp 345-351.

Hartland S. and Vohra D. K., 1980, "*Effect of Interdrop Forces on the Coalescence of Drops in Close-Packed Dispersions*", Journal of Colloid and Interface, v 77, n 2, pp 295-316.

Hunter R. J., 1993, "*Introduction to Modern Colloidal Science*" Oxford Science Publications.

Hatim G., 1999, "*Design of Surfactant Enhanced Electrokinetic System for Hydrocarbons Removal from Clayey Soils in Pilot Scale Conditions*". M. Sc. Thesis. Concordia University.

Hahn W. J., 1994, "*High Temperature Reprocessing of Petroleum Oily Sludges*". Society of Petroleum Engineers, Vol. 9, No. 3, pp. 179-182.

Hilmi A., Luong J. H. T., and Nguyen A., 1999, "*Development of Electrokinetic Capillary Electrophoresis Equipped with Amperometric Detection for Analysis of Explosive Compounds*". Analytical Chemistry, v 71, n 4, Feb 15, p 873-878.

Jahanbakhshi P., 1996, "*Removal of Diesel Fuel from Contaminated Soil Using Electrokinetic Technology*". Internal Report, Under Supervision of Dr. Elektorowicz, Concordia University.

Jean D. S., Lee d. J. and Wu J. C. S., 1999, "*Separation of Oil from Oily Sludge by Freezing and Thawing*". Department of Chemical Engineering, National Taiwan University. Wat. Res. Vol. 33, No. 7, pp. 1756-1759.

Jesien W., 1995. "*Behaviour of Surfactants in Various Conditions (Vol. I)*". Internal Report, Under Supervision of Dr. Elektorowicz, Concordia University.

Jesien W., 1996. "*Behaviour of Surfactants in Various Conditions (Vol III)*". Internal Report, Under Supervision of Dr. Elektorowicz, Concordia University.

Joffe L. and Knieper L., 2000. "*Electrocoagulation Technology: Quickly Removes Barium, Total Suspended Solids from a Water-Retention Pond for Fractions of a Cent o per gallon*". Industrial Wastewater Journal.

Johnson L. A., Satchwell R. N., Glaser R. R., and Brecher L. E., Nov. 9, 1993. U.S. Pat. 5,259,945.

Kim S. O., Moon S. H., and Kim K. W., 2000. "*Enhanced Electrokinetic Soil Remediation for Removal of Organic Contaminants*". Environmental Technology. Vol. 21, No. 4, pp. 417-426.

Kokal S., Tang T., Schramm L., and Sayegh S., 1995 "*Electrokinetic and Adsorption Properties of Asphaltenes*" Colloids and Surfaces A: Physicochemical and Engineering Aspects, v 94, n 2-3, p 253-265.

Kuriakose A. P., and Manjooran K. B., 2001. "*A Low Cost Processing Aid from Oil Refinery Waste for Compounding Rubber Blends*". Iranian Polymer Journal, Vol. 10, No. 3, pp. 165-172.

Kuriakose A. P., and Manjooran K. B., 2001. "*Bitumenous Paints from Refinery Sludge*". Surface and coatings technology, No. 145, pp. 132-138

Lageman R., 1989, "*Electrokinetic Reclamation: State of Art*", Demonstration of Remedial Action Technologists for Contaminated Land and Groundwater, Geokinetics, Poortweg, the Netherlands.

Lagrega M. D., Evans J. C., Acuna C. O., Zarlinski S. J., and Hall, D. S., 1990. "*Stabilization of Acidic Refinery Sludges*". Journal of Hazardous Materials, Vol. 24, No. 2-3, pp. 169-187.

Lal, B., Mishra, S., Ramesh, K. C., and Jyot, J. 2000. "*Oilzapper: an Effective Bioremediation Tool*". In Proceedings of the International Seminar on Oily Sludge Management pp. 1-2

Levine S., Bowen B. and Partridge S.J., 1989, Colloid Surfaces, 38, 325-345 in Yan N. and Masliyah J. H., 1993, "*Solids-Stabilized Oil-Water Emulsions: Scavenging of Emulsion Droplets by Fresh Oil Addition*", Colloids and Surfaces A: Physicochemical and Engineering Aspects 75, pp 123-132

Lee J. M., Lim K. H. and Smith D. H., 2002, "*Formation of Two-Phase Multiple Emulsions by Inclusion of Continuous Phase into Dispersed Phase*", Langmuri, 18, pp 7334-7340.

Lomax E. G., 1996. "*Amphoteric Surfactants*". Surfactant Science Series. Second edition. Vol. 59. Marcel Dekker, Inc.

Loehr R. C., Martin J. H., and Neuhauser E. F., 1992. "*Land Treatment of an Aged Oily Sludge. Organic Loss and Change in Soil Characteristics*". Water Research, Vol. 26, No. 6, pp. 805-815.

Leeman J. E., 1988. "*Hazardous Waste Minimization: Part V Waste Minimization in the Petroleum Industry*." JAPCA 38, no. 6: 814-822.

Maini G., Sharman A. K., Christopher J., and Sunderland G., 2000. "*Electrokinetic Remediation of Metals and Organics From Historically Contaminated Soil*". Journal of Chemical Technology and Biotechnology, v 75, n 8, p 657-664.

Marks R. E., Field S. D., Wojtanowicz A. K., and Britenbeck G. A., 1992. "*Biological Treatment of Petrochemical Wastes for Removal of Hazardous*

Polynuclear Aromatic Hydrocarbon Constituents". Wat. Sci. Tech. Vol. 25, No. 3, pp. 213-220.

Menon V. B. and Wasan D. T., 1986, "*Particle-Fluid Interactions with Application to Solid-Stabilized Emulsions*", Colloids and Surfaces, 19, pp 89-105

Mukarji A., 2000. "*Assam Oil Refineries Contaminating Water by Dumping Sludge*". The Hindustan Times, New Delhi.

Miller B. H., Sheehan W. J., Swanberg C. J., and Matthys P., 1994. "*Waste Minimization and Resource Recovery Using Centrifugation and Thermal Desorption*". In J. P. Hager, Conference Proceedings from Extraction Processing and Treatment of Minimization Waste, Miner. Met. Mater. Soc., Warrendale, Pa.

Miyasaki M. T., 1998, "*Method and Apparatus for Recovering the Fuel Value of Crude Oil Sludge*". United States Patent, 5,755,389

Myers D., 1992. "*Surfactant Science and Technology*". Second edition. VCH Publishers.

Namer J. and Ganczarczyk J. J., 1994. "*Fractal Dimensions and Shape Factors of Digested Sludge Particle Aggregates*", Water Pollution Research Journal of Canada, v 29, n 4, p 441-455.

Norssair F.H., 1995. "*Electrolysis of Emulsion of Diesel Fuel in Surfactant and Suspension of Soil Contaminated by Diesel Fuel*". Internal Report, Under Supervision of Dr. Elektorowicz, Concordia University.

Norssair F.H., 1996a. "*Use of Cationic Surfactant for the Separation Processes of Diesel Fuel from Sediments*". Internal Report, Under Supervision of Dr. Elektorowicz, Concordia University.

Norssair F.H., 1996b. "*Use of Amphoteric Surfactant for the Separation Processes of Diesel Fuel from Sediments*". Internal Report, Under Supervision of Dr. Elektorowicz, Concordia University.

Nelson W. L., 1958. "*Petroleum Refinery Engineering*". Chemical Engineering Series. McGraw-Hill.

Omar, A.M.A, Mohamed M. S., and Ibrahim H., 2002. "*Recovery of Residual Emulsifiable Oil from Waste Water by Flotation*" Lubrication Science, v 14, n 2, p 275-284.

Ontario Environmental Protection Act, R.R.O. 1990, Regulation 347.

Pamukcu S, Wittle J. K., 1992. "*Electrokinetic Removal of Selected Heavy Metals from Soil*". Environmental Progress. Vol. 11, No. 3.

Pamukcu S., Filipova I., and Wittle J. K., 1995. "*The Role of Electroosmosis in Transporting PAH Compounds in Contaminated Soils*". Electrochemical Society Proceeding. Vol. 12, pp. 252-263.

Pelton R. H., 2002, "*Selected Topics in Colloid and Surface Science*" Class note, McMaster University.

Petrisor I.G., Dobrota S., Lazar I., Voicu A., Stefanescu M., and Kuperberg M., 2001. "*Bioremediation of Soils Contaminated With Oily Sludge: A Romanian Field Study*". AEHS Contaminated Soil Sediments and Water, Aug. 2001 International Issue, 48-50.

PCRA, 2003, "*Sustainable Development – Challenges and Opportunities*" Petroleum Conservation Research Association, India.

Pileni P., 2001, "Mesosstructured Fluids in Oil-Rich Regions: Structural and Templating Approaches", Langmuir, 17, pp 7476-7486.

Podol'skaya V. I., Yakubenko L. N. and Ul'berg Z. R., 2001, "*Electrokinetic and transmembrane potentials as factors of cell adaptation to cyanide compounds*", Kolloidnyj Zhurnal, v 63, n 4, pp 498-504.

Puskas S., Balazs J., Farkas A., Regdon I., Berkesi O., and Dekany I., 1996, "*The Significance of Colloidal Hydrocarbons in Crude Oil Production Part 1. New Aspects of the Stability and Rheological properties of Water-in-Oil Emulsions*", Colloids and Surfaces A: Physicochemical and Engineering Aspects 113, pp 279–293

Rasmussen G. P., 1994. "*New Desorption Process Treats Refinery K and F Wastes in Demo Trial*." Oil and Gas Journal, v 92, n 2, p 48-51.

Ripley I. S., and Needham A. H., 1998, "*Treatment of Waste Petroleum*" United States Patent, 5,853,563.

Rizakos T., 1994. "*A Comparison of the Performance of Graphite and Steel Electrodes during Electroosmotic Processes*". Internal Report, Under Supervision of Dr. Elektorowicz, Concordia University.

Podol'skaya V. L., Yakubenko L. N., Ul'berg Z. R., 2001. "*Electrokinetic and Transmembrane Potentials as Factors of Cell Adaptation to Cyanide Compounds*". Kolloidnyj Zhurnal, v 63, n 4, p 498-504

Rhodes A., 1994. "*New Process Effectively Recovers Oil from Refinery Waste Streams*". Oil and Gas Journal, v 92, n 33, p 92-94.

Santos B., 1999, "*Process to Refine Petroleum Residues and Sludges into Asphalt and/or other Petroleum Products*" United States Patent, 5,922,189.

Scamehorn J. F., and Haewell J. H., 1988, "*Surfactant –Based Treatment of Aqueous Process Streams*" from "Surfactants in chemical/ process Engineering" by Wasan D. T., Ginn M. E., and Shah D. O., Surfactant Science Series, Marcel Dekker Inc., Volume 28.

Schindler T., 1992. El Digest. pp. 8-12. In Silva, L. J., Sealock, L. J., Elliott, D. C. and Baker, E. G., 1998. "*Petroleum Sludge Treatment*". Wiley Encyclopedia Series in Environmental Science, Environmental Analysis and Remediation. Vol. 6, pp. 3686-3695.

Schmitt T. M., 2001. "*Analysis of Surfactant*". Surfactant Science Series. Second edition. Vol. 96. Marcel Dekker, Inc.

Spellman F. R., 1997, "*Dewatering Biosolids*". Technomic Publishing Company, Inc.

Shie J. L., Chang C. Y., Wu J. P., and Lee C. H., 2000. "*Resources Recovery of Oil Sludge by Pyrolysis: Kinetics Study*". Journal of Chemical Technology and Biotechnology, Vol. 75, No. 6, pp. 443-450.

Shiba S., Hino S., Hirata Y., Seno T., 2000. "*Removal of Heavy Metal from Soil and Groundwater by In-Situ Electrokinetic Remediation*", Water Science and Technology, v 42, n 7-8, p 335-343.

Smoluchowski M., (1917) Z. Phys. Chem. (Leipzig) 92, 129–168. In Hunter, R. J., 1993. "*Introduction to Modern Colloidal Science*" Oxford Science Publications.

Spearman M. K., and Zagola S. J., 1992. "*The Development of a Waste Minimization Program at Amoco Oil Company*". Wat. Sci. Tech., Vol. 25, No. 3, pp. 107-116.

Silva L. J., Sealock L. J., Elliott D. C. and Baker E. G., 1998. "*Petroleum Sludge Treatment*". Wiley Encyclopedia Series in Environmental Science, Environmental Analysis and Remediation. Vol. 6, pp. 3686-3695.

Shieh Y. S. and Sheehan W. J., 1992. "*Integrated Refinery Waste Management*". Wat. Sci. Tech. Vol. 25. No.3, pp. 273-275.

Sjoblom J., Aske N., Auflem I. H., Brandal O., Havre T. E., Saether O., Westvik A., Johnsen E. E., Kallevik H., 2003, "*Our Current Understanding of Water-in-Crude Oil emulsions. Recent Characterization Techniques and High Pressure Performance*", Advances in Colloid and Interface Science, 100-102, pp 399-473.

Sullivan A. P. and Kilpatrick P. K., 2002, "*The Effects of Inorganic Solid Particles on Water and Crude Oil Emulsion Stability*", American Chemical Society, Industrial and Engineering Chemistry Research, v 41, n 14, pp 3389-3404

Taha M. R., 1996. "*Micellar Electrokinetic Remediation of TNT from Soil*". Louisiana State University.

Tay J. H. and Jeyaseelan S., 1993. "*Dewatering Characteristics of Oily Sludge*". Wat. Sci. Tech. Vol. 28, No. 1, pp. 249-256.

Thalasso F., Van der Burgt J., O'flaherty V., and Colleran E., 1999, "*Large-scale Anaerobic Degradation of Betaine*", Journal of Chemical Technology and Biotechnology, v 74, n 12, Dec, 1999, p 1176-1182.

U.S. Army, 1999. "*Engineering and Design Lubricants and Hydraulic Fluids*". CECW-ET Washington, DC 20314-1000 Manual, No. 1110-2-1424 28.

Verwey E. J. W. and Overbeek J. Th. G., 1948, "*Theory of the Stability of Lyophobic Colloids*", Elsevier, Amsterdam

Wall W., Li J., and El R. Z., 2002. "*Electrically Driven Microseparation Methods for Pesticides and Metabolites Part VII: Capillary Electrophoresis and Electrochromatography of Derivatized and Underivatized Phenol Pesticidic Metabolites. Preconcentration and Laser Induced Fluorescence Detection of Dilute Samples*". Journal of Separation Science, v 25, n 15-17, December, 2002, p 1231-1244.

Wagner H., 1981 "*Process for the Preparation of Sulfobetaines*", United States Patent, 4,259,191 to Th. Goldschmidt AG.

Wright R. A D., and Noorvhuys B. R., 1991. "*Treatment and Disposal of Oily Solids*". Proceedings of the First International Conference on Health, Safety and Environment in Oil and Gas Exploration and Production, Part 2, pp. 521-526. Published by Society of Petroleum Engineers of AIME.

Yan N., Kurbis C., and Masliyah J. H., 1997, "*Continuous Demulsification of Solids-Stabilized Oil-in-Water Emulsions by the Addition of Fresh Oil*", American Chemical Society, Industrial and Engineering Chemistry Research, v 36, n 7, pp 2634-2640

Yan N. and Masliyah J. H., 1993, "*Solids-Stabilized Oil-Water Emulsions: Scavenging of Emulsion Droplets by Fresh Oil Addition*", Colloids and Surfaces A: Physicochemical and Engineering Aspects 75, pp 123-132

Yan N. and Masliyah J. H., 1995, "characterization and Demulsification of Solids-Stabilized Oil-in-Water Emulsions, Part 1. Partitioning of Clay Particles and

Preparation of Emulsions”, *Colloids and Surfaces A: Physicochemical and Engineering Aspects* 96, pp 229–242

Yan N. and Masliyah J. H., 1996, “*Demulsification of Solids-Stabilized Oil-Water*”, *Colloids and Surfaces A: Physicochemical and Engineering Aspects* 117, pp 15–25

Yan N. and Masliyah J. H., 1996, “*Effect of pH on Adsorption and Desorption of Clay Particles at Oil-Water Interface*”, *Journal of Colloid and Interface Science* 181, pp 20–27

Yellamraju A., 1995.”*Behaviour of Surfactants in Various Conditions (Vol. II)* ”. Internal Report, Under Supervision of Dr. Elektorowicz, Concordia University.

Yan N., Gray M. R., and Masliyah J. H., 2001, “*On Water-in-Oil Emulsions Stabilized by Fine Solids*”, *Colloids and Surfaces A: Physicochemical and Engineering Aspects* 193, pp 97–107

Yan N., Gray M. R., and Masliyah J. H., 2001, “*On Water-in-Oil Emulsions Stabilized by Fine Solids*”, *Colloids and Surfaces A: Physicochemical and Engineering Aspects* 193, pp 97–107

Yellamraju A., 1996.”*Behaviour of Surfactants in Various Conditions (Vol. IV)* ”. Internal Report, Under Supervision of Dr. Elektorowicz, Concordia University.

Zaki N., Schorling P. C., and Rahimian I., 2000, “*Effect of Asphaltene and Resins on the Stability of Water-in-Waxy Oil Emulsions*”, *Petroleum Science and Technology*, v 18, n 7, pp 945-963

Zhang X., Basaran O. A., and Wham R. M., 1995, “*Theoretical Prediction of Electric Field-Enhanced Coalescence of Spherical Drops*”, *AIChE Journal*, 41 (7), pp 1629-1639.

Appendix A

A-1) Characteristics of oily sludge before and after the experiment

Table A-1 Water content in the samples

Sample #	Mass of sample, g	Volume of water, ml	Water Content (% w)
1	25.47	4.6	18.06
2	25.17	1.7	6.75
3	25.2	1.85	7.34
4	25.32	1.9	7.5
5	25.14	1.8	7.16

Table A-2 Volatile hydrocarbon content in the samples

Sample #	Mass of sample, g	Residue (% w)	Water Content (% w)	Light Hydrocarbon Content (% w)
1	2.3657	73.93	18.06	55.87
2	2.0656	38.55	6.75	31.8
3	4.0224	39.05	7.34	31.71
4	6.6287	36.63	7.5	29.13
5	1.9789	34.61	7.16	27.45

Table A-3 Solid content in the samples

Sample #	Mass of sample, g	Residue, g	Solid Content (% w)
1	2.3657	0.0615	2.6
2	2.0656	0.3979	19.26
3	4.0224	0.6878	17.1
4	6.6287	1.16	17.5
5	1.9789	0.3289	16.62

Table A-4 Non - Volatile hydrocarbon content in the samples

Sample #	Water Content (% w)	Light Hydrocarbon Content (% w)	Solid Content (% w)	Non-VOC Content (% w)
1	18.06	55.87	2.6	23.47
2	6.75	31.8	19.26	42.19
3	7.34	31.71	17.1	43.85
4	7.5	29.13	17.5	45.87
5	7.16	27.45	16.62	48.84

A-2) Sustainable development

For millions of years, before man became a major player of the Earth, there was a natural balance between organisms. By interfering of human species into the natural world, Ecological imbalance, Environmental degradation, and rapid depletion of natural resources and associated began which is major threat to the sustainable economic development.

“Sustainable Development” and “Environmental protection” are related. At the 1992 UN Conference on Environment and Development, Rio, UNCED Principle #3 characterized sustainable development, as “the right to development must be fulfilled so as to equitably meet developmental and environmental needs of present and future generation.” Principle #4 further states “in order to achieve sustainable development, environmental protection shall constitute an integral part of the development process and cannot be considered in isolation from it” (PCRA, 2003).

Sustainable development means economic development and improvement in standards of living by considering future generations. Bruntland in 1987 defined the environmental sustainability as “Development that means the needs of the present without compromising the ability of future generation to meet their own needs.” One way to achieve this goal by industries is generating less waste and useful bi-products, which could be used for commercial advantage.

Energy is a very important part of economic development and environmental challenges. The way that we deal with the energy issues in a global perspective will be significant in achieving sustainable development. Over the next few decades, oil is still will remain as the single largest source of primary energy (Einar, 2002).

One of the most important challenges in the world's today is the question of how efficiency can increase by means of sustainable growth. The answer is by supporting and promoting the development of renewable energy systems and developing technologies that use the fossil energy source more efficiently (Einar, 2002).

Here are some elements, which can help the world attain sustainable development and environment protection (PCRA, 2003):

- ❖ Population stabilization
- ❖ New Technologies / technology transfer
- ❖ Efficient use of natural resources
- ❖ Waste reduction and pollution prevention
- ❖ Integrated environmental systems management
- ❖ Refining market economy
- ❖ Education
- ❖ Perception and attitude change
- ❖ Social and cultural changes

A new technology, which focuses on sustainable development can solve the pollution problems in the past and prevent new problems in the future. These processes should minimize waste products and changing them to recyclable products.

A-3) Pollution prevention and waste minimization

Pollution prevention is the reduction or elimination of discharges or emissions to the environment. Pollution prevention can be accomplished by reducing the generation of wastes at their source (source reduction) or by using, reusing or reclaiming wastes once they are generated (CHMR, 1996).

Waste minimization is an environmentally responsible approach to management of wastes and supports using all environmentally sound methods including source reduction and resource recovery (Spearman and Zagula, 1992). Resource recovery, volume reduction and waste minimization are the primary choices to reduce environmental problems (Shieh and Sheehan, 1992). A good pollution prevention method must eliminate the generation of waste instead of developing complex and costly treatment and might save thousands of dollars in treatment and disposal costs.

In a refinery, waste reduction practice includes preventing hydrocarbon loss and reducing expenses associated with waste disposal. This result increases operation efficiency and lowers expenses.

Petroleum refinery wastes result from processes designed to remove different contaminants from crude oil such as water, sulfur, nitrogen, and heavy metals. Small changes in personnel practices, housekeeping, inventory control, waste stream segregation, material handling and scheduling improvements, spill and leak prevention can reduce a large amount of waste. Here are some examples in petroleum refineries (CHMR, 1996):

- Segregation of oily waste streams from relatively clean rainwater run off to reduce the amount of oily sludges. Because a big part of the refinery waste comes from oily sludges found in combined process storm sewers.
- Having regularly inspection of petroleum refinery systems for leaks. For example, checking hoses, pipes, valves, pumps and seals are very important.
- Reducing the amount of water that is used for cleaning of equipment and trying to reuse rinse waters to reduce net waste generation.
- Using correct pressures, temperatures and mixing ratios for optimum recovery of products can reduce the amount of waste production.
- Reducing transfer of solids to waste system by paving run off areas.

A-4) Environmental regulations

Petroleum refining operations generate the highest amount of hazardous wastes in the petroleum industry. A major part of this waste is wastewaters. By treating the wastewaters the amount of contaminant must be reduced until the effluent meets discharge requirement specified in the Clean Water Act. Major sources of wastewaters include processing operations where water comes in direct contact with oil-hydrocarbons and from oily discharges from heat exchangers and cooling towers. There are also other sources of wastewater including storage and handling operations, storm water runoff, and spills of oil and oily waters.

Primary treatment separates the wastewater to oil, water and solids. There are different methods for separating such as gravity separation, centrifuging, mechanical and thermal emulsion breaking and also by using chemicals. The water is further processed through secondary and tertiary treatments.

In the United State the discharge from wastewaters are regulated under RCRA and Clean Water Act. EPA has regulations to identify hazardous solid wastes associated with water treatment and oil recovery from wastewaters. Table 2-4 shows a summary of the oily wastes and sludges that EPA has identified them as hazardous wastes. The EPA has established an industry and EPA hazardous waste number for these wastes, also described briefly about the wastes stream and listed the basis or the classification.

Table A-5 Petroleum Sludge Hazardous Waste List (Silva et al., 1998)

Industry and EPA Hazardous Waste Number	<u>Hazardous Waste</u>	EPA Basis for Listing
F037	<p>Petroleum refinery primary oil-water-solids separation sludge: any sludge generated from the gravitational separation of oil-water-solids during the storage or treatment of process wastewaters and oily cooling wastewaters from petroleum refineries. Such sludges include, but are not limited to, those generated in oil-water-solids separators; tanks and impoundment; ditches and other conveyances; sumps; and storm water units receiving dry weather flow. Sludge generated in storm water units that do not receive dry weather flow, sludge generated from non-contact once-through cooling waters segregated for treatment from other processes or oily cooling waters, sludges generated in aggressive biological treatment units as defined in 261.31(b)(2) (including sludges generated in one or more additional units after wastewaters have been treated in aggressive biological treatment units) and K051 wastes are not included in this listing.</p>	Toxic waste
F038	<p>Petroleum refinery secondary (emulsified) oil-water-solids separation sludge: any sludge and/or float generated from the physical and/or chemical separation of oil-water-solids in process wastewaters and oily cooling wastewaters from petroleum refineries. Such wastes include, but are not limited to, all sludges and floats generated in induced air flotation (IAF) units, tanks and impoundments, and all sludges generated in DAF units. Sludges</p>	Toxic waste

	generated in storm water units that do not receive dry weather flow, sludges generated from noncontact once-through cooling waters segregated for treatment from other process or oily cooling waters, sludges and floats generated in aggressive biological treatment units as defined in 261.31(b)(2) (including sludges and floats generated in one or more additional units after wastewaters have been treated in aggressive biological treatment units) and F037, K048, and K051 wastes are not included in this listing.	
K048	Dissolved air flotation (DAF) float from the petroleum refining industry.	Toxic waste
K049	Slop oil emulsion from the petroleum refining industry.	Toxic waste
K050	Heat-exchanger bundle cleaning sludge from the petroleum refining industry.	Toxic waste
K051	API separator sludge from the petroleum refining industry.	Toxic waste
K052	Tank bottoms (leached) from the petroleum refining industry.	Toxic waste

Reportable quantities (RQs) for releases of CERCLA hazardous substances at one pound is established by section 102 (b) of CERCLA, unless a substance has a different RQ established under section 311 (b) of the Clean Water Act. Section 102 (a) of CERCLA is about the authorization of EPA to adjust these RQs by regulation.

If a CERCLA hazardous substance has been released in a quantity that equals or exceeds its RQ, under CERCLA section 103 (a), the person in charge of a vessel or

facility must immediately notify the National Response Center (40 CFR 302.6). The owner or operator of that facility must immediately state a local response authorizes (section 304 of the Emergency Planning and Community Right-to-Know Act of 1986 (EPCRA)). Table 2-4 shows some information about the seven kinds of oily wastes and sludges that are listed by EPA as hazardous substances.

The EPA evaluation is based on their physical, chemical and toxicological properties. The examined primary criteria are aquatic toxicity, mammalian toxicity (oral, dermal and inhalation), ignitability, reactivity, chronic toxicity and potential carcinogenicity. For each property, EPA ranks hazardous substances on a scale with an RQ level of 1, 10, 100, 1000, or 5000 pound. Evaluation of each hazardous substance is based on its various primary criteria. Each hazardous substance base on its particular intrinsic properties may receive several tentative RQ values. The lowest RQs becomes “primary criteria RQ” for that substance.

After the primary criteria RQs, secondary adjustment criteria are done by further evaluation of substances for their susceptibility to certain degradative processes.

Information about each of the regulated refinery sludge has been shown in Table 2-5. This information includes an inventory of the hazardous constituents for which they were listed. “Statutory RQ” lists the RQs for hazardous substances established by section 102 of CERCLA. The “Statutory Code” indicates the statutory source for designating each substance. Number 4 means that the source is RCRA section 3001. “Waste Number” is an identification number that is assigned to substances by RCRA regulations.

Table A-6 Hazardous Substances and Reportable Quantities

EPA Hazardous Waste Number	Hazardous Constituents for Which Listed	Statutory ^a		Final RQ Category ^b	Pound (kg)
		RQ	Code		
F037	Benzene, benzo(a)pyrene chrysene, lead, chromium	1	4	X	1 (0.454)
F038	All constituents for which treatment standards are specified for multisource leachate (wastewaters and nonwastewaters) under 40 CFR 268.43(a), Table CCW	1	4	X	1 (0.454)
K048	Hexavalent chromium, lead	1	4	X	10 (4.54)
K049	Hexavalent chromium, lead	1	4	X	10 (4.54)
K050	Hexavalent chromium	1	4	X	10 (4.54)
K051	Hexavalent chromium, lead	1	4	X	10 (4.54)
K052	Lead	1	4	X	10 (4.54)

^a RQ : 1= indicates 1-lb RQ is CERCLA statutory RQ; Code: 4 = indicates source is RCRA Section 3001

^b X = associated with reportable quantity 1 lb; A = associated with reportable quantity 10 lbs.

In “Category” column letters “X” and “A” are used to show the reportable quantities of 1 and 10 pounds, respectively. The reportable quantity adjustment for each hazardous substance is provided by “Pounds (kg)” column.

The exact amount of petroleum sludge from oil refineries (K048 – K052 wastes) is not available. Table 2-6 shows an estimation amount provided by the American Petroleum Institute. This table shows that in 1982, 851300 wet tons per year of sludge was produced. The largest part of the waste is K048 – DAF float, K049 – slop oil emulsion solids, and K051 – API separator sludge (Silva et al, 1998).

Table A-7 K-Listed Refinery U.S. Waste Generation (Silva et al., 1998)

	Project Disposal Rates	Wet Tons/yr
K048	<u>DAF Float</u>	308,000
<u>K049</u>	Slop oil emulsion solids	144,000
K050	Heat-exchanger bundle cleaning solids	1,300
K051	API separator sludge	393,000
K052	Leaded gasoline tank bottoms	5,000
	Total	851,300

- **Disposal**

When the treatment of oil wastes has been completed, the residue from treatment must be disposed. Land farming is the most common method for disposing oily wastes and

sludges. Land farming uses biological degradation and immobilization to treat the wastes and landfilling in facilities that is permitted by EPA.

The EPA was forced by the 1984 Hazardous and Solid Waste Amendments to RCRA to establish Land Disposal Restrictions, or “Land bans”, for RCRA characteristic and listed hazardous wastes. Land disposal includes but is not limited to “any placement of such hazardous waste in a landfill, surface impoundment, waste pile, injection well, land treatment facility, salt dome formation, salt bed formation, or underground mine or cave” (RCRA section 3004 (k), 42 USC 6924 (k)).

A certificate must be issued by treatment facility for each shipment of waste or treatment residue of a restricted waste to the land disposal facility. This certificate must state the waste or treatment residue that has been treated in compliance with the applicable performance standard specified in subpart D of this part and the applicable prohibitions set forth in section 268.32 or RCRA section 3004 (d) (Silva et al., 1998).

Appendix B

Glossary

Anthropogenic organic compounds: Man-made organic compounds. Some are volatile; others tend to stay dissolved in water instead of evaporating.

API: American Petroleum Institute

Betains: One of the main groups of amphoteric surfactant

Cell S: 1.5 liter of initial oily sludge was poured into cell S without any preparation. This cell had no electrical connection.

Cell SA: The mixture of 1 liter of sludge and 500 ml of 0.005 M Gen (Amphoteric Surfactant) was shaken for 4 hours at 75 rpm. This mixture was poured in Cell SA. There was no electrical connection for this cell.

Cell SE (1.5): This cell contained 1.5 liter of initial sludge without surfactant. The voltage was 1.5 volt per cm.

Cell SAE (1.5): 1 liter of sludge plus 500 ml of 0.005 M Gen was shaken for 4 hours at 75 rpm and was poured in this cell. The applied voltage was 1.5 volt per cm.

Cell AE (1.5): This cell contained 1.5 liter of 0.005 M Gen without any sludge. The applied voltage gradient for this cell was 1.5 volt per cm.

Cell SE (0.5): This cell contained 1.5 liter of initial sludge without surfactant. The applied voltage was 0.5 volt per cm.

Cell SAE (0.5): 1 liter of sludge plus 500 ml of 0.005 M Gen was shaken for 4 hours at 75 rpm and was poured in this cell. The applied voltage was 0.5 volt per cm.

Cell AE (0.5): This cell contained 1.5 liter of 0.005 M Gen without sludge. The applied voltage for this cell was 0.5 volt per cm.

Coalescence: The coalescence behavior can be described in three steps: droplets approaching each other, the process of film thinning/drainage, and film rupture leading to droplet-droplet coalescence.

Colloid Stability: When a specified process that causes the colloid to become a macrophase, such as aggregation, does not proceed at a significant rate.

Contact angle: an angle formed between two substances, as determined by their surface tensions, when in contact.

CMC: Critical micelle concentration

CWA: Clean Water Act

DAF: Dissolved Air Floatation

Demulsification: Process of "breaking" or separating an emulsion into its component parts.

DLVO Theory: An acronym for a theory of the stability of colloidal dispersions developed by Derjaguin, Landau, Verwey and Overbeek. The theory was developed to predict the stability against aggregation of electrostatically charged particles in a dispersion.

Effective potential: Zeta potential

Electric Double Layer: An idealized description of the distribution of free charges in the neighborhood of an interface.

Electrolyte: A conducting medium in which the flow of electric current takes place by migration of ions.

Electro-demulsification: The break down of the water-in-oil emulsions by electrical forces

Electrokinetic: A general adjective referring to the relative motions of charged species in an electric field. The motions may be either of charged, dispersed species or of the continuous phase, and the electric field may be either an externally applied field or else created by the motions of the dispersed or continuous phases. Electrokinetic measurements are usually aimed at determining Zeta Potentials.

Electrophoresis: The process whereby an electric charge is used to separate charged molecules in a mixture according to charge and size.

Electro-osmosis: The motion of liquid through a porous medium caused by an imposed electric field.

Electrophoresis: The motion of colloidal species caused by an imposed electric field.

EPA: Environment Protection Act

Flocculation: The process of gathering particles to form larger masses or flocs (usually gelatinous in form).

Fractal: Fractal geometry is a method for characterizing structures of fine particles

Fractal dimension: A number that quantitatively describes how an object fills its space.

GHG: Green House Gas

Heteroatom: any atom besides carbon and hydrogen.

HLB: This represents the Hydrophile-Lipophile balance which basically means the balance between water-loving and water-hating constituents of the molecule. An HLB of 1 represents a very hydrophobic material or having very low water solubility. A higher HLB value indicates a higher degree of water solubility. HLB values range from 0 to 20.

Horizontal separation: break down of the water-in-oil emulsions in x-axis

Horizontal movements: electro-osmotic and electrophoretic movements in the x-axis

Hydrophobic: Water hating or having a strong aversion to water.

Hydrophilic: Water loving or having a strong affinity for water.

LSHL: Low Sulfur Heavy Stock

NCP: National Contingency Plan

Oil-in-water emulsion: when oil is the dispersed phase it is oil-in-water emulsion

Petroleum sludge: oily sludge

Sedimentation Potential: The potential difference at zero current caused by the sedimentation of dispersed species. This mechanism of potential difference generation is known as the Dorn effect; sedimentation potential is sometimes referred to as Dorn potential.

Streaming Potential: The potential difference at zero current created when liquid is made to flow through a porous medium.

Surface-active material: Materials that act like surfactant.

Refinery waste: residuals of all petroleum acquisition, transportation, storing and refining operations

RCRA: Resource Conservation and Recovery Act

Vertical separation: break down of the water-in-oil emulsions in y-axis

Water-in-oil emulsion: when water is the dispersed phase it is a water-in-oil emulsion

Wettability: The relative affinity of a liquid for a surface, measured by the contact angle formed between the liquid and the surface. (If the contact angle is zero complete wettability occurs. If the contact angle is greater than 90 degrees the condition is one of non-wettability).

Zeta potential: Zeta potential (ζ) is the potential across the interface of all solids and liquids. Specifically, the potential across the diffuse layer of ions surrounding a charged

colloidal particle, which is largely responsible for colloidal stability. Also called electrokinetic potential.